

AD-A240 185



TECHNICAL REPORT 3L-91-11

2

US Army Corps
of Engineers

KA-III, PHASE C, M-1 PROPELLANT TESTS: DEFLAGRATION IN PARTIAL CONFINEMENT

by

Charles E. Joachim

Structures Laboratory

DEPARTMENT OF THE ARMY

Waterways Experiment Station, Corps of Engineers
3909 Halls Ferry Road, Vicksburg, Mississippi 39180-6199

DTIC
ELECTE
SEP 11 1991
S D D



July 1991

Final Report

Approved For Public Release; Distribution is Unlimited

91-10272



Prepared for US DoD Explosives Safety Board,
Norwegian Defence Construction Service, and
Safety Services Organisation, Ministry of Defence, United Kingdom

91 9 10 073

REPORT DOCUMENTATION PAGE			Form Approved OMB No. 0704-0188	
<small>Public reporting burden for this collection of information is estimated to average 1 hour per response, including the time for reviewing instructions, searching existing data sources, gathering and maintaining the data needed, and completing and reviewing the collection of information. Send comments regarding this burden estimate or any other aspect of this collection of information, including suggestions for reducing this burden, to Washington Headquarters Services, Directorate for Information Operations and Reports, 1215 Jefferson Davis Highway, Suite 1204, Arlington, VA 22202-4302, and to the Office of Management and Budget, Paperwork Reduction Project (0704-0188), Washington, DC 20503</small>				
1. AGENCY USE ONLY (Leave blank)	2. REPORT DATE July 1991	3. REPORT TYPE AND DATES COVERED Final report		
4. TITLE AND SUBTITLE KA-III, Phase C, M-1 Propellant Tests: Deflagration in Partial Confinement		5. FUNDING NUMBERS		
6. AUTHOR(S) Charles E. Joachim				
7. PERFORMING ORGANIZATION NAME(S) AND ADDRESS(ES) USAE Waterways Experiment Station, Structures Laboratory, 3909 Halls Ferry Road, Vicksburg, MS 39180-6199		8. PERFORMING ORGANIZATION REPORT NUMBER Technical Report SL-91-11		
9. SPONSORING / MONITORING AGENCY NAME(S) AND ADDRESS(ES) US DoD Explosives Safety Board, Norwegian Defence Construction Service, and Safety Services Organisation, Ministry of Defence, United Kingdom		10. SPONSORING / MONITORING AGENCY REPORT NUMBER		
11. SUPPLEMENTARY NOTES				
12a. DISTRIBUTION / AVAILABILITY STATEMENT Approved for public release; distribution is unlimited		12b. DISTRIBUTION CODE		
13. ABSTRACT (Maximum 200 words) <p>When a propellant material is stored under confined conditions, US and NATO explosives safety regulations require that the safety hazard quantity-distance (Q-D's) used for Hazard Class 1.1 (mass detonating) explosives be applied, rather than the less restrictive Q-D's normally used for propellants and other Class 1.3 materials. This is based on the assumption that high gas pressures produced by an accidental burning of propellant in a confined volume will cause the burning (deflagration) to transition to a detonation. To test this assumption, a series of experiments were conducted in which increasing amounts of propellants were ignited and burned inside a heavy concrete structure with an internal chamber volume of 5 m³. Pressure and temperatures were measured inside the chamber, in a connecting exhaust vent, and in the free field beyond the exhaust vent pipe. Although there was no evidence that a detonation occurred, the high gas pressures produced by burning of the largest propellant charge (250 kg) were sufficient to fail the structure.</p>				
14. SUBJECT TERMS Deflagration/detonation M-1 propellant		Munitions storage Propellant burn		15. NUMBER OF PAGES 143
				16. PRICE CODE
17. SECURITY CLASSIFICATION OF REPORT UNCLASSIFIED	18. SECURITY CLASSIFICATION OF THIS PAGE UNCLASSIFIED	19. SECURITY CLASSIFICATION OF ABSTRACT	20. LIMITATION OF ABSTRACT	

PREFACE

The KA-III Test Program was a series of explosive tests conducted as a follow-on to the Defense Nuclear Agency's (DNA) MISERS GOLD EVENT (June 1989). The KA-III, Phase A and B tests were jointly sponsored by DNA and the Norwegian Defence Construction Service, and subjected several Norwegian structures previously tested on MISERS GOLD to detonation effects of fuel-air explosives (FAE), conventional bombs, and high explosive charges. The KA-III, Phase C Test Program was sponsored by the US Department of Defense Explosives Safety Board (DDESB), the Norwegian Defence Construction Service (NDCS), and the Safety Services Organisation (SSO) of the Ministry of Defence, United Kingdom.

The KA-III Test Program was conducted on the DNA's MISERS GOLD Test Bed at the White Sands Missile Range. LCDR W. F. Taylor was the DNA Test Director and Mr. R. A. Flory, Washington Research Center, was Program Coordinator. The DDESB, NDCS, and SSO Technical Monitors for Phase C were Dr. C. E. Canada, Mr. Arnfinn Jenssen, and Dr. N. J. M. Rees, respectively.

The KA-III, Phase C, propellant burn study was performed by the Explosion Effects Division (EED), Structures Laboratory (SL), US Army Engineer Waterways Experiment Station (WES). Mr. Charles E. Joachim, EED, was Project Manager and is the author of this report. The work was performed under the general supervision of Mr. L. K. Davis, Chief, EED, and Mr. Bryant Mather, Chief, SL. Field support was provided by Messrs. D. P. Hale, EED, and W. W. Tennant, WES Engineering and Construction Services Division. Messrs. J. W. Johnson and D. P. Biggs, WES Instrumentation Services Division, provided timing and firing and instrumentation support for the field tests. Messrs. R. Edgar and R. Campbell, Ballistec Systems, Inc., Quebec, Canada provided digital recording and final data plots of all transducer-time histories.

COL Larry B. Fulton, EN, was the Commander and Director of WES, and Dr. Robert W. Whalin was the Technical Director.



i

Accession For	
NTIS GRA&I	J
DTIC TAB	
Unannounced	
Justification	
By	
Distribution	
Availability	
Dist	Avail
A-1	

CONTENTS

	Page
PREFACE	i
LIST OF FIGURES	iv
LIST OF TABLES	xi
CONVERSION FACTORS, SI (METRIC) TO NON-SI UNITS OF MEASUREMENT	xii
SECTION 1 INTRODUCTION	1
1.1 BACKGROUND AND REQUIREMENT	1
1.2 OBJECTIVES	2
SECTION 2 TEST PROCEDURES	3
2.1 GENERAL APPROACH	3
2.2 TEST STRUCTURE	3
2.3 PROPELLANT DESCRIPTION	4
2.4 ARMING AND FIRING	5
2.5 INSTRUMENTATION	6
2.6 VIDEO COVERAGE	7
SECTION 3 TEST RESULTS	8
3.1 INSTRUMENTATION PERFORMANCE	8
3.2 RESULTS OF TEST C-1 (10-kg Charge)	8
3.3 RESULTS OF TEST C-2 (25-kg Charge)	9
3.4 RESULTS OF TEST C-3 (100-kg Charge)	10
3.5 RESULTS OF TEST C-4 (250-kg Charge)	11
SECTION 4 ANALYSIS OF RESULTS	13
SECTION 5 CONCLUSIONS	15
SECTION 6 RECOMMENDATIONS	16
REFERENCES	17

CONTENTS (Continued)

	Page
APPENDIX A1 TEST C-1, 10-kg M-1 PROPELLANT BURN, DATA-TIME HISTORIES	56
APPENDIX A2 TEST C-2, 25-kg M-1 PROPELLANT BURN, DATA-TIME HISTORIES	72
APPENDIX A3 TEST C-3, 100-kg M-1 PROPELLANT BURN, DATA-TIME HISTORIES	91
APPENDIX A4 TEST C-4, 250-kg M-1 PROPELLANT BURN, DATA-TIME HISTORIES	109

LIST OF FIGURES

	Page
1. MISERS GOLD test site location	18
2. Vertical cross-section of horn antenna bunker with vent pipe attached. The M-1 propellant charge was placed in a cardboard box for Tests C-1, C-2, and C-3 and poured directly on the bunker floor for Test C-4	19
3. Test C-2 charge (25 kg of M-1 propellant) placed in a cardboard box on the floor of the bunker with booster (electric match surrounded by 50 gm of pistol powder) laid on the top surface of the charge	20
4. Test C-3 charge (100 kg of M-1 propellant) placed in four cardboard boxes taped together, with booster laid on the surface of the charge	20
5. Chamber pressure gage mount (ABI180) directly below vent pipe. Note: accelerometer mounting bracket (lower left) was left over from MISERS GOLD EVENT	21
6. Water filled cylinder with five pressure gages. Note pipe with 90° elbow connecting the cylinder to the interior of horn antenna bunker	21
7. Vent pipe with one free-field, side-on overpressure gage (ABE173). Cables are seen for two internal vent pipe transducers: thermal flux gage (TF192, left) and side-on overpressure gage (ABE172)	22
8. Instrumentation layout (plan view) showing internal and external transducer locations. Five pressure gages were attached to the water filled cylinder which was connected to the chamber via the air-filled pipe (upper left corner of drawing)	23
9. Recording bunker protecting digital recording system. A shallow cable ditch can be seen running (left to center background) from the recording bunker to the horn antenna bunker	24
10. Plan view of external airblast instrumentation and photo marker locations	25
11. Test C-1: length of exhaust gas plume (from end of vent pipe) as a function of relative time. Zero-time was not recorded, so all times are relative to an arbitrarily chosen start time	26
12. Test C-1: measured peak pressures as a function of distance from the center of the 10-kg M-1 propellant charge	27

LIST OF FIGURES (Continued)

	Page
13. Test C-1: thermal flux at mid-length in the vent pipe (Gage TF191) versus the differential of measured temperature (Gage THC190) with respect to time. Each data point represents a * "pair" of values; an x-value from a given dT/dt , and a y-value from the thermal flux record corresponding to the same time instant (after zero time) as the dT/dt value	28
14. Test C-1: calculated pseudo-thermal flux (from temperature measurements of Gage THC190) in the bunker chamber compared to measured thermal flux-time histories in the vent pipe (Gages TF191 and TF192)	29
15. Test C-2: length of exhaust gas plume (from end of vent pipe) as a function of relative time. Zero-time was not recorded, so all times are relative to an arbitrarily chosen start time	30
16. Test C-2: measured peak pressures as a function of distance from the center of the 25-kg M-1 propellant charge	31
17. Test C-2: thermal flux at mid-length in the vent pipe (Gage TF191) versus the differential of measured temperature (Gage THC190) with respect to time. Each data point represents a "pair" of values; an x-value from a given dT/dt , and a y-value from the thermal flux record corresponding to the same time instant (after zero time) as the dT/dt value	32
18. Test C-2: calculated pseudo-thermal flux (from temperature measurement of (Gage THC190) in the bunker chamber compared to measured themal flux-time histories in the vent pipe (Gages (TF191 and TF192)	33
19. Test C-3: length of exhaust gas plume (from end of vent pipe) as a function of relative time. Zero-time was not recorded so all times are relative to an arbitrarily chosen start time	34
20. Test C-3: measured peak pressures as a function of distance from the center of the 100-kg M-1 propellant charge	35
21. Test C-3: thermal flux at mid-length in the vent pipe (Gage TF191) versus the differential of measured temperature (Gage THC190) with respect to time. Each data point represents a "pair" of values; an x-value from a given dT/dt , and a y-value from the thermal flux record corresponding to the same time instant (after zero time) as the dT/dt value	36

LIST OF FIGURES (Continued)

	Page
22. Test C-3: calculated pseudo-thermal flux (from temperature measurement of (Gage THCl90) in the bunker chamber compared to measured themal flux-time histories in the vent pipe (Gages (TF191 and TF192)	37
23. Test C-4: length of exhaust gas plume (from end of vent pipe) as a function of relative time. Zero-time was not recorded so all times are relative to an arbitrarily chosen start time	38
24. Test C-4: measured peak pressure as a function of distance from the center of the 250-kg M-1 propellant charge	39
25. Peak overpressure versus distance from the center of the M-1 propellant charge, KA-III, Phase C	40
26. Peak chamber pressure versus M-1 propellant loading density, KA-III, Phase C; comparison with previous data from BRL tests with one and three ignition points of propellant charge	41
27. Peak overpressure at end of vent pipe versus chamber loading density; KA-III, Phase C	42
28. Peak total free-field pressure versus distance from the center of the M-1 propellant charge, KA-III, Phase C	43
29. Peak thermal flux versus distance from the center of the M-1 propellant charge; KA-III, Phase C. Note: chamber thermal flux data are calculated from thermocouple measurements	44
30. Peak thermal flux versus M-1 propellant loading density, KA-III, Phase C	45
31. Peak chamber temperature versus loading density, KA-III, Phase C; comparison with previous data from BRL model test with one and three ignition points of propellant charge	46
A1-1. Test C-1, airblast overpressure-time history at mid-length inside the vent pipe, Gage ABEl71	57
A1-2. Test C-1, airblast overpressure-time history at the exterior end of the vent pipe, Gage ABEl72	58
A1-3. Test C-1, free-field airblast overpressure-time history at 0.3-m from the end of vent pipe, Gage ABEl73	59
A1-4. Test C-1, free-field airblast overpressure-time history at 0.9-m from the end of the vent pipe, Gage ABEl74	60

LIST OF FIGURES (Continued)

	Page
A1-5. Test C-1, free-field airblast overpressure-time history at 2.1-m from end of vent pipe, Gage ABE175	61
A1-6. Test C-1, free-field airblast overpressure-time history at 4.5-m from end of vent pipe, Gage ABE176	62
A1-7. Test C-1, free-field airblast total pressure-time history at 2.1-m from end of vent pipe, Gage ABE178	63
A1-8. Test C-1, chamber airblast pressure-time history, Gage ABI180 .	64
A1-9. Test C-1, chamber airblast pressure-time history, Gage ABI182 .	65
A1-10. Test C-1, chamber (water filled cylinder) airblast pressure-time history, Gage ABI184	66
A1-11. Test C-1, chamber (water filled cylinder) airblast pressure-time history, Gage ABI185	67
A1-12. Test C-1, chamber (water filled cylinder) airblast pressure-time history, Gage ABI187	68
A1-13. Test C-1, chamber temperature, Gage THC190	69
A1-14. Test C-1, thermal flux-time history at mid-length inside the vent pipe, Gage ABE191	70
A1-15. Test C-1, thermal flux-time history at the exterior end of the vent pipe, Gage ABE192	71
A2-1. Test C-2, airblast overpressure-time history at mid-length inside the vent pipe, Gage ABE171	73
A2-2. Test C-2, airblast overpressure-time history at the exterior end of the vent pipe, Gage ABE172	74
A2-3. Test C-2, free-field airblast overpressure-time history at 0.3-m from the end of vent pipe, Gage ABE173	75
A2-4. Test C-2, free-field airblast overpressure-time history at 0.9-m from the end of the vent pipe, Gage ABE174	76
A2-5. Test C-2, free-field airblast overpressure-time history at 2.1-m from end of vent pipe, Gage ABE175	77
A2-6. Test C-2, free-field airblast overpressure-time history at 4.5-m from end of vent pipe, Gage ABE176	78

LIST OF FIGURES (Continued)

	Page
A2-7. Test C-2, free-field airblast total pressure-time history at 0.9-m from end of vent pipe, Gage ABE177	79
A2-8. Test C-2, free-field airblast total pressure-time history at 2.1-m from end of vent pipe, Gage ABE178	80
A2-9. Test C-2, chamber airblast pressure-time history, Gage ABI180	81
A2-10. Test C-2 chamber airblast pressure-time history, Gage ABI181B	82
A2-11. Test C-2, chamber airblast pressure-time history, Gage ABI182	83
A2-12. Test C-2, chamber airblast pressure-time history, Gage ABI183T	84
A2-13. Test C-2, chamber (water filled cylinder) airblast pressure-time history, Gage ABI185	85
A2-14. Test C-2, chamber (water filled cylinder) airblast pressure-time history, Gage ABI186	86
A2-15. Test C-2, chamber (water filled cylinder) airblast pressure-time history, Gage ABI187	87
A2-16. Test C-2, chamber temperature, Gage THC190	88
A2-17. Test C-2, thermal flux-time history at mid-length inside the vent pipe, Gage TF191	89
A2-18. Test C-2, thermal flux-time history at the exterior end of the vent pipe, Gage TF192	90
A3-1. Test C-3, airblast overpressure-time history at mid-length inside the vent pipe, Gage ABE171	92
A3-2. Test C-3, airblast overpressure-time history at the exterior end of the vent pipe, Gage ABE172	93
A3-3. Test C-3, free-field airblast overpressure-time history at 0.3-m from the end of vent pipe, Gage ABE173	94
A3-4. Test C-3, free-field airblast overpressure-time history at 0.9-m from the end of the vent pipe, Gage 174	95
A3-5. Test C-3, free-field airblast overpressure-time history at 2.1-m from end of vent pipe, Gage ABE175	96
A3-6. Test C-3, free-field airblast overpressure-time history at 4.5-m from end of vent pipe, Gage ABE176	97

LIST OF FIGURES (Continued)

	Page
A3-7. Test C-3, free-field airblast total pressure-time history at 2.1-m from end of vent pipe, Gage ABEH178	98
A3-8. Test C-3, chamber airblast pressure-time history, Gage ABI180	99
A3-9. Test C-3, chamber airblast pressure-time history, Gage ABI181B	100
A3-10. Test C-3, chamber airblast pressure-time history, Gage ABI182	101
A3-11. Test C-3, chamber (water filled cylinder) airblast pressure-time history, Gage ABI185	102
A3-12. Test C-3, chamber (water filled cylinder) airblast pressure-time history, Gage ABI186	103
A3-13. Test C-3, chamber (water filled cylinder) airblast pressure-time history, Gage ABI187	104
A3-14. Test C-3, chamber (water filled cylinder) airblast pressure-time history, Gage ABI188	105
A3-15. Test C-3, chamber temperature, Gage THC190	106
A3-16. Test C-3, thermal flux-time history at mid-length inside the vent pipe, Gage TF191	107
A3-17. Test C-3, thermal flux-time history at the exterior end of the vent pipe, Gage TF192	108
A4-1. Test C-4, airblast overpressure-time history at mid-length inside the vent pipe, Gage ABE171	110
A4-2. Test C-4, airblast overpressure-time history at the exterior end of the vent pipe, Gage ABE172	111
A4-3. Test C-4, free-field airblast overpressure-time history at 0.3-m from the end of vent pipe, Gage ABE173	112
A4-4. Test C-4, free-field airblast overpressure-time history at 0.9-m from the end of the vent pipe, Gage ABE174	113
A4-5. Test C-4, free-field airblast overpressure-time history at 2.1-m from end of vent pipe, Gage ABE175	114
A4-6. Test C-4, free-field airblast overpressure-time history at 4.5-m from end of vent pipe, Gage ABE176	115

LIST OF FIGURES (Concluded)

	Page
A4-7. Test C-4, free-field airblast total pressure-time history at 0.9-m from end of vent pipe, Gage APFH177	116
A4-8. Test C-4, chamber airblast pressure-time history, Gage ABI180 .	117
A4-9. Test C-4, chamber airblast pressure-time history, Gage ABI181B .	118
A4-10. Test C-4, chamber airblast pressure-time history, Gage ABI182 .	119
A4-11. Test C-4, chamber airblast pressure-time history, Gage ABI183T	120
A4-12. Test C-4, chamber (water filled cylinder) airblast pressure-time history, Gage ABI185	121
A4-13. Test C-4, chamber (water filled cylinder) airblast pressure-time history, Gage ABI186	122
A4-14. Test C-4, chamber (water filled cylinder) airblast pressure-time history, Gage ABI187	123
A4-15. Test C-4, chamber (water filled cylinder) airblast pressure-time history, Gage ABI188	124
A4-16. Test C-4, chamber temperature, Gage THC190	125
A4-17. Test C-4, thermal flux-time history at mid-length inside the vent pipe, Gage TF191	126
A4-18. Test C-4, thermal flux-time history at the exterior end of the vent pipe, Gage TF192	127

LIST OF TABLES

	Page
1. KA-III, Phase C: Configuration Parameters for M-1 Propellant Charges	47
2. Test C-1 (Loading Density 2 kg/m ³): Pre-Test Gage Location and Digital System Set-up Data	48
3. Test C-2 (Loading Density 5 kg/m ³): Pre-Test Gage Location and Digital System Set-up Data	49
4. Test C-3 (Loading Density 20 kg/m ³): Pre-Test Gage Location and Digital System Set-up Data	50
5. Test C-4 (Loading Density 50 kg/m ³): Pre-Test Gage Location and Digital System Set-up Data	51
6. Test C-1 (Loading Density 2 kg/m ³): Gage Location and Peak Measured Data	52
7. Test C-2 (Loading Density 5 kg/m ³): Gage Location and Peak Measured Data	53
8. Test C-3 (Loading Density 20 kg/m ³): Gage Location and Peak Measured Data	54
9. Test C-4 (Loading Density 50 kg/m ³): Gage Location and Peak Measured Data	55

CONVERSION FACTORS, SI (METRIC) TO NON-SI
UNITS OF MEASUREMENT

SI (Metric) units of measurement used in this report can be converted to Non-SI units as follows:

Divide	By	To Obtain
calories per square centimeter-second	0.2712459	BTU per square foot-seconds
cubic metres	0.02831685	cubic feet
degrees Celsius*	$1.8\text{ C} + 32$	degrees Fahrenheit
kilograms	0.45359237	pound (mass)
kilograms per cubic metre	16.01846	pounds (mass) per cubic foot
kilopascals	6.894757	pounds (force) per square inch
metres	0.3048	feet
square metres	0.9290304	square feet

* To obtain Fahrenheit (F) temperature readings from Celsius (C) readings, use the following formula: $F = 1.8\text{ C} + 32$. To obtain kelvin (K) readings, use: $K = C + 273.14$.

KA-III, PHASE C
M-1 PROPELLANT TESTS: DEFLAGRATION IN PARTIAL CONFINEMENT

SECTION 1

INTRODUCTION

1.1 BACKGROUND AND REQUIREMENT

In order to maintain a satisfactory level of combat readiness, the armed forces of NATO nations must store large amounts of ammunition and propellant for artillery and naval guns. Ammunition usually contains high explosives that are classified as Class 1.1 explosion hazards by US and NATO guidelines, due to the fact that they will "mass detonate"; i.e., an accidental explosion of a single round will sympathetically detonate the entire mass of ammo rounds in close proximity. Consequently, large separation distances, or "Quantity Distances (Q-D's)," are required between a given quantity of stored ammunition and other magazines (or other ammo storage or explosive operations areas), inhabited buildings, public traffic routes, etc.

Under most conditions, propellants may burn, but they will not mass detonate. They are therefore designated as Hazard Class 1.3 materials, and are subject to much less restriction and have much smaller Q-D's than 1.1 materials. The theory exists, however, that if propellant is stored in a chamber or other confined area, an accidental fire could quickly ignite the propellant mass and rapidly produce a large volume of combustion gases. Because this rapid buildup of gases can only vent through the relatively small entrance into the chamber, the chamber becomes highly pressurized. The theory postulates that such high pressures can cause the deflagration of the propellant to transition to a detonation. Consequently, propellant stored under confined conditions must be classified as a mass-detonating explosive, or Hazard Class 1.1, instead of 1.3. This, in turn, requires much larger "buffer zones", or Quantity-Distance (Q-D) separations between magazines, inhabited buildings, public traffic routes, etc.

1.2 OBJECTIVES

The objective of the Phase C tests was to determine the combination of confinement pressure and loading density required for M-1 propellant to transition from deflagration to detonation, in the event of an accidental

fire. The tests also measured the temperatures, thermal flux and internal and external pressures generated by the deflagration of the various propellant loading densities.

SECTION 2

TEST PROCEDURES

2.1 GENERAL APPROACH

Following the MISERS GOLD explosion test (1 June 1989) at White Sands Missile Range, NM, several relatively undamaged, full-scale structures were available for further testing at the MISERS GOLD site (Figure 1). The KA-III Test Series was developed to exploit these structures in an extensive program of tests to evaluate the detonation effects of conventional (i.e., non-nuclear) munitions. Phase C of the KA-III Series was planned to consist of up to five deflagration and/or detonation tests, using M-1 propellant, inside a small concrete bunker. The Phase C plan called for increasing the propellant loading density with each successive test (loading densities of 2, 5, 20, 50 and 100 kg/m³)* until either (a) a transition from burning to a detonation occurred, or (b) the structure failed from the buildup of internal pressures. The test program would be terminated at either point.

2.2 TEST STRUCTURE

The test structure, known as the Horn Antenna Bunker (MISERS GOLD Structure #6410G), had internal dimensions of 1.4 m (side-to-side), 1.9 m (front-to-back) and 1.9 m (height). The reinforced concrete walls, roof, and floor of the structure were 30 cm thick. For the KA-III-C tests, the bunker was modified by the addition of a vent tube welded into the observation port opening, and by strengthening of the access hatch to resist internal pressures from the propellant burn tests. The vent tube cross-sectional area was selected to simulate the chamber and access tunnel proportions of the Shallow Underground Tunnel/Chamber Explosion Test conducted at China Lake, CA, in 1988. The chamber and access tunnel at China Lake had the following dimensions (volume, cross-sectional area and length):

Chamber: $V_c = 331.2 \text{ m}^3$	Tunnel: $V_t = 132.5 \text{ m}^3$
$A_c = 18.4 \text{ m}^2$	$A_t = 5.3 \text{ m}^2$
$L_c = 18 \text{ m}$	$L_t = 25 \text{ m}$

* A table of factors for converting SI (metric) units of measurement to non-SI units is presented on page xii.

The volume of the Horn Antenna Bunker (V_b) was 5 m^3 . If the vent area ratio (vent area/chamber volume) of the China Lake facility is applied to the bunker test design, then

$$\begin{aligned} A_t/V_c &= 5.3/331.2 = 0.016, & A_v/V_b &= 0.016, \\ A_v &= 0.016 \times 5.0 = 0.08 \text{ m}^2. \end{aligned}$$

A steel pipe was selected whose diameter gave a vent area closest to this value. The pipe was 35.6 cm (14 in.) in diameter, with an extra heavy (12.7 mm, or 0.50 in.) wall thickness. With an inside diameter of 33.02 cm (13 in.), this pipe provided a vent area of:

$$A_v = 3.1416 \times (33.02/2)^2 = 0.0857 \text{ m}^2.$$

For the tunnel and vent pipe, the following ratios apply:

$$L_v/L_t = (A_v/A_t)^{1/2}$$

The length of pipe required was computed from this ratio as:

$$L_v = L_t (A_v/A_t)^{1/2} = 25 (0.0857/5.3)^{1/2} = 3.18 \text{ m}.$$

The Horn Antenna Bunker with vent tube attached is shown in plan view in Figure 2.

2.3 PROPELLANT DESCRIPTION

The M-1 propellant used in the Phase C test program was demilitarized material obtained from the US Army Armament, Munitions and Chemical Command's Rock Island (Illinois) Arsenal (stock number 1376-451-2881). It was shipped to the White Sands Missile Range in metal-lined, wooden containers (type M-24) with a stated propellant weight of 64 kg in each canister. The actual propellant weight in each canister was found to average approximately 45 kg. The propellant grains were examined at WES under an electron microscope, and average dimensions were obtained. The propellant grain was cylindrical, with a single perforation (a perforation is a hole through the entire length of the

grain cylinder). The grains were nominally 5 mm long, with a 1.1-mm outside diameter, a 0.5-mm inside diameter, and, a 0.36 mm WEB (web thickness). Shipping labels indicated the material was all from Lot No. RAD 69214.

For Tests C-1 - C-3, the M-1 propellant charge was placed in a cardboard box at the center of the chamber floor (Figure 3). For Test C-3, four boxes were taped together, as shown in Figure 4. The individual boxes were 4.92 cm wide, 6.50 cm long, and 4.92 cm deep. For Test C-4, the propellant was poured onto the floor, forming an approximately conical shape. Charge weight, volume, and surface area data for each test are given in Table 1.

2.4 ARMING AND FIRING

Atlas electric matches were used to initiate all M-1 propellant burns. The match was placed in a plastic bag along with a booster charge of 50 grams of smokeless pistol powder to assure ignition. The electric match lead wires were connected to separate leads of a 4-conductor shielded cable which exited the bunker through a cable grommet installed in the hatch cover. The firing line was approximately 200 m long, running from the bunker to a sandbagged junction box containing a 12-volt battery and a single-pole, double-throw relay. The shorted side of the relay was connected to the cable from the electric match, and the other side to the test event control system.

All tests were computer controlled from North Park Bunker #1. The event controller provided relay signals to start the Digistar digital system at T-100 msec. A closure at T-0 msec (zero-time) switched the firing line from short to 12 volts, which initiated the electric match. After the deflagration and/or detonation was complete, the firing control unit was disconnected from the firing line and the test area inspected for possible hazards by a reentry team consisting of the WES blaster, WES Project Officer, and DNA Site Safety Officer. When no visual signs of internal burning were evident, the bunker was approached from the rear and a hand-held, digital, temperature meter was attached to the thermocouple cable to monitor the temperature inside the bunker chamber. The hatch cover was reopened when the temperature monitor indicated that the internal temperature had fallen below 130°F. A ventilation duct, connected to an exhaust fan, was then placed inside the chamber through the open hatch to exhaust fumes from the chamber. When gas sampling indicated

that the carbon dioxide content of the interior was safe, personnel were then allowed to reenter the bunker for cleanup and instrumentation work.

2.5 INSTRUMENTATION

Instrumentation for all Phase C tests included four flush-mounted airblast pressure gages on the interior bunker walls. Two pressure gages were mounted on the center of the side wall (right side as observed from outside through the vent pipe); one at a height of 63 cm and the other at 1.27 cm. The other two internal gages were mounted at the center (mid-height and mid-width) of the front (under the vent pipe, Figure 5) and rear walls. The pressure gages were placed in mounts that were glued with epoxy into holes drilled through the bunker concrete wall. These gage mounts included a metal baffle system and nylon bushings to protect the airblast gages from direct heating by the burning propellant.

Five additional airblast gages were mounted on a water-filled cylinder which was connected to the bunker interior through an air-filled steel vent pipe, 12.7 mm in diameter (inside) and 2.8 m long. The pipe penetrated the chamber wall at the upper rear corner of the chamber (wall on right side), with the other end connected to the water-filled cylinder through a 90° elbow (Figure 6). The vent pipe was instrumented at two internal points for side-on airblast and thermal flux measurements. Four additional side-on airblast pressure gages were installed on the ground surface outside the bunker along the extended vent pipe centerline to measure side-on overpressure, and two total-pressure probe gage mounts were placed along the extended centerline of the vent pipe. The vent pipe, with the first of the four free-field, side-on overpressure gages, is shown in Figure 7. The temperature inside the bunker during the propellant burns was monitored with a Type K thermocouple, mounted in the hatch cover. Gage locations are shown in Figure 8. Gage types, locations, and predicted peak values are given in Tables 2 through 5.

Kulite Model HKS-375 series pressure gages were used in all locations where predicted peak pressures exceeded 1.5 MPa. Kulite XT-190 Series gages were used for lower pressures. Thermal flux measurements were made with Medtherm Model #64-250SB-17 heat flux transducers. These gages use a

Schmidt-Boelter thermopile with a capacity of 250 BTU/ft²-sec, with an over-range capability of 150%. Bunker temperatures during propellant burns were monitored with Medtherm Model TC-K1212UP thermocouples. These gages use a Type K Chromel/Alumel junction. Temperatures were digitally recorded during the burns.

Transducer analog signals were digitized and recorded by Ballistech Systems, Incorporated (BSI) using their Digistar II digital system. The transducer signals were transmitted to the recording bunker (Figure 9) on 4-conductor, shielded cable (approximately 200 m long) with a floating ground. Each channel was electrically calibrated at the digitizer by the equivalent voltage method. The digital records were field processed for quick-look data assessments. BSI provided final, filtered time-history plots at a later date. These plots are presented in Appendix A1 through A4.

2.6 VIDEO COVERAGE

A VHS video camera was used to obtain visual data on the external effects of the propellant burn. The camera was positioned to provide coverage of the bunker, vent tube and a region approximately 25 m to the front of the vent tube. The video camera was started just prior to each test and ran unattended. There was no visual zero time indicator. Photo markers were emplaced on both sides of the extended vent tube centerline to provide reference points from which to estimate flame spread and other visual effects. The markers were 61-cm square plywood sheets, attached to 10-cm square posts and painted with alternating 30-cm black and white squares. Photo marker locations are shown in Figure 10.

SECTION 3

TEST RESULTS

3.1 INSTRUMENTATION PERFORMANCE

Because preshot predictions of the peak overpressure levels expected in the bunker from the propellant burns were too high, a number of gages failed to record useful records on Tests C-1 and C-2. Of the 20 data channels on Test C-1, eight produced good quantitative data, eight produced records useful for a qualitative analysis, and four produced no data. On Test C-2, seven channels provided good quantitative data, ten produced qualitative information, and two had no data. Nineteen channels were operational on Tests C-3 and C-4, with 15 providing good records on C-3 and 11 on C-4. One channel was overdriven on Test C-3, and seven on C-4, but these still produced useful qualitative information.

For all tests, the data was digitized at a rate of one sample per 220 micro-seconds, which gave a nominal recording time of 60 seconds on each channel.

3.2 RESULTS OF TEST C-1 (10-kg Charge)

The initial visual indication of the internal M-1 propellant burn was black smoke that was projected some 3 meters beyond the end of the vent pipe. The smoke quickly changed to flame and, by 4 seconds after (assumed) initiation, the flame extended approximately 5 meters from the end of the pipe. Total duration of the external flame was approximately 11 seconds. The position of the fire plume is plotted versus time in Figure 10. Since the video does not have a zero (initiation) time indicator, an arbitrary start time was assumed. As shown in Figure 11, the initial gas flow out the vent pipe had a velocity of 3.47 m/sec. Although not seen in the video, an orange vapor or smoke persisted more than an hour after burning ceased, seeping out through the antenna port, vent pipe and around the imperfectly-sealed hatch cover.

Measured peak pressure data are presented in Table 6. Peak side-on overpressures (Figure 12) produced by the burning of the 10-kg M-1 propellant charge were very low. Pressures beyond the vent pipe were higher than the

very low transducer signals indicated for the overpressure inside the bunker. This fact suggests that uncombusted gas and propellant was carried outside and secondary burning occurred in the vented gas plume. When the bunker was reentered, the propellant charge container (cardboard box) was charred but not destroyed, indicating a lack of sufficient oxygen during deflagration. The video record shows the presence of a pulsing flame in the gas plume released through the vent pipe. Herrera (1984) reports that, in an earlier study, unburned propellant was transported outside a similar test structure in a plume with overpressures on the order of 1.6 kPa.

The temperature history recorded by the thermocouple inside the bunker on Test C-1 was differentiated with respect to time by computing the slope between digitized data points. This yielded a value, " dT/dt ", for each time interval sampled. In Figure 13, the different dT/dt values obtained from the thermocouple record have been matched with the thermal flux levels recorded for the same time intervals, at the mid-point of the vent pipe, by Gage TF191. These "pairs" of dT/dt and thermocouple readings are used as x and y values for the data points shown in Figure 12. A linear least squares fit to the data in Figure 12 therefore relates the temperature time differential to the thermal flux. Although the thermocouple (Gage THC190), located in the bunker hatch cover directly above the burning propellant, was separated from the thermal flux transducer by a distance of 2.55 m, this curve provides a crude method for relating temperature to a "pseudo"-thermal flux. Applying the relation shown in Figure 12, a pseudo-thermal flux-time history was calculated from the temperature history (Gage (THC190)). The calculated pseudo-thermal flux for the chamber is compared with the measured flux in the vent pipe (Gages TF191 and TF192) in Figure 14. As shown here, the calculated and measured data are in good agreement.

3.3 RESULTS OF TEST C-2 (25-kg Charge)

The initial visual indication of the M-1 propellant burn inside the bunker for Test C-2 was a glowing plume projected some 3 meters beyond the end of the vent pipe, within approximately one second after initiation. The plume of smoke and flame quickly extended, reaching a length of 10 m after approximately 10 seconds. The position of the leading edge of the plume is plotted versus time in Figure 15. As shown in the figure, the initial plume

velocity was 3.13 m/sec. Although it continued to burn violently, the length of the plume decreased after 10 seconds, retreating to the end of the vent pipe. Total duration of the external gas plume was approximately 18 seconds. The orange residual vapor observed after Test C-1 was not present after burning of the Test C-2 propellant charge had ceased.

Measured peak pressure and thermal flux data are presented in Table 7. Peak side-on overpressures (Figure 16) produced inside the bunker by the burning of the 25-kg propellant charge were very low. Although the peak external overpressures were approximately 20 percent higher for Event C-2 than for Event C-1, the results still indicated that uncombusted gas and unburned propellant were carried outside by the gas plume for external burning. Once again, when the bunker was reentered, the propellant charge container (cardboard box) was charred but not destroyed, indicating a deficiency of oxygen during deflagration. The video recording again showed the presence of a pulsing flame in the gas plume released through the vent pipe.

As was done for Test C-1, the temperature history recorded by the thermocouple on Test C-2 was differentiated with respect to time (dT/dt) by computing the slope between digitized data points. Thermal flux values recorded at the mid-point of the vent pipe (Gage TF191) are plotted versus dT/dt in Figure 16. An "eyeball" fit was made to the data through the point $(dT/dt) = 0$ and $Q = 3.459 \text{ cal/m}^2\text{-sec}$. Applying the relation shown in Figure 17, a pseudo thermal flux-time history was calculated from the temperature history. The calculated pseudo-thermal flux for the chamber is compared with the measured flux in the vent pipe (Gages TF191 and TF192) in Figure 18. As shown here, the calculated and measured data are in good agreement.

3.4 RESULTS OF TEST C-3 (100-kg Charge)

The initial visual indication of the propellant burn in Test C-3 was a smoke plume projected some 1.5 meters beyond the end of the vent pipe within approximately 0.2 seconds. The plume of smoke and flame reached a length of 16 m in approximately 6 seconds. The position of the leading edge of the plume is plotted versus an arbitrary time in Figure 19. As shown in Figure 18, the initial plume velocity was 5.58 m/sec, which was slightly higher than seen on the first two experiments. Although it continued to burn

violently, the length of the plume began to decrease after 6 seconds, retreating towards the end of the vent pipe. At approximately 11 seconds, a violent gas exhaust was noted, which had an estimated velocity of 29.5 m/sec and a duration of about one second. This sudden jet ripped up clods of earth from the ground surface, throwing them into the air at velocities approaching 11 m/sec. The total duration of the external gas plume, including the late jetting phenomena, was approximately 12 seconds. The orange residual vapor observed after Test C-1 was again observed after burning of the Test C-3 propellant charge ceased, although it did not persist once ventilation of the bunker was begun.

Measured peak pressure and thermal data are presented in Table 8. Peak side-on overpressures (Figure 20) produced by the burning of the 100-kg propellant charge were still low compared to predictions. The data presented in Figure 19 show a consistent trend of decreased side-on overpressure with distance from the center of the bunker. The attenuation rate increases beyond the end of the vent pipe, where the jet was allowed to expand in three dimensions. The results still indicated that uncombusted gas and unburned propellant are carried outside by the gas plume for external burning. Once again, when the bunker was reentered, the propellant charge container (cardboard box) was found to be charred but not destroyed, indicating a deficiency of surplus oxygen during deflagration. The video recording showed the presence of a pulsing flame in the gas plume released through the vent pipe.

Thermal flux values recorded at the mid-point of the vent pipe (Gage TF191) were again matched with dT/dt values from the thermocouple gage, as shown in Figure 21. An eyeball-fitted line was forced through the point $(dT/dt) = 0$ and $Q = 3.459 \text{ cal/m}^2\text{-sec}$. The calculated pseudo-thermal flux (Gage THC190) for the chamber is compared with the measured flux in the vent pipe (Gages TF191 and TF192) in Figure 22. As shown here, the calculated and measured data are in good agreement. All three time-histories show the presence of a later peak at about 15 seconds after initiation. This peak occurs in the vent pipe first, indicating movement back into the chamber from the free-field outside the bunker. This is postulated to be an indication of reignition of hot gages, progressing from the exterior back into the bunker.

3.5 RESULTS OF TEST C-4 (250-kg Charge)

The initial visual indication of the propellant burn for Test C-4 was a smoke plume projected some 1.3 meters beyond the end of the vent pipe within approximately 0.3 seconds. The plume of smoke and flame quickly extended from the vent, filling the video field of view (a distance greater than 25 m) in approximately 5.3 seconds. The position of the leading edge of the plume is plotted versus an arbitrary time in Figure 23. The initial plume velocity was 3.88 m/sec, which is slightly higher than seen on the first two experiments but less than that measured from Test C-3. Shortly afterwards (at approximately 6 sec), the structure failed, releasing all internal pressure in the process. The remaining unburned propellant then burned rapidly in the oxygen-rich outside air.

In Test C-4, the Horn Antenna Bunker clearly failed from excess internal pressure. Visual observation of the post-test structure showed that the concrete bond to the reinforcing rods had failed, and the rods were pulled out of the concrete. Only a small number of rods showed necked-down sections characteristic of tensile failure of the steel. At the time of failure, the hatch cover and roof section were hurled high into the air. The video record shows the hatch cover, although tumbling, moving with an average velocity upward velocity of 33.3 m/sec shortly after failure. Similarly, the roof section moved upward at an average velocity of 11.4 m/sec.

Measured peak pressure and thermal data for Test C-4 are presented in Table 9. Peak side-on overpressures (Figure 24) produced by the burning of the 250-kg propellant charge were the highest measured in this test series, but still seemed relatively low by weapons effects standards. The data presented in Figure 24 shows a consistent trend of decreasing side-on overpressure with distance from the center of the bunker. The attenuation rate increases beyond the end of the vent pipe, where the jet was allowed to expand in three dimensions.

SECTION 4

ANALYSIS OF RESULTS

The peak overpressures measured in the Phase C tests are plotted versus distance from the center of the burn chamber in Figure 25. Least squares fit lines are shown for Tests C-1 and C-3 (vent tube and free-field data). Average peak pressures are plotted in Figure 25 for the overpressure measurements in the chamber and water-filled cylinder. The measured peak chamber pressures are plotted versus the chamber loading densities in Figure 26.

The Ballistic Research Laboratories (BRL) conducted a series of experiments modeling the KA-III/Phase C experiments prior to the actual tests. The model chamber was 25.4 cm in diameter by 184 cm long, with a volume of 93180 cm³ (0.93 m³). The vent tube was 10 cm in diameter by 257 cm long, with a volume of 2047 cm³. Venting was further restricted at the chamber/tube interface by a 5.1 cm diameter opening. The BRL data (unpublished) is shown for comparison in Figure 26. A significant difference is seen in the model results between experiments using one-point ignition and three-point ignition. The additional ignition points increased the energy release rate, which apparently increased the measured peak overpressures. As seen in Figure 26, the model and prototype results from experiments using one-point ignition are in good agreement.

The pressures measured at the end of the vent pipe for each test are plotted versus loading density in Figure 27. Peak exit pressure increases as the loading density to the 1.653 power, for loading densities greater than 5 kg/m³. For loading densities below 5 kg/m³, the relatively large chamber volume appears to inhibit the exit pressures.

Figure 28 is a plot of peak total pressure versus distance from the center of the M-1 propellant charge. Total-pressure gages were positioned outside the bunker along the extended vent pipe centerline to measure jetting effects. The side-on pressure gage located at the same range as the successful total-pressure measurement (Gage ABE178) on Test C-3 was over-driven, indicating an overpressure in excess of 70 kPa. For Test C-4, the side-on pressure gage at the same 0.9 m location as the total-pressure

gage recorded a peak of 34.5 kPa, which appears to be abnormally low when compared to the data trend. Therefore, these total-pressure measurements indicate that jetting is not a significant problem compared to the fire and gas plume hazards outside the vent tube.

Figure 29 gives a comparison of thermal flux versus distance from the center of M-1 propellant charge. Chamber thermal flux is calculated from the thermocouple records. The thermocouple was located beneath the bunker hatch cover, directly above the charge. This distance was approximately 1.5 m above the charge surface. The thermal flux measurements from Test C-4 were over-driven, so the actual peak data are somewhat greater. The peak thermal flux data in Figure 29 shows the effects of loading density and distance from the source. Thermal flux increased with increasing propellant loading density and, at any particular loading density, the flux decreased with distance.

Thermal flux is plotted versus loading density in Figure 30. The calculated chamber thermal flux indicates that the energy release increased in almost linear proportion to the propellant loading density. The vent pipe measurements show a two-slope relation, with a lower flux gradient at lower loading densities ($< 5 \text{ kg/m}^3$). At greater loading densities, the curve essentially parallels the thermal flux-loading density relation for the chamber.

Chamber temperature is plotted versus propellant loading density in Figure 31. Temperature data from the BRL model tests are included in Figure 31 for comparison. The KA-III chamber temperature measurements were made at the thermocouple location; i.e., beneath the bunker hatch cover directly above the center of the propellant charge. Thermocouples for the BRL model experiments were located at the chamber wall. As shown in Figure 31, the number of ignition points influenced peak chamber temperature. The model test data also indicates an increase in temperature with loading density. This trend is not seen in the KA-III data.

SECTION 5

CONCLUSIONS

While the peak overpressures measured during the KA-III/Phase C experiments were relatively low, these experiments demonstrate that a serious flame and gas venting problem exists in front of a storage chamber exit. The catastrophic failure of the bunker roof from Test C-4 indicates that structural failure may occur, releasing the gas pressures from a propellant burn before the internal pressures can build enough to cause a transition from a deflagration to a detonation.

The pressures generated are a direct function of the loading density. It is suggested that, when M-1 propellant is stored in underground facilities with sufficient overburden to prevent cover venting, an accidental burn will produce far greater overpressures at loading densities above 50 kg/m^3 than was indicated by the KA-III/Phase C Tests. Rupture of the bunker roof substantially reduced the pressures generated by Test C-4.

Chamber overpressures are also a function of the number of burn ignition points. The BRL model tests demonstrated that higher pressures are generated when more than one ignition point is used. Exit pressures are a function of chamber volume, below a loading density of 5 kg/m^3 . The test data indicates a similar volume relation exists for thermal flux at loading densities below 5 kg/m^3 . The peak chamber temperatures measured in the KA-III/Phase C tests were essentially constant, irrespective of loading density.

SECTION 6

RECOMMENDATIONS

Additional testing should be done to investigate the effect of gas pressures from propellant burns in underground storage situations where cover rupture will not occur. These tests should include a measurement system to collect data on heat release rate (related to the change in mass of the unburned propellant with respect to time) of the propellant burn. This quantity is proportional to the product of the burn rate and propellant surface area. These data are required to fully assess the influence of the surface burn area on the deflagration gas pressures generated.

REFERENCES

Herrera, William R., Vargas, Luis M., Bowles, Patricia M., Baker, Dr. Wilfred E., "A Study of Fire Hazards from Combustible Ammunition, Effects of Scale and Confinement (Phase II)," Final Report, December 1984, Southwest Research Institute, San Antonio, Texas 78284

Zardos, Steve; unpublished data (personal communication), US Army Laboratory Command, Ballistic Research Laboratory, Aberdeen Proving Ground, Maryland 21005-5066

PERMANENT HIGH EXPLOSIVE TEST SITE

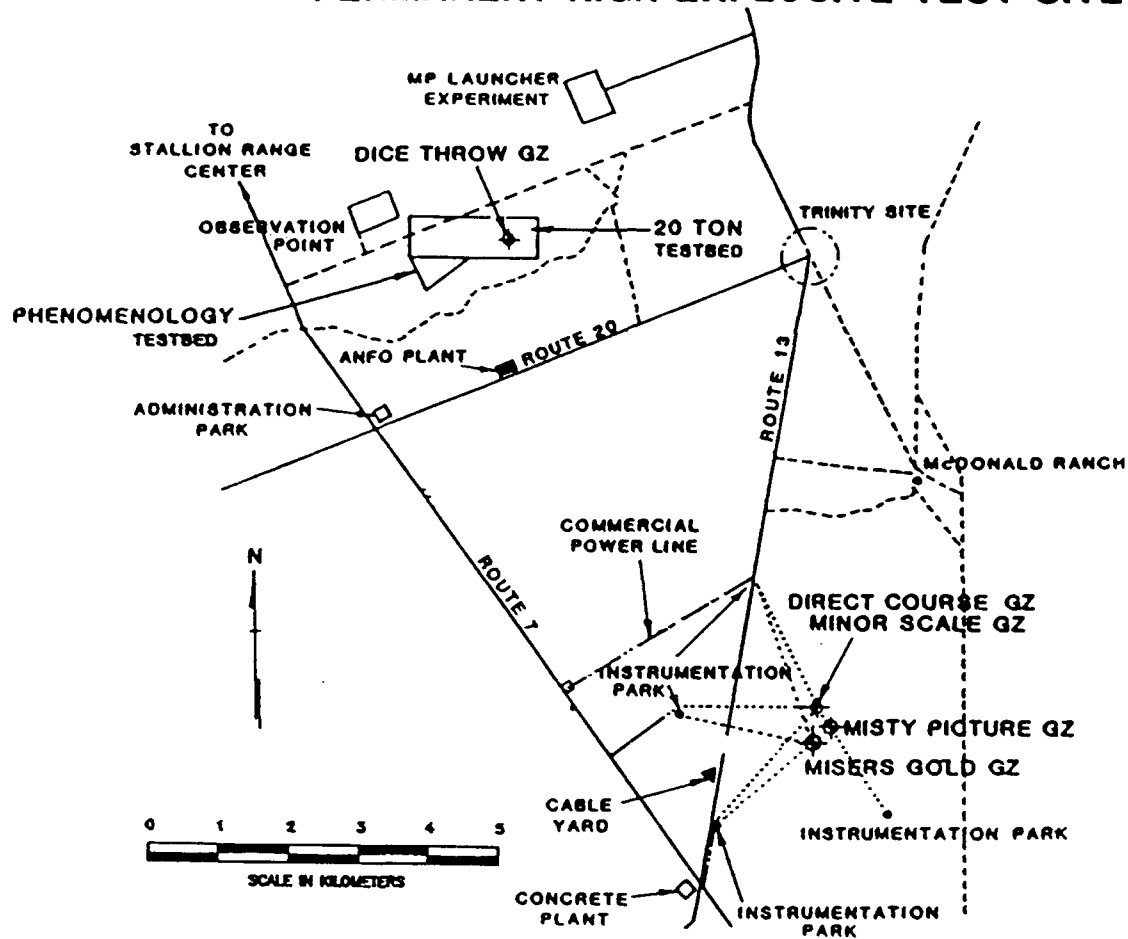


Figure 1. MISERS GOLD test site location.

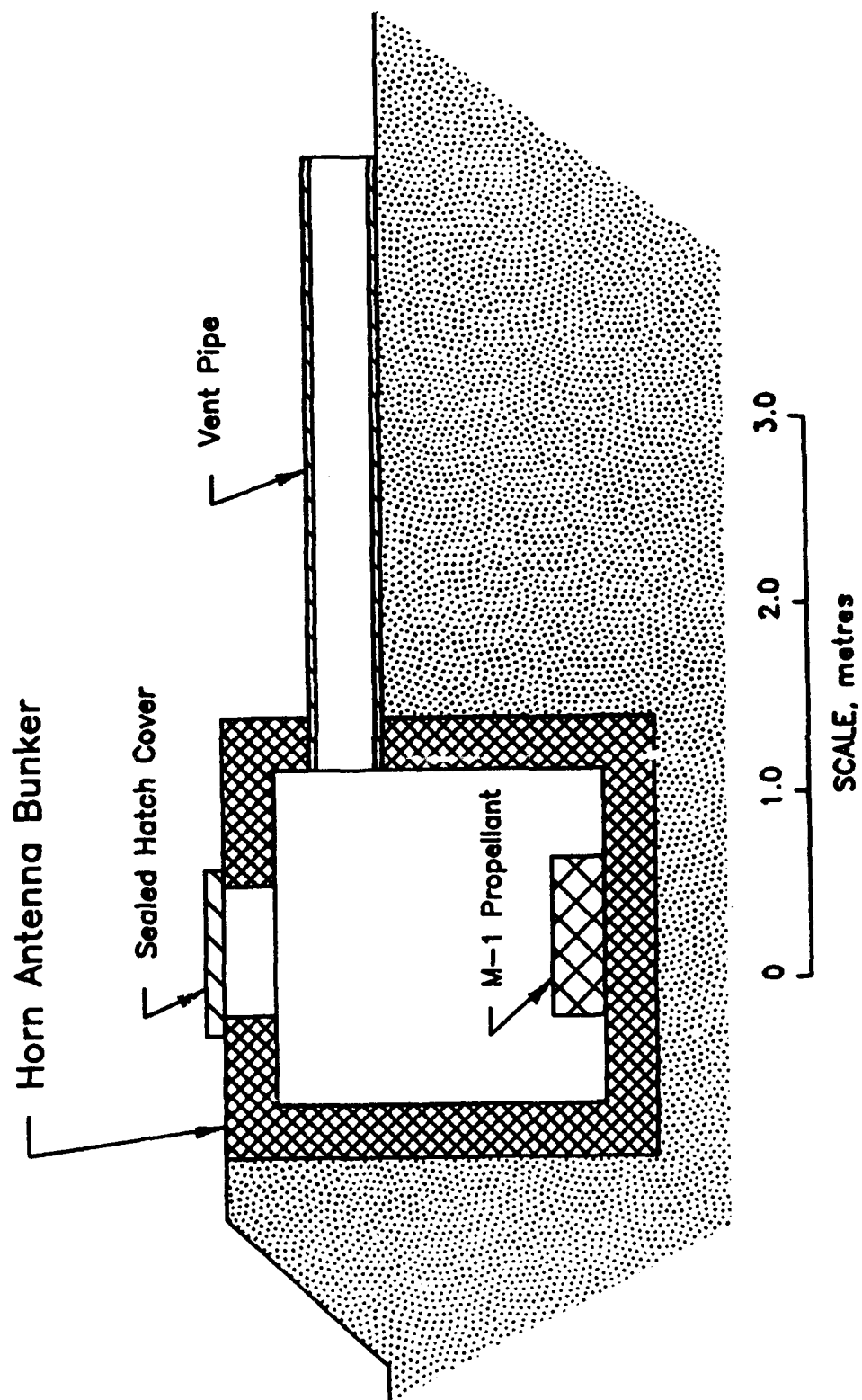


Figure 2. Vertical cross-section of horn antenna bunker with vent pipe attached. The M-1 propellant charge was placed in a cardboard box for Tests C-1, 2, and 3 and poured directly on the bunker floor for Test C-4.



Figure 3. Test C-2 charge (25 kg of M-1 propellant) placed in a cardboard box on the floor of bunker with booster (electric match surrounded by 50 gm of pistol powder) laid on the surface of the charge.



Figure 4. Test C-3 charge (100 kg of M-1 propellant) placed in four cardboard boxes taped together, with booster laid on the surface of the charge.

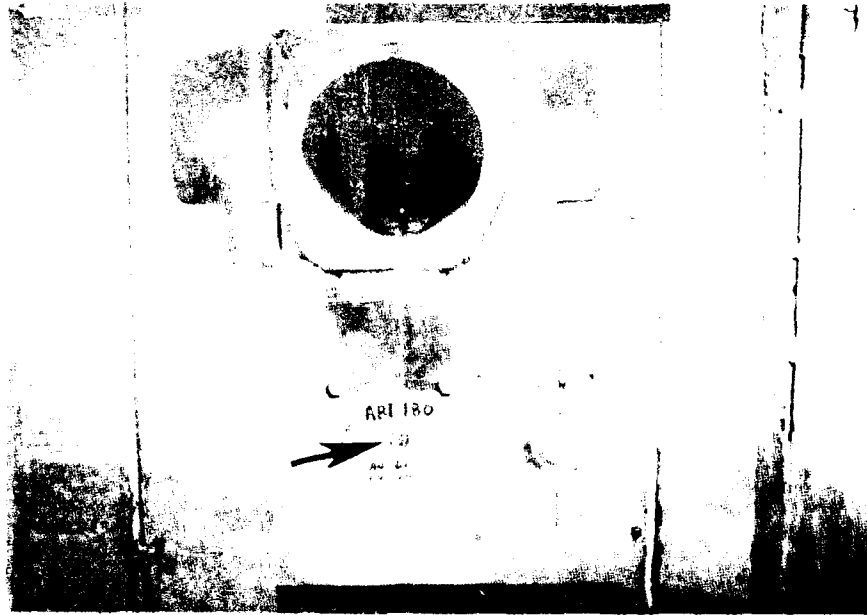


Figure 5. Chamber pressure gage mount (ABI180) directly below vent pipe. Note: accelerometer mounting bracket (lower right) was left over from MISERS GOLD EVENT.



Figure 6. Water filled cylinder with five pressure gages. Note pipe with 90° elbow connecting cylinder to interior of horn antenna bunker.

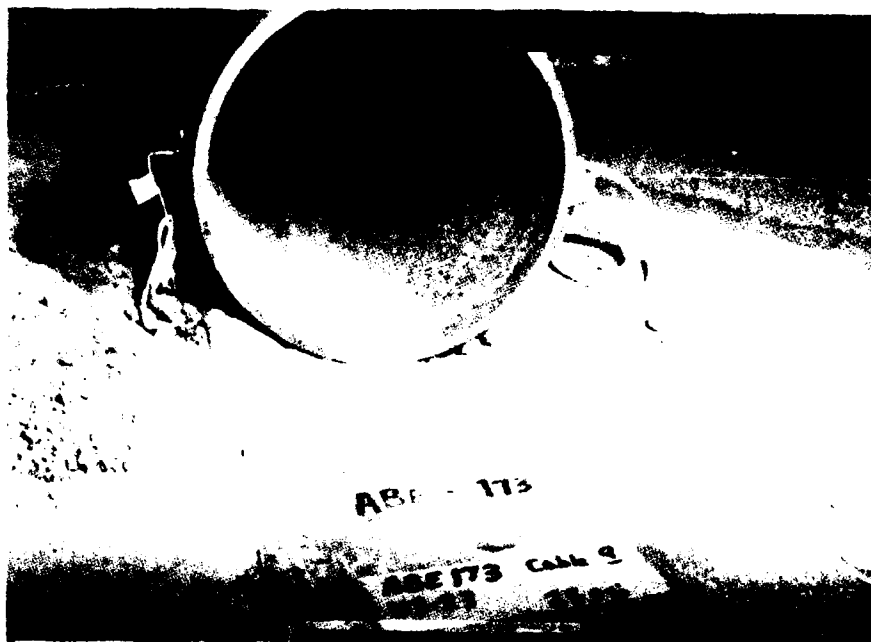
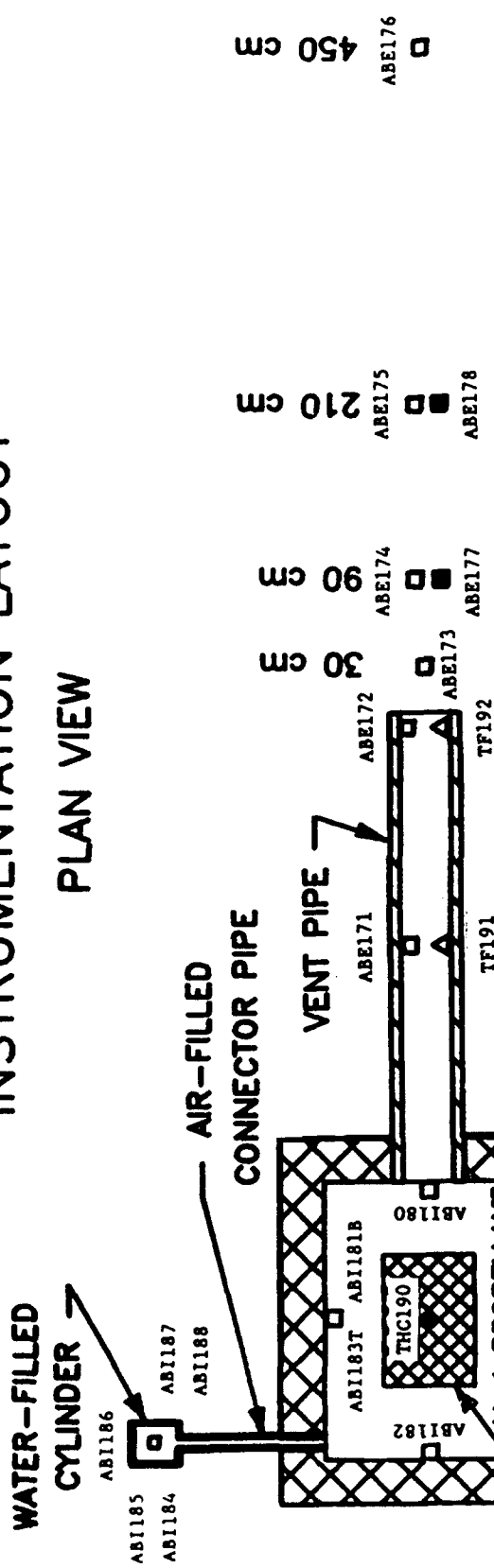


Figure 7. Vent pipe with one free-field, side-on overpressure gage (ABE173). Cables are seen for two internal vent pipe transducers; thermal flux gage (TF192, left) and side-on overpressure gage (ABE172).

INSTRUMENTATION LAYOUT

PLAN VIEW



LEGEND

- OVERPRESSURE
- TOTAL PRESSURE
- △ THERMAL FLUX
- THERMOCOUPLE

HORN ANTENNA BUNKER

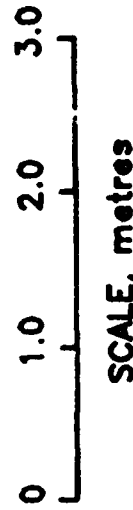


Figure 8. Instrumentation layout (plan view) showing internal and external transducer locations. Five pressure gages were attached to the water filled cylinder which was connected to the chamber via the air-filled pipe (upper left corner of drawing).



Figure 9. Recording bunker protecting digital recording system. A shallow cable ditch can be seen running (left to center background) from the recording bunker to the horn antenna bunker.

EXTERNAL INSTRUMENTATION AND PHOTO MARKER LOCATIONS PLAN VIEW

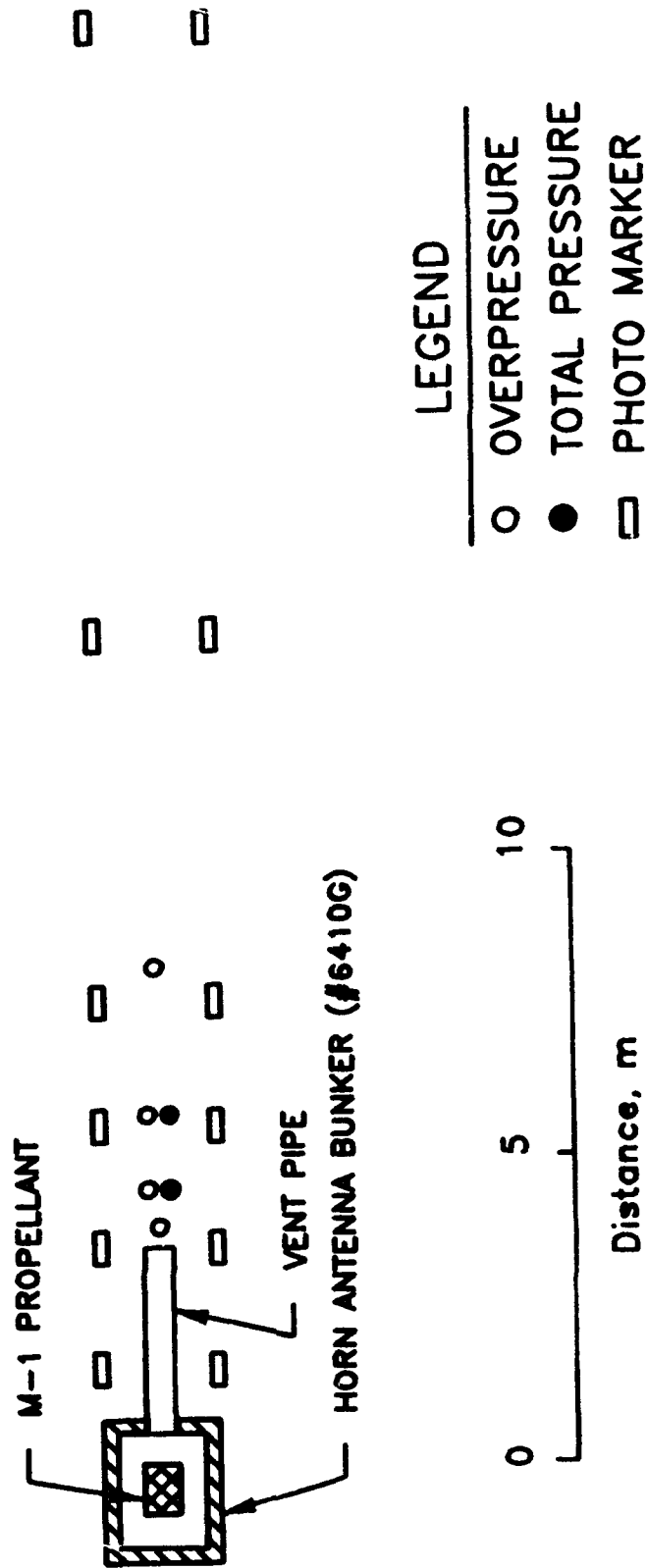


Figure 10. Plan view of external airblast instrumentation and photo marker locations.

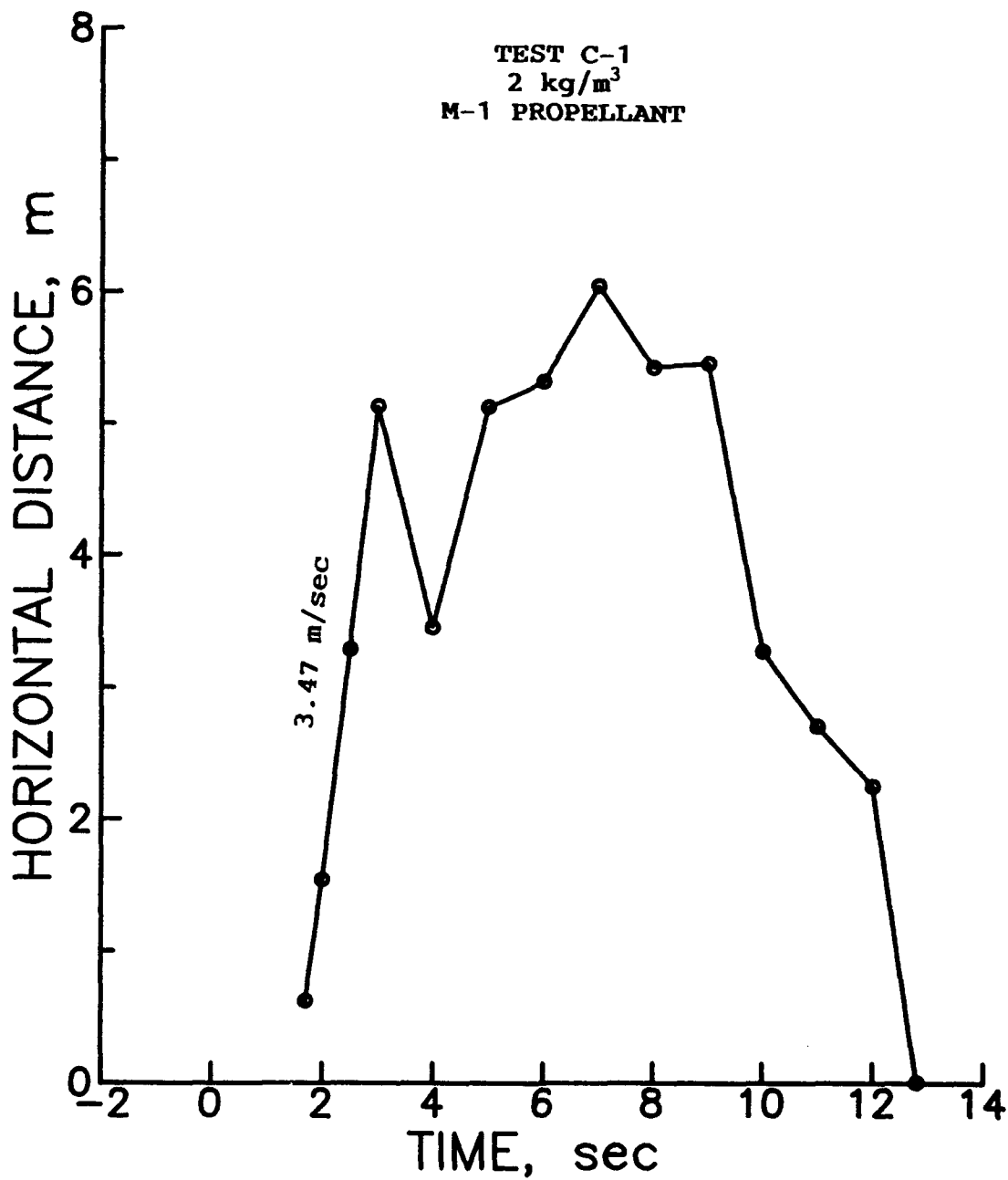


Figure 11. Test C-1: length of exhaust gas plume (from end of vent pipe) as a function of relative time. Zero-time was not recorded, so all times are relative to an arbitrarily chosen start time.

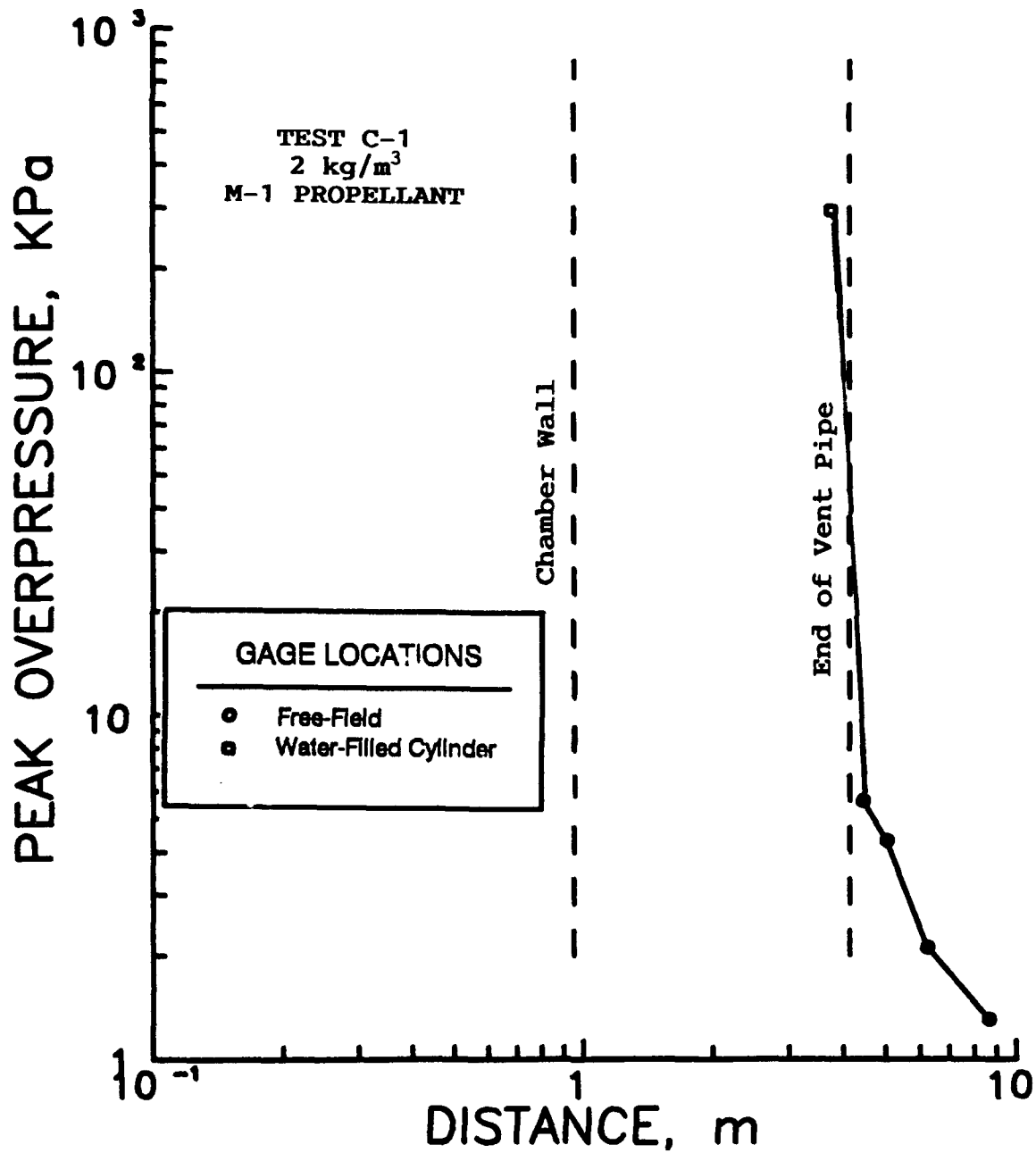


Figure 12. Test C-1: measured peak pressures as a function of distance from the center of the 10-kg M-1 propellant charge.

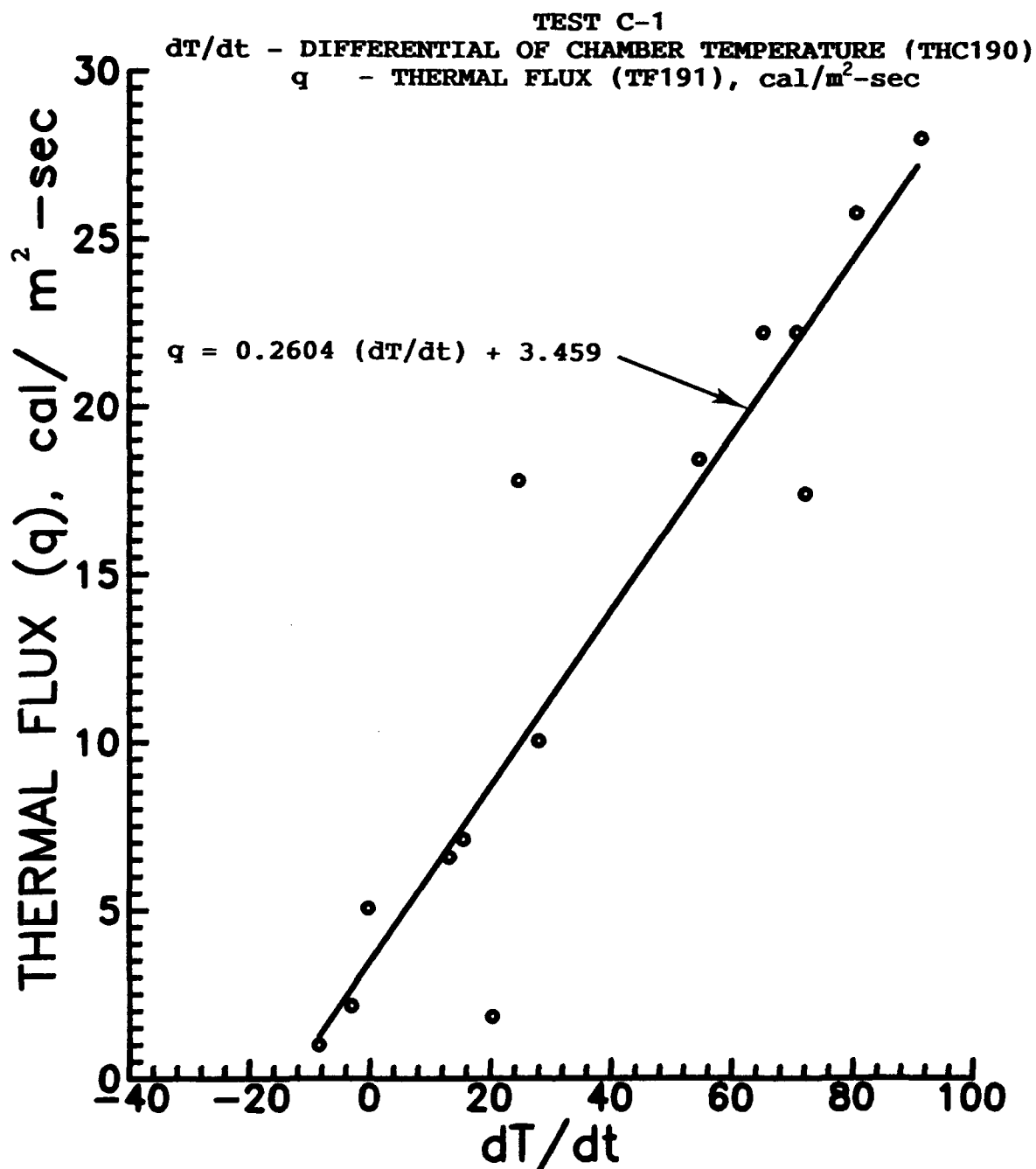


Figure 13. Test C-1: thermal flux at mid-length in the vent pipe (Gage TF191) versus the differential of measured temperature (Gage THC190) with respect to time. Each data point represents a "pair" of values; an x-value from a given dT/dt , and a y-value from the thermal flux record corresponding to the same time instant (after zero time) as the dT/dt value.

TEST C-1 THERMAL FLUX

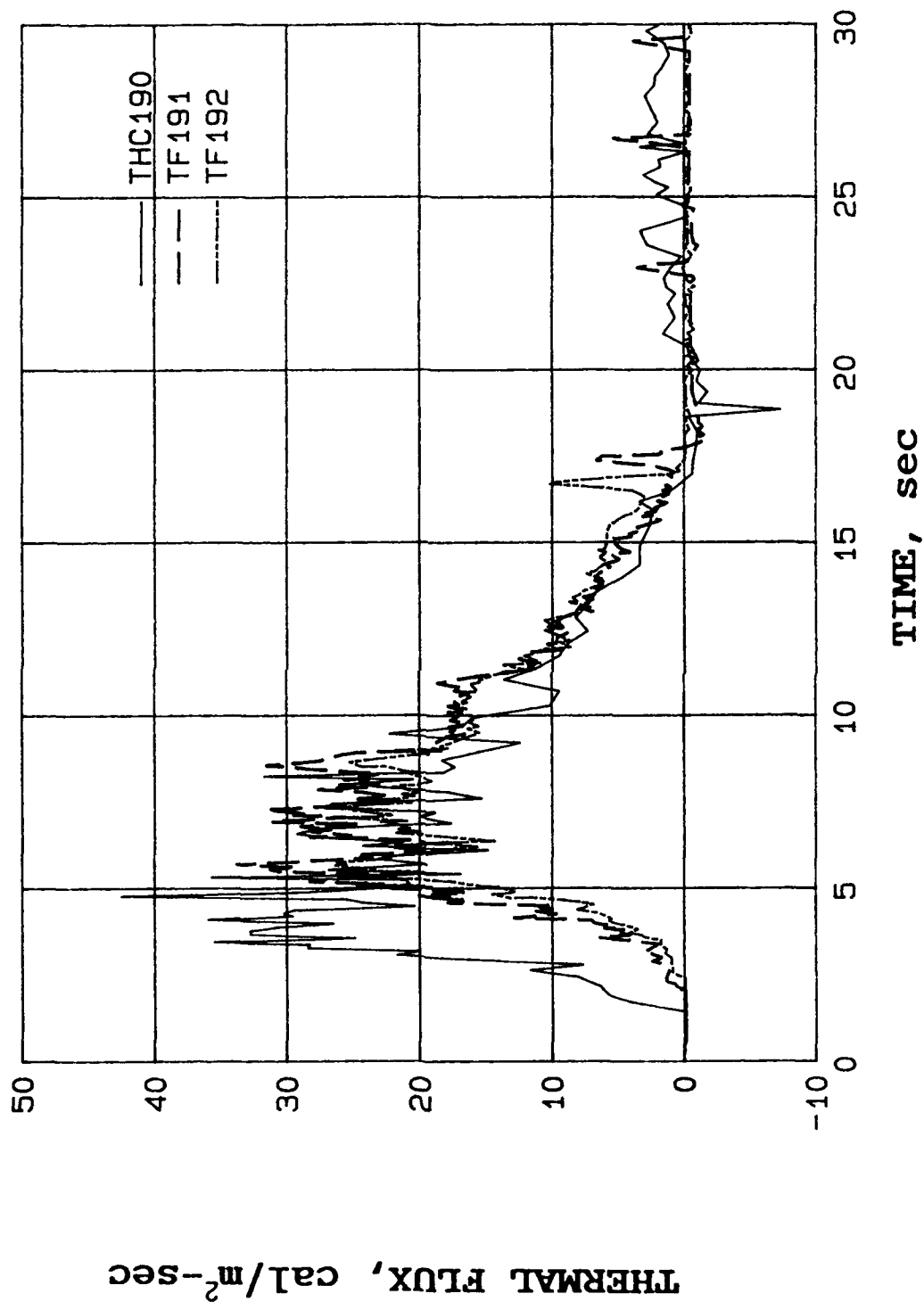


Figure 14. Test C-1: calculated pseudo-thermal flux (from temperature measurements of Gage (THC190) in the bunker chamber compared to measured thermal flux-time histories in the vent pipe (Gages TF191 and TF192).

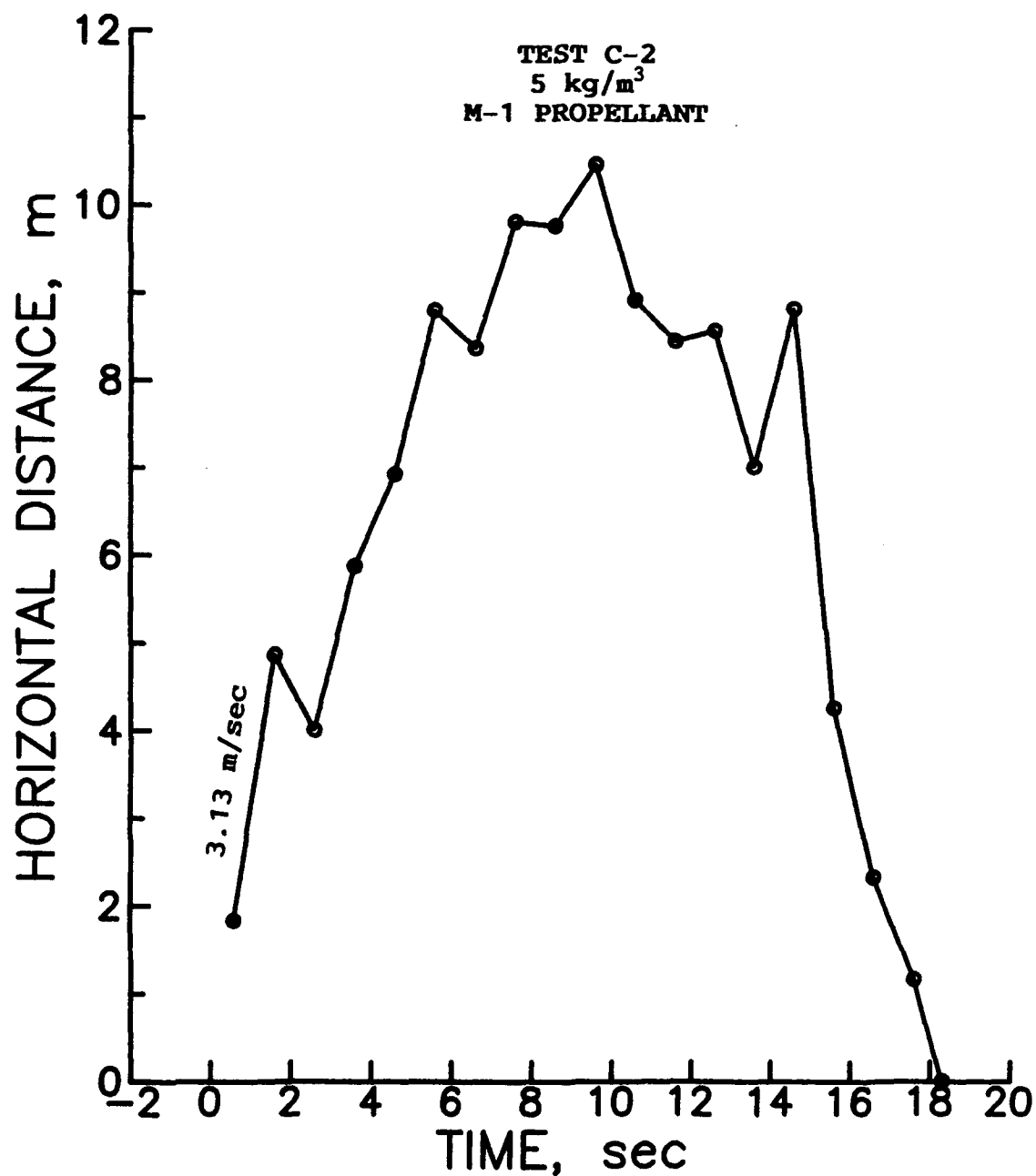


Figure 15. Test C-2: length of exhaust gas plume (from end of vent pipe) as a function of relative time. Zero-time was not recorded, so all times are relative to an arbitrarily chosen start time.

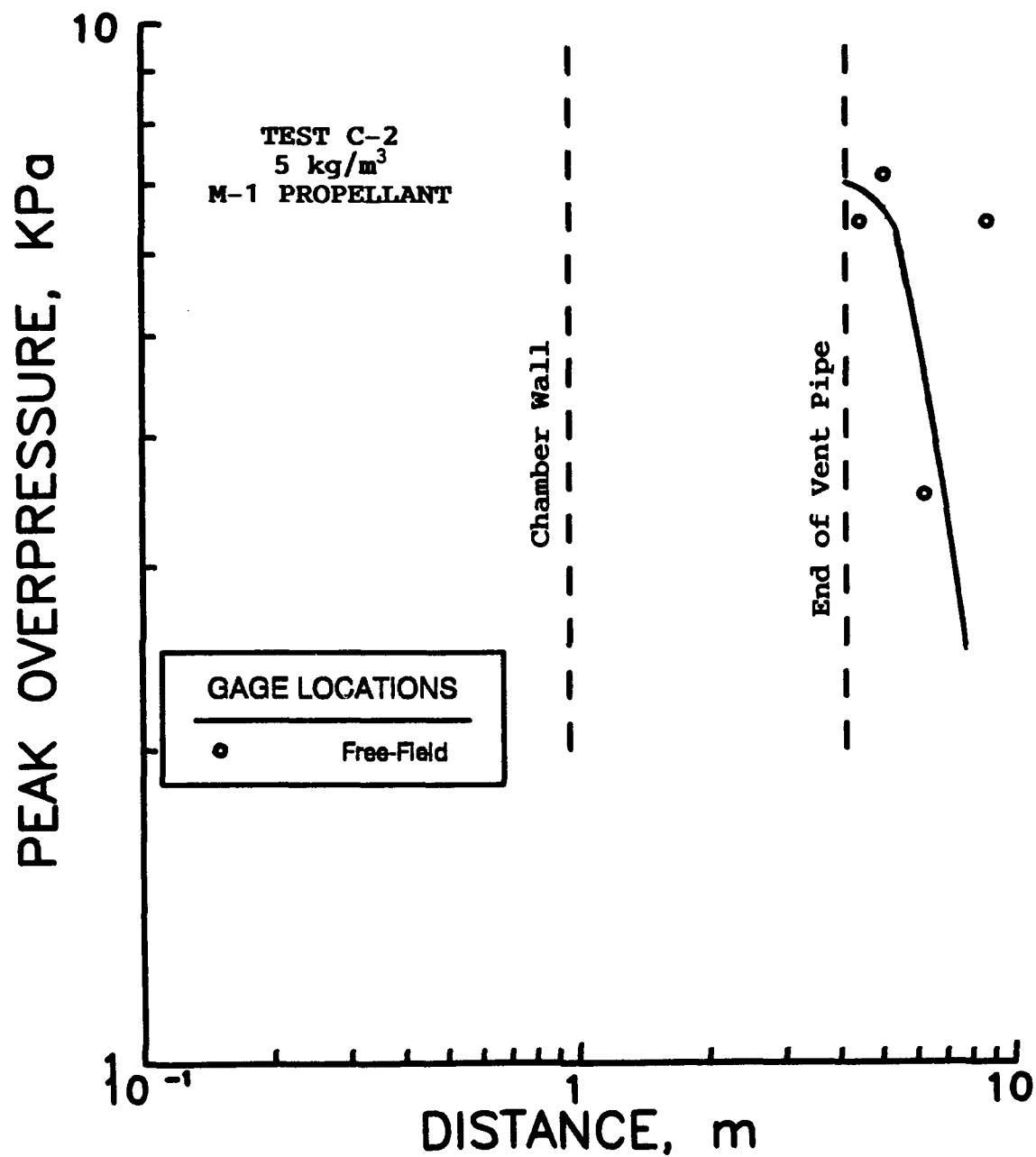


Figure 16. Test C-2: measured peak pressures as a function of distance from the center of the 25-kg M-1 propellant charge.

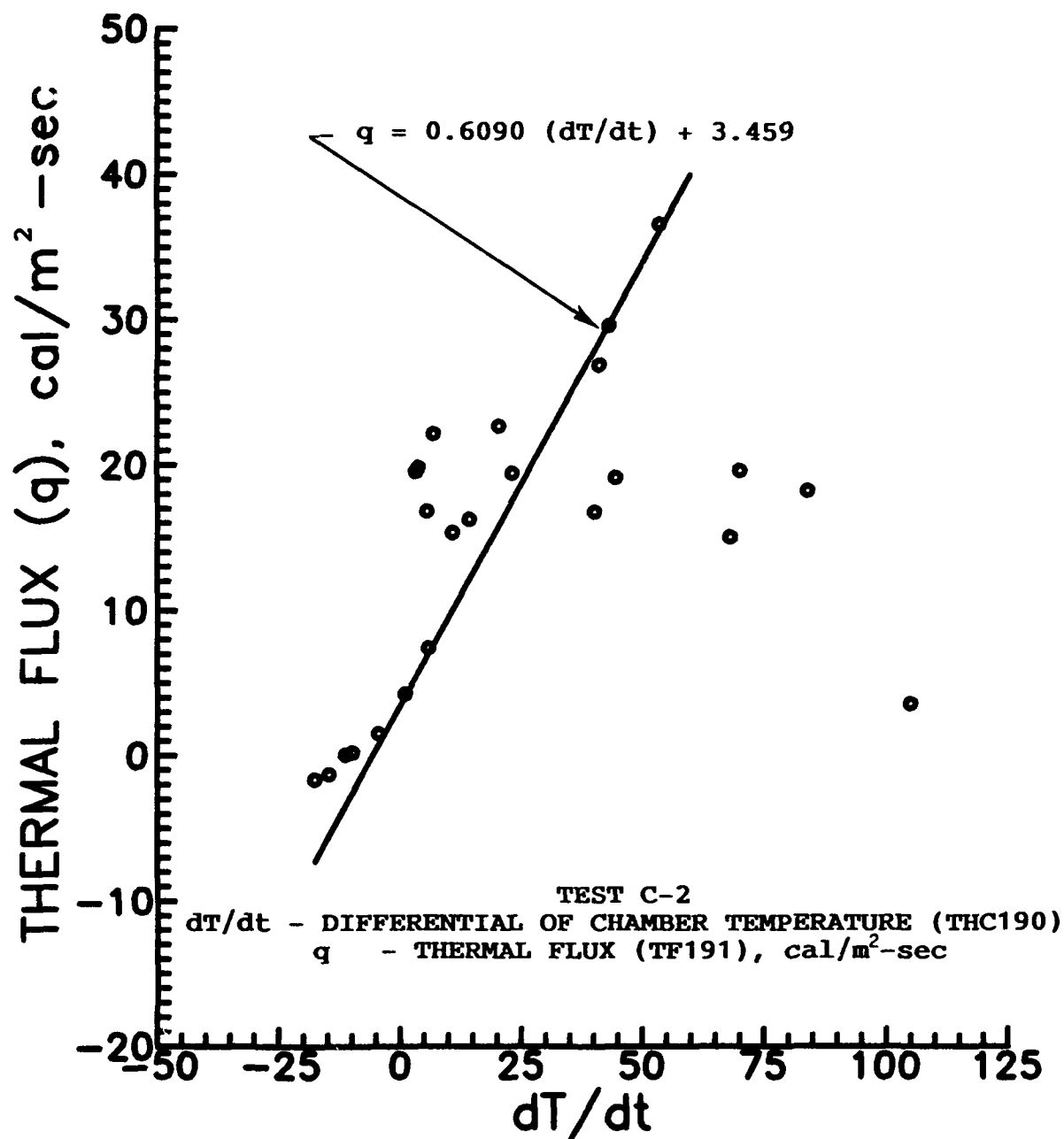


Figure 17. Test C-2: thermal flux at mid-length in the vent pipe (Gage TF191) versus the differential of measured temperature (Gage THC190) with respect to time. Each data point represents a "pair" of values; an x-value from a given dT/dt , and a y-value from the thermal flux record corresponding to the same time instant (after zero time) as the dT/dt value.

TEST C-2 THERMAL FLUX

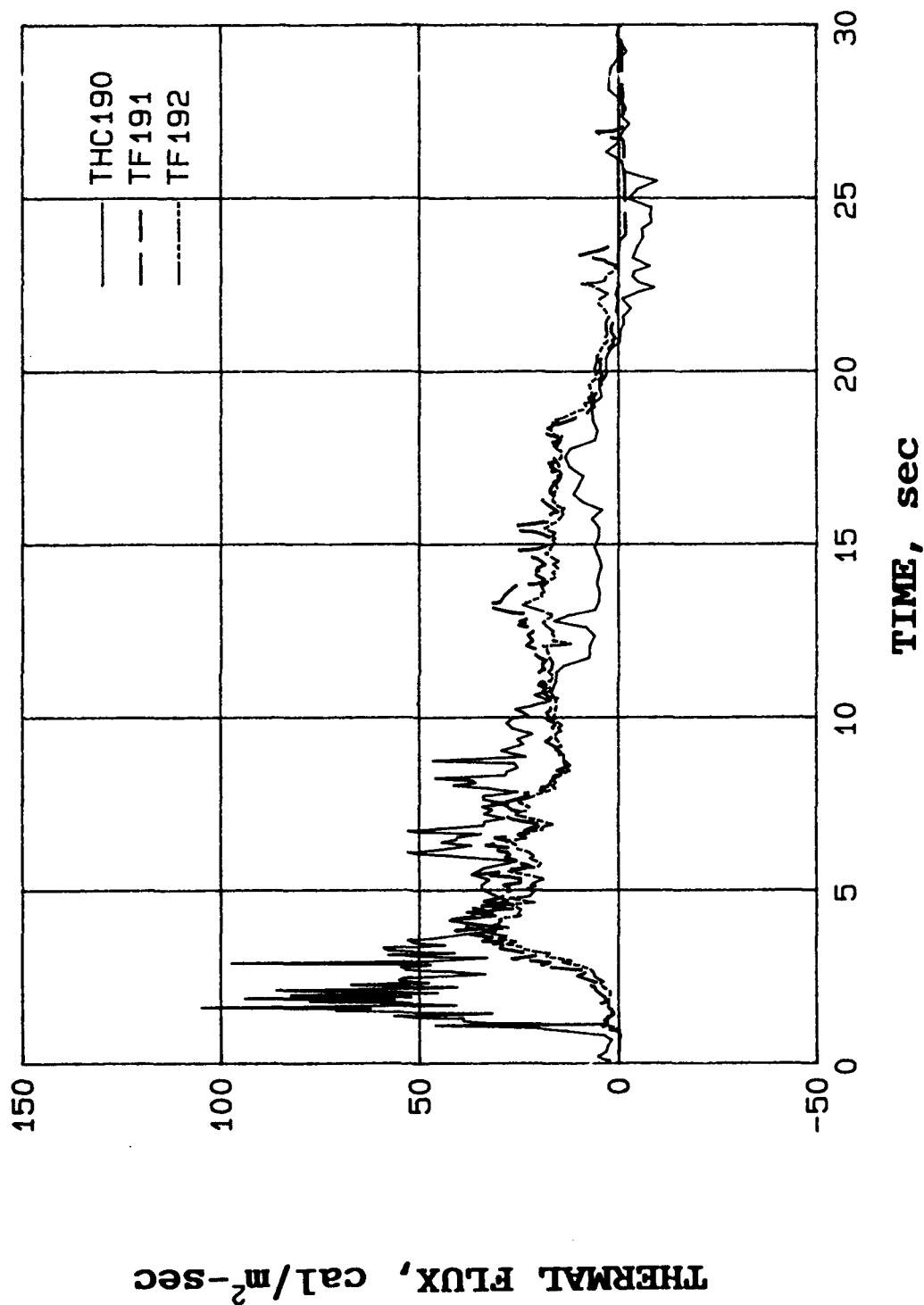


Figure 18. Test C-2: calculated pseudo-thermal flux (from temperature measurements of Gage (THC190) in the bunker chamber compared to measured thermal flux-time histories in the vent pipe (Gages TF191 and TF192).

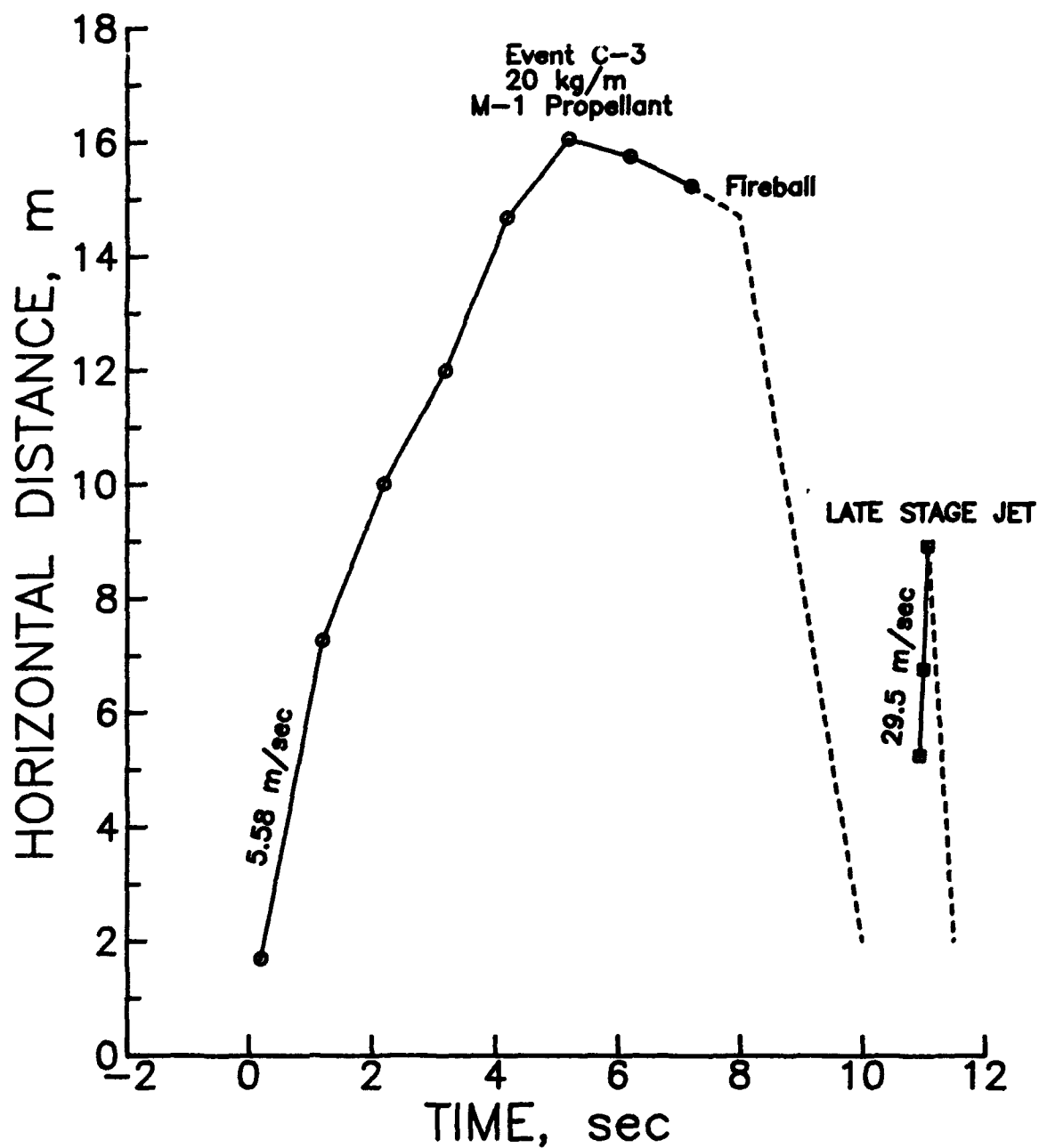


Figure 19. Test C-3: length of exhaust gas plume (from end of vent pipe) as a function of relative time. Zero-time was not recorded, so all times are relative to an arbitrarily chosen start time.

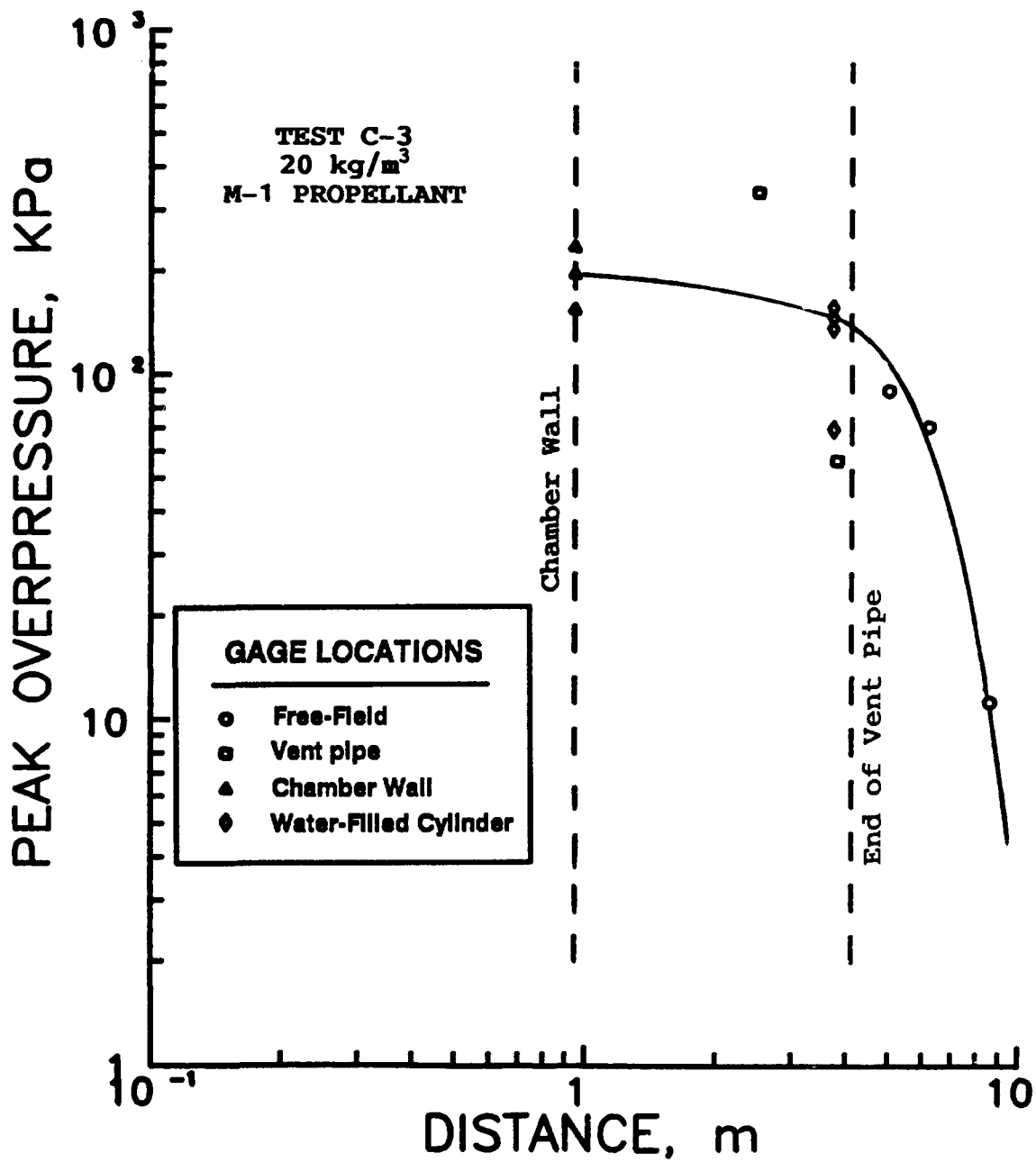


Figure 20. Test C-3: measured peak pressures as a function of distance from the center of the 100-kg M-1 propellant charge.

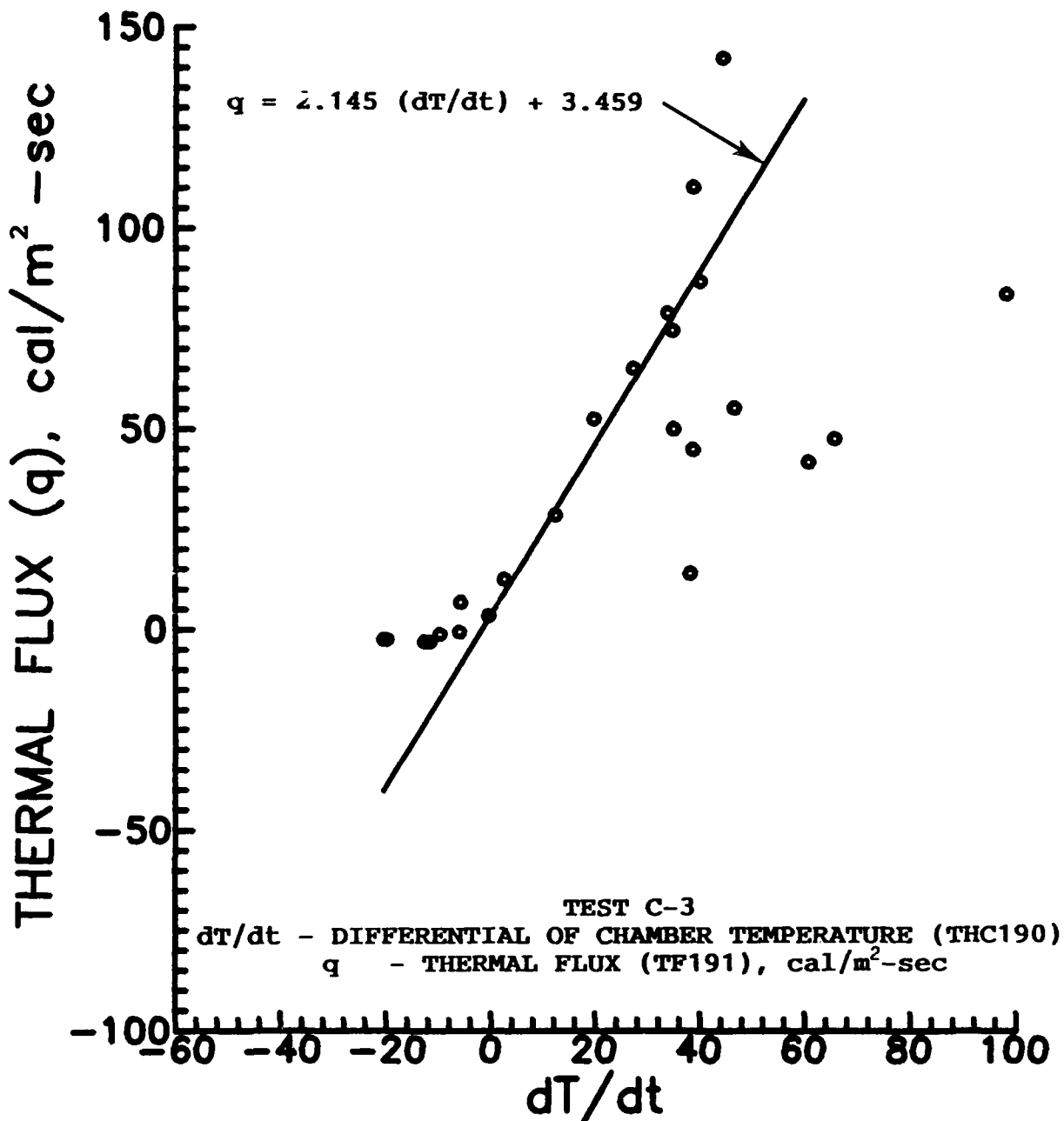


Figure 21. Test C-3: thermal flux at mid-length in the vent pipe (Gage TF191) versus the differential of measured temperature (Gage THC190) with respect to time. Each data point represents a "pair" of values; an x-value from a given $\frac{dT}{dt}$, and a y-value from the thermal flux record corresponding to the same time instant (after zero time) as the $\frac{dT}{dt}$ value.

TEST C-3 THERMAL FLUX

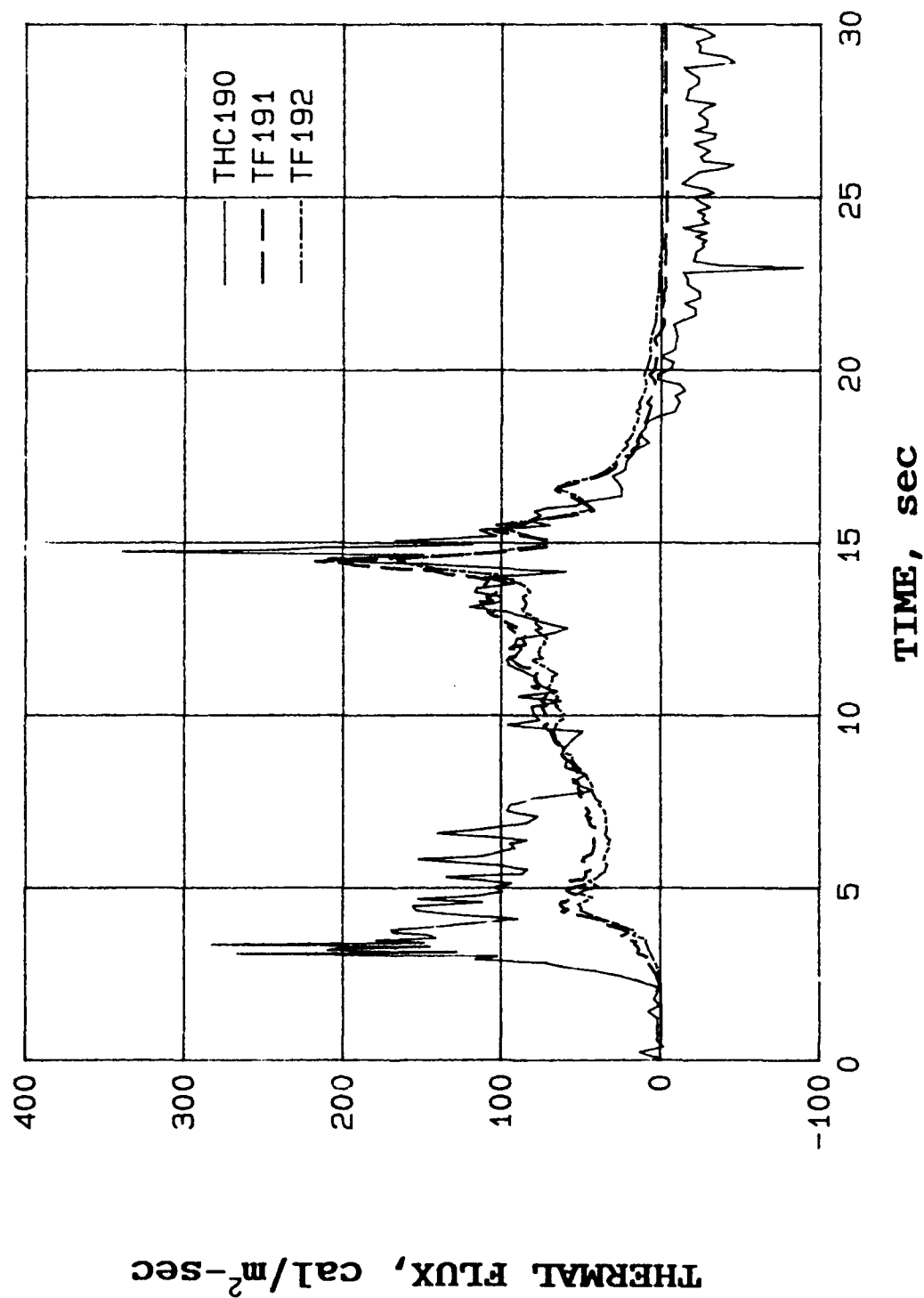


Figure 22. Test C-3: calculated pseudo-thermal flux (from temperature measurement of Gage THC190) in the bunker chamber compared to measured thermal flux-time histories in the vent pipe (Gages TF191 and TF192).

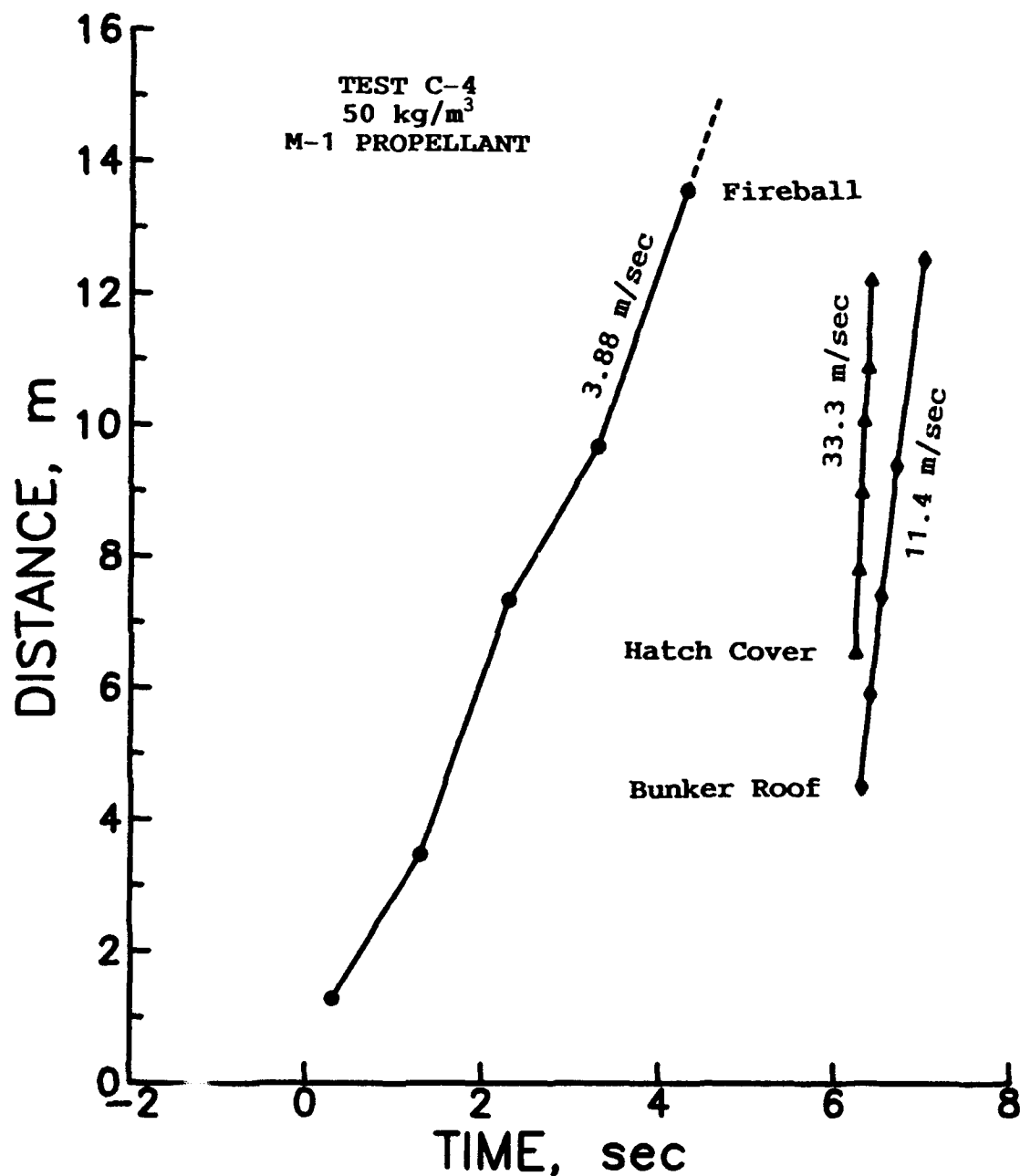


Figure 23. Test C-4: length of exhaust gas plume (from end of vent pipe) as a function of relative time. Zero-time was not recorded, so all times are relative to an arbitrarily chosen start time.

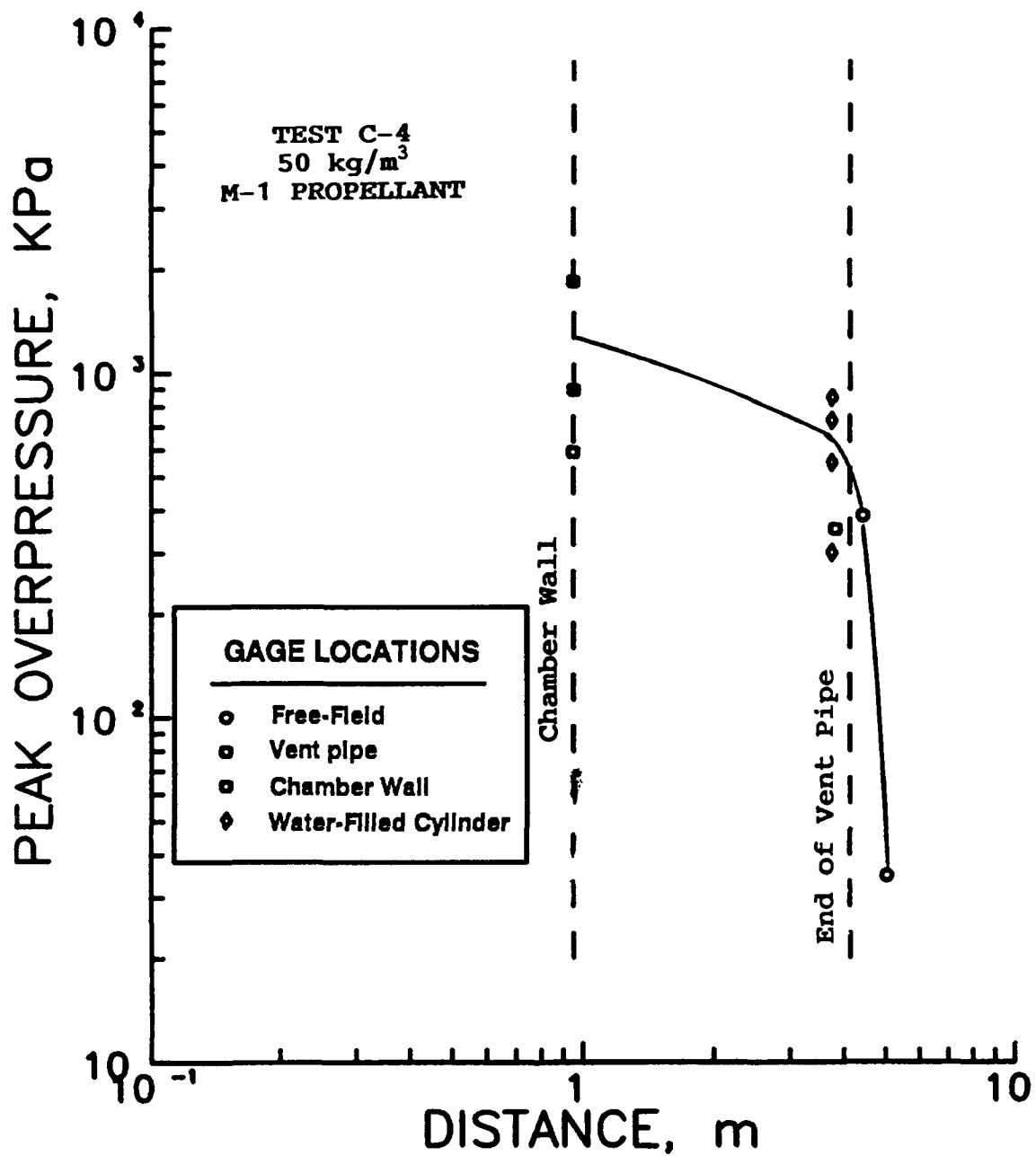


Figure 24. Test C-4: measured peak pressures as a function of distance from the center of the 250-kg M-1 propellant charge.

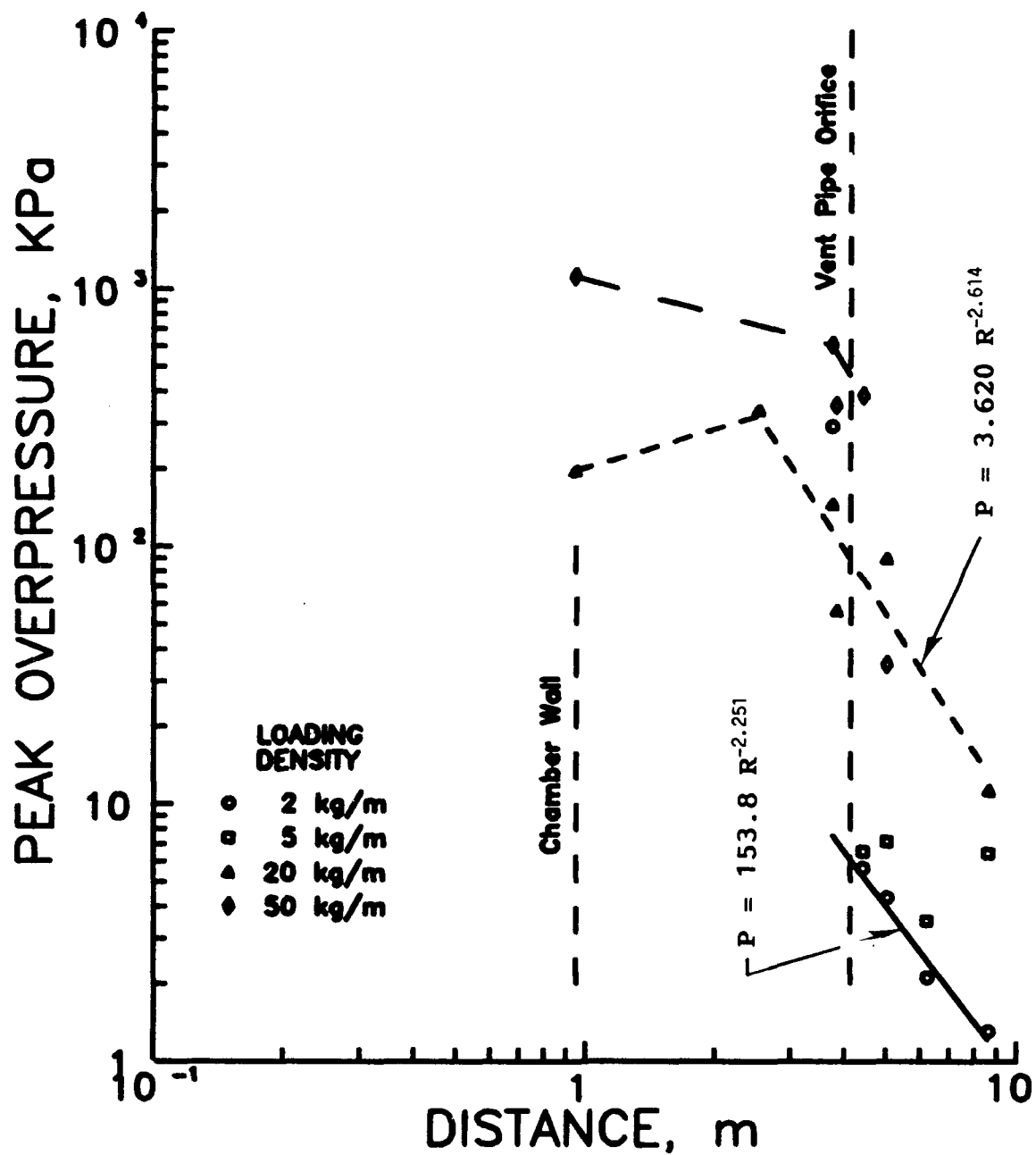


Figure 25. Peak overpressure versus distance from the center of the M-1 propellant charge, KA-III, Phase C.

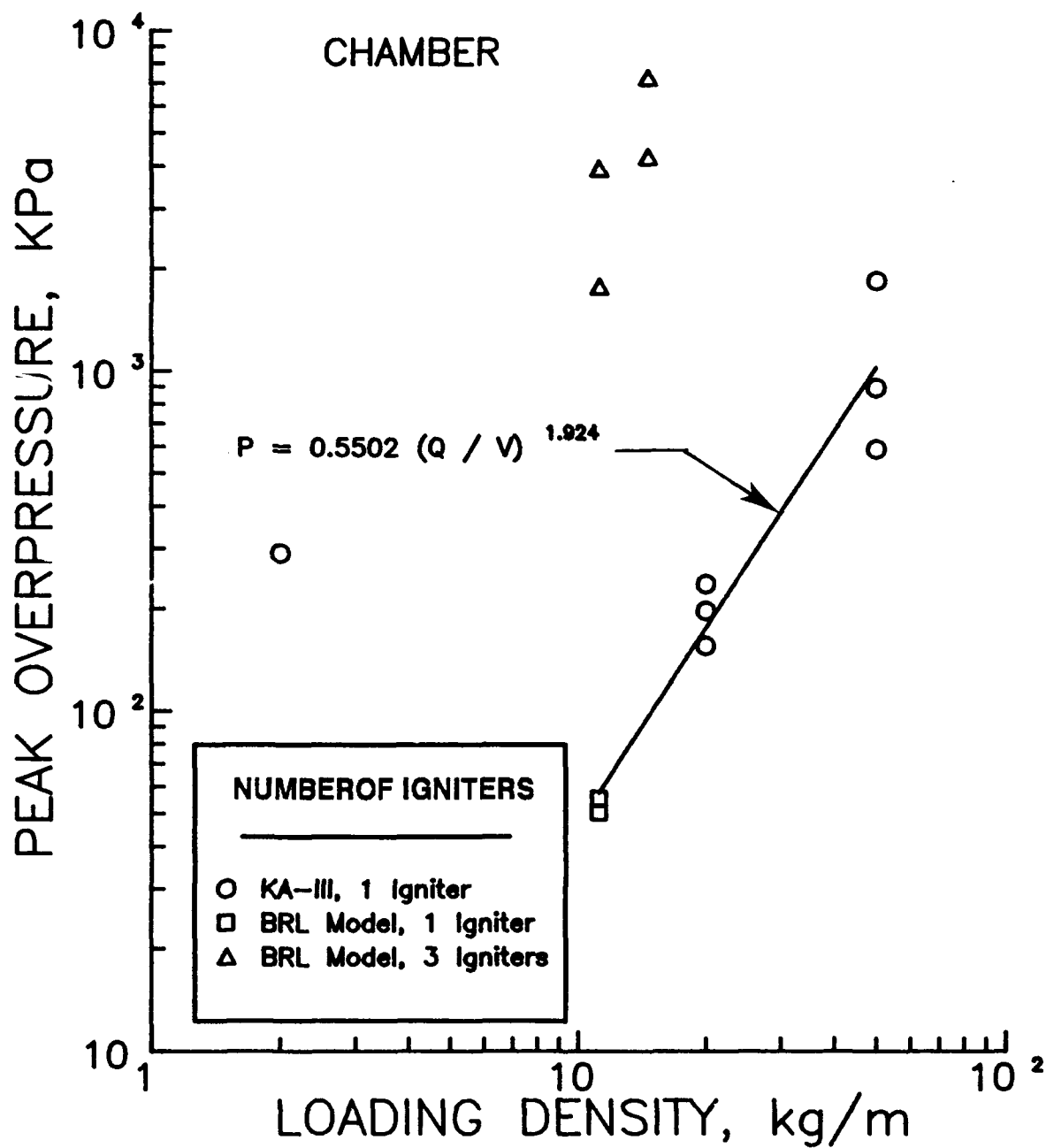


Figure 26. Peak chamber pressure versus M-1 propellant loading density, KA-III, Phase C; comparison with previous data from BRL tests with one and three ignition points of propellant charge.

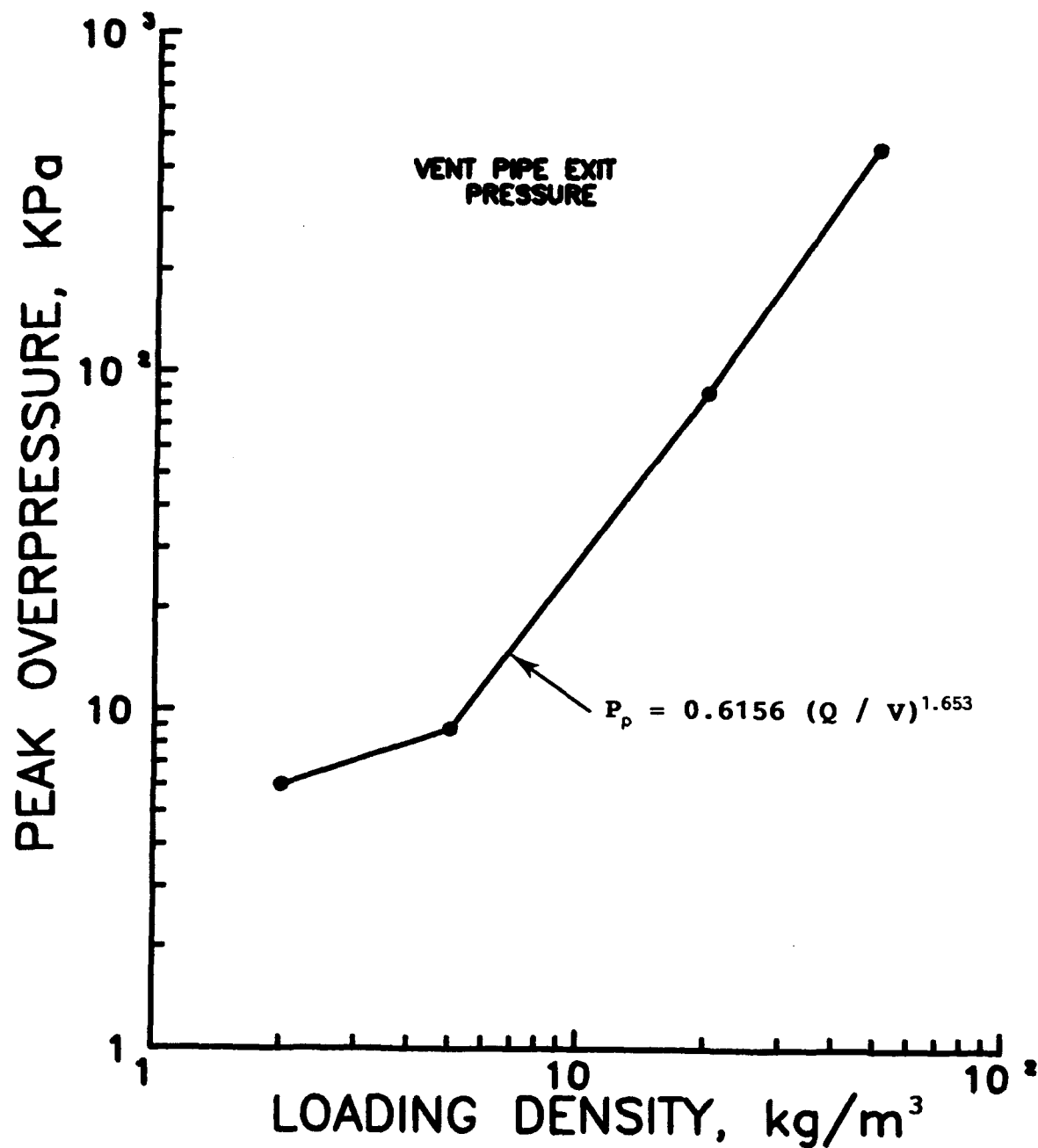


Figure 27. Peak overpressure at end of vent pipe versus chamber loading density; KA-III, Phase C.

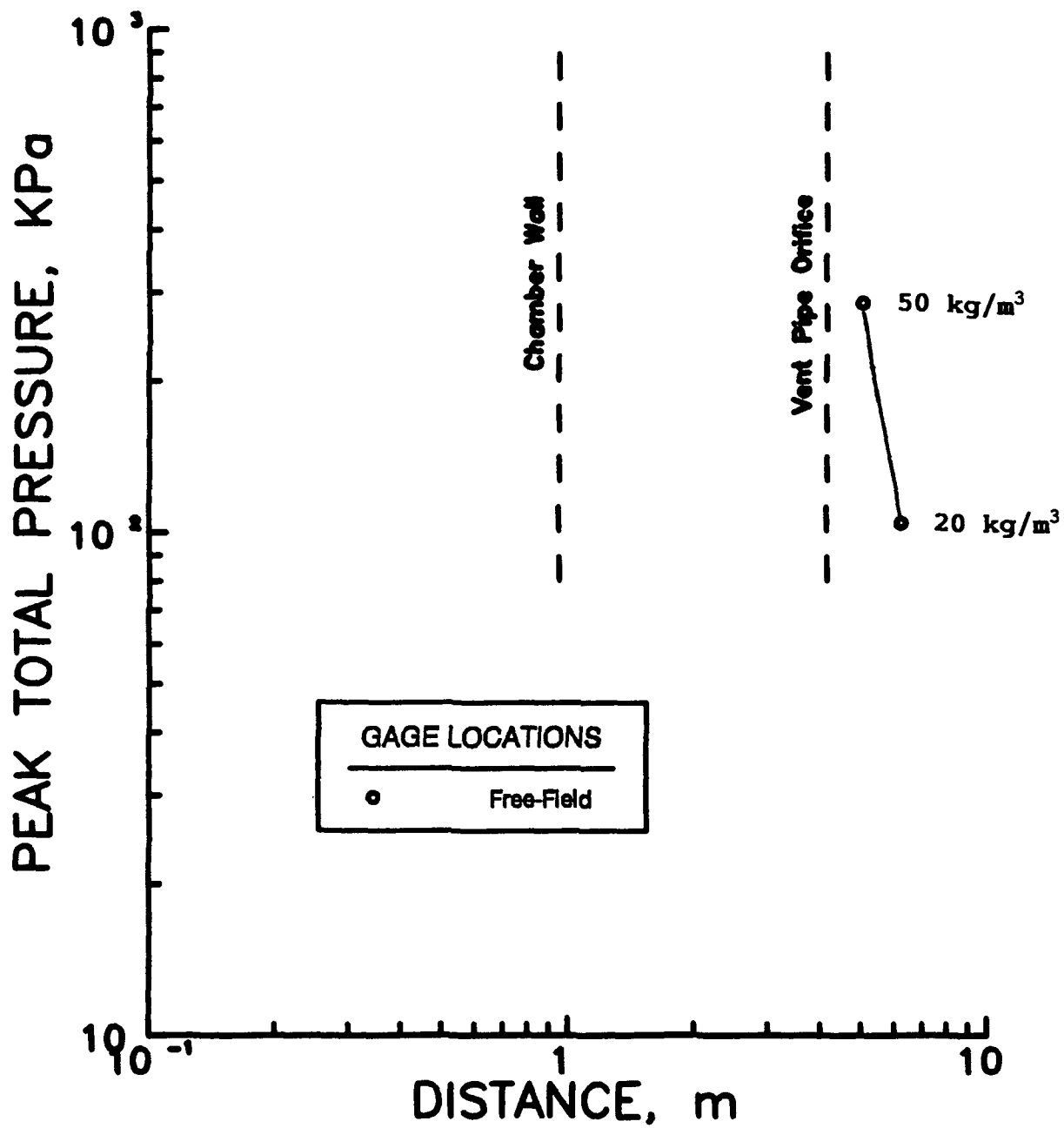


Figure 28. Peak total free-field pressure versus distance from the center of the M-1 propellant charge, KA-III, Phase C.

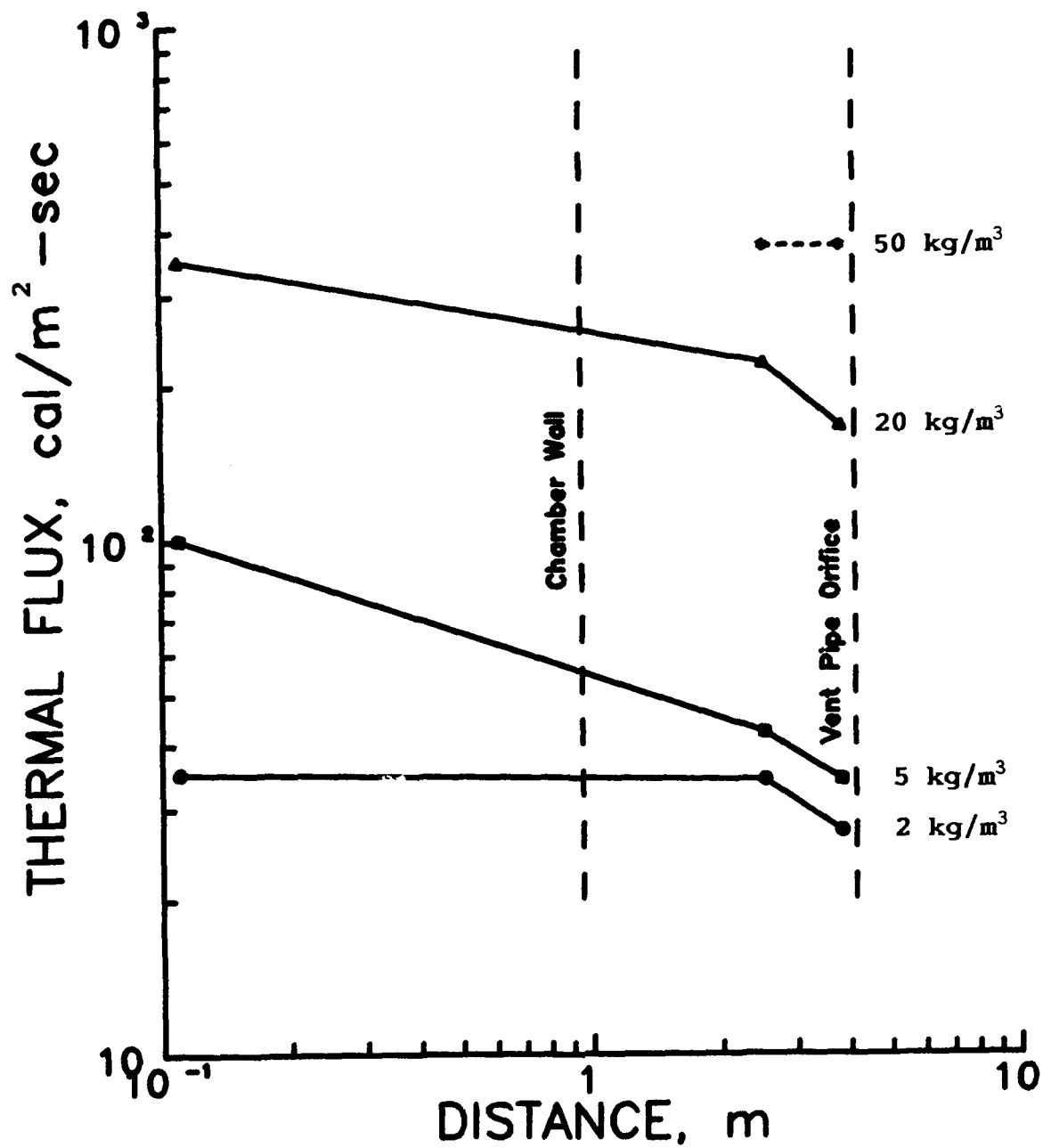


Figure 29. Peak thermal flux versus distance from the center of the M-1 propellant charge; KA-III, Phase C. Note: chamber thermal flux data are calculated from thermocouple measurements.

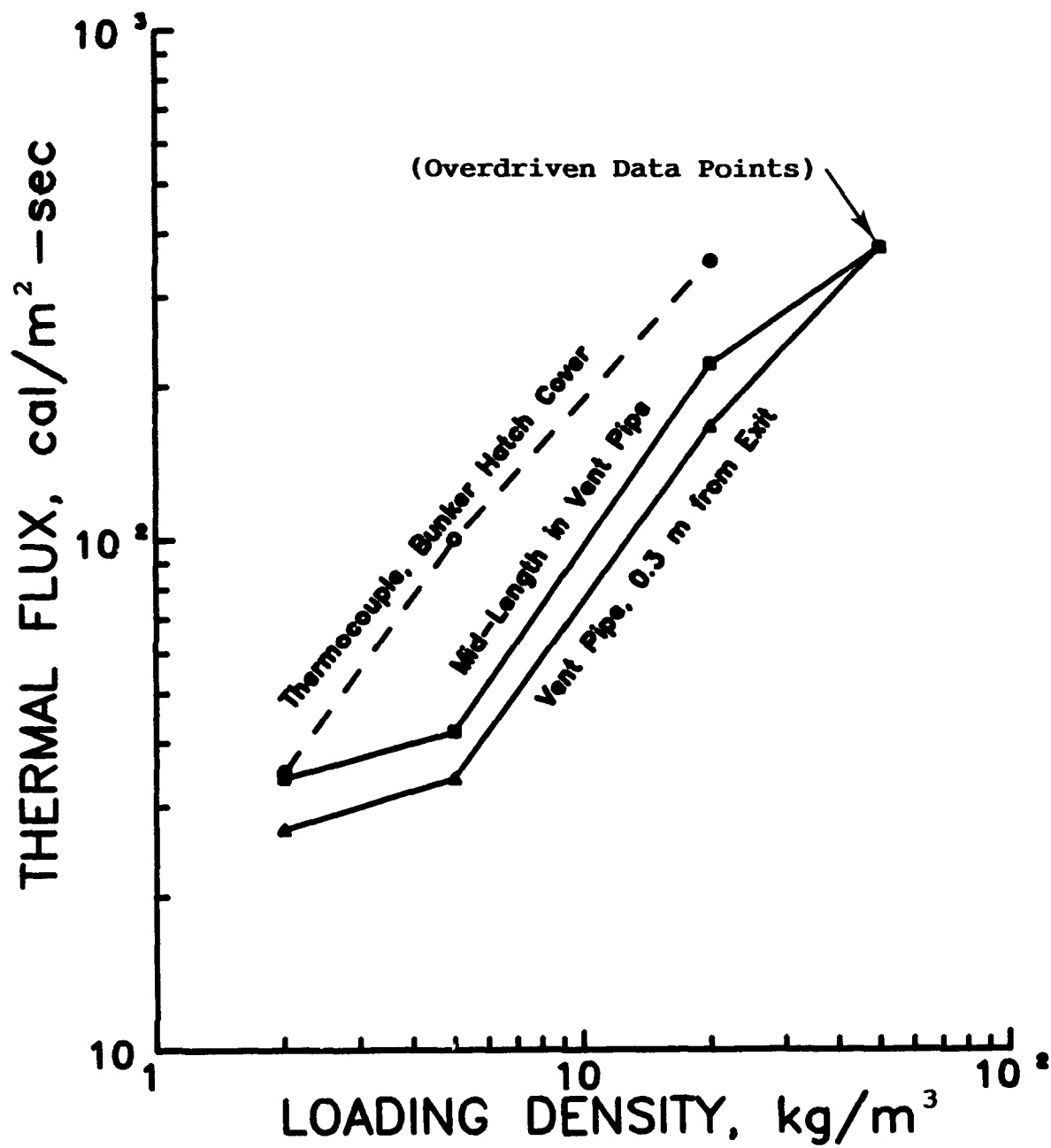


Figure 30. Peak thermal flux versus M-1 propellant loading density, KA-III, Phase C.

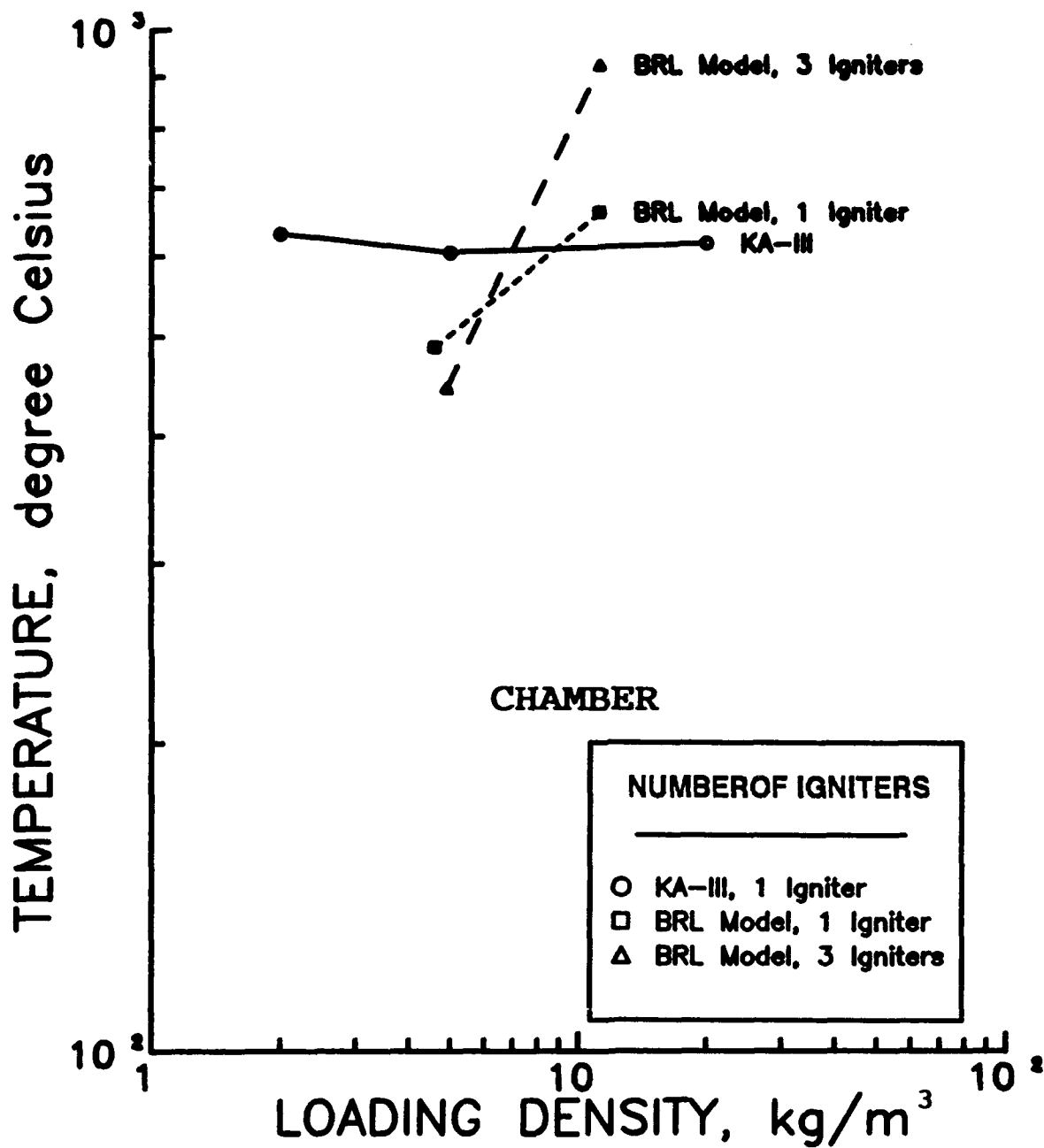


Figure 31. Peak chamber temperature versus loading density, KA-III, Phase C; comparison with previous data from BRL model test with one and three ignition points of propellant charge.

Table 1 KA III, Phase C: Configuration Parameters for M-1 Propellant Charges

<u>Test</u>	<u>Charge Weight (kg)</u>	<u>Charge Surface Area (m²)</u>	<u>Charge Volume (m³)</u>	<u>Surface Area To Volume Ratio (m⁻¹)</u>
C-1	10	0.1334	0.01771	7.796
C-2	25	0.1334	0.04277	3.118
C-3	100	0.5335	0.1771	3.118
C-4	250	1.95*	0.4277	4.547

*Estimated

Table 2 Test C-1 (Loading Density 2 kg/m³): Pre-Test Gage Location and Digital System Set-up Data.

Designation	Transducer			Measurement Type	Digital Channel Set-Up	
	Model	Sensitivity	Location		Predicted Full-Scale	Excitation Voltage Volts
ABE171	XT-190-100	139 mv/MPa	Vent Tube, 1.6 m from Portal	Side-on Pressure	276 kPa	10
ABE172	XT-190-100	181 mv/MPa	Vent Tube, 0.3 m from Portal	Side-on Pressure	138 kPa	10
ABE173	XT-190-25	423 mv/MPa	Free-Field, 0.3 m from Portal	Side-on Pressure	138 kPa	10
ABE174	XT-190-25	615 mv/MPa	Free-Field, 0.9 m from Portal	Side-on Pressure	48.3 kPa	10
ABE175	XT-190-10	930 mv/MPa	Free-Field, 2.1 m from Portal	Side-on Pressure	13.8 kPa	10
ABE176	XT-190-5	1577 mv/MPa	Free-Field, 4.5 m from Portal	Side-on Pressure	6.89 kPa	10
ABE177	HKS-500	54.1 mv/MPa	Free-Field, 0.9 m from Portal	Total Pressure	1380. kPa	10
ABE178	HKS-500	54.5 mv/MPa	Free-Field, 2.1 m from Portal	Total Pressure	689. kPa	10
ABI180	XT-190-200	77.5 mv/MPa	Front Wall of Chamber	Chamber Pressure	965. kPa	10
ABI181B	XT-190-200	85.7 mv/MPa	Right Wall of Chamber (1/3 Height)	Chamber Pressure	965. kPa	10
ABI182	XT-190-200	94.4 mv/MPa	Back Wall of Chamber	Chamber Pressure	965. kPa	10
ABI183T	XT-190-200	94.9 mv/MPa	Right Wall of Chamber (2/3 Height)	Chamber Pressure	1380. kPa	10
ABI184	XT-190-50	303 mv/MPa	Water Filled Cylinder	Chamber Pressure	345. kPa	10
ABI185	XT-190-100	173 mv/MPa	Water Filled Cylinder	Chamber Pressure	689. kPa	10
ABI186	HKS-500	24.5 mv/MPa	Water Filled Cylinder	Chamber Pressure	3450. kPa	5
ABI187	HKS-1000	2.18 mv/MPa	Water Filled Cylinder	Chamber Pressure	6890. kPa	5
ABI188	HKS-5000	0.728 mv/MPa	Water Filled Cylinder	Chamber Pressure	34.5 kPa	5
THC190	K	0.040 mv/°C	Chamber Hatch Cover	Chamber Temperature	1000°C	1
TF191	64-250SB-17	0.461 mv/[cal/m ² -sec]	Vent Tube, 1.6 m from Portal	Thermal Flux	36.6 cal/m ² -sec	10
TF192	64-250SB-17	0.461 mv/[cal/m ² -sec]	Vent Tube, 0.3 m from Portal	Thermal Flux	36.6 cal/m ² -sec	10

Table 3 Test C-2 (Loading Density 5 kg/m³): Pre-Test Gage Location and Digital System Set-up Data.

Designation	Model	Sensitivity	Location	Measurement Type	Digital Channel Set-Up	
					Predicted Full-Scale	Excitation Voltage Volts
ABE171	XT-190-100	139 mv/MPa	Vent Tube, 1.6 m from Portal	Side-on Pressure	276 kPa	10
ABE172	XT-190-100	181 mv/MPa	Vent Tube, 0.3 m from Portal	Side-on Pressure	138 kPa	10
ABE173	XT-190-25	423 mv/MPa	Free-Field, 0.3 m from Portal	Side-on Pressure	138 kPa	10
ABE174	XT-190-25	615 mv/MPa	Free-Field, 0.9 m from Portal	Side-on Pressure	48.3 kPa	10
ABE175	XT-190-10	930 mv/MPa	Free-Field, 2.1 m from Portal	Side-on Pressure	13.8 kPa	10
ABE176	XT-190-5	1577 mv/MPa	Free-Field, 4.5 m from Portal	Side-on Pressure	6.89 kPa	10
ABE177	HKS-500	54.1 mv/MPa	Free-Field, 0.9 m from Portal	Total Pressure	1380. kPa	10
ABE178	HKS-500	54.5 mv/MPa	Free-Field, 2.1 m from Portal	Total Pressure	689. kPa	10
ABI180	XT-190-200	77.5 mv/MPa	Front Wall of Chamber	Chamber Pressure	965. kPa	10
ABI181B	XT-190-200	85.7 mv/MPa	Right Wall of Chamber (1/3 Height)	Chamber Pressure	965. kPa	10
ABI182	XT-190-200	94.4 mv/MPa	Back Wall of Chamber	Chamber Pressure	965. kPa	10
ABI183T	XT-190-200	94.9 mv/MPa	Right Wall of Chamber (2/3 Height)	Chamber Pressure	1380. kPa	10
ABI184	XT-190-50	303 mv/MPa	Water Filled Cylinder	Chamber Pressure	345. kPa	10
ABI185	XT-190-100	173 mv/MPa	Water Filled Cylinder	Chamber Pressure	689. kPa	10
ABI186	HKS-500	24.5 mv/MPa	Water Filled Cylinder	Chamber Pressure	3480. kPa	5
ABI187	HKS-1000	2.18 mv/MPa	Water Filled Cylinder	Chamber Pressure	6890. kPa	5
ABI188	HKS-5000	0.728 mv/MPa	Water Filled Cylinder	Chamber Pressure	34.5 kPa	5
THC190	K	0.040 mv/°C	Chamber Hatch Cover	Chamber Temperature	1000°C	1
TF191	64-250SB-17	0.461 mv/[cal/m ² -sec]	Vent Tube, 1.6 m from Portal	Thermal Flux	36.6 cal/m ² -sec	10
TF192	64-250SB-17	0.461 mv/[cal/m ² -sec]	Vent Tube, 0.3 m from Portal	Thermal Flux	36.6 cal/m ² -sec	10

Table 4 Test C-3 (Loading Density 20 kg/m³): Pre-Test Gage Location and Digital System Set-up Data.

Designation	Transducer			Location	Measurement Type	Digital Channel Set-up	
	Model	Sensitivity				Predicted Full-Scale	Excitation Voltage Volts
ABE171	XT-190-100	77.5 mv/MPa		Vent Tube, 1.6 m from Portal	Side-on Pressure	1380 kPa	10
ABE172	XT-190-100	178 mv/MPa		Vent Tube, 0.3 m from Portal	Side-on Pressure	689 kPa	10
ABE173	XT-190-25	423 mv/MPa		Free-field, 0.3 m from Portal	Side-on Pressure	138 kPa	10
ABE174	XT-190-25	615 mv/MPa		Free-field, 0.9 m from Portal	Side-on Pressure	138 kPa	10
ABE175	XT-190-10	930 mv/MPa		Free-field, 2.1 m from Portal	Side-on Pressure	68.9 kPa	10
ABE176	XT-190-5	1577 mv/MPa		Free-field, 4.5 m from Portal	Side-on Pressure	34.5 kPa	10
ABE177	HKS-500	54.1 mv/MPa		Free-field, 0.9 m from Portal	Total Pressure	3450. kPa	10
ABE178	HKS-500	54.5 mv/MPa		Free-field, 2.1 m from Portal	Total Pressure	3450. kPa	10
AB1180	HKS-1000	10.3 mv/MPa		Front Wall of Chamber	Chamber Pressure	6890. kPa	10
AB1181B	XT-190-200	85.7 mv/MPa		Right Wall of Chamber (1/3 Height)	Chamber Pressure	1380. kPa	10
AB1182	HKS-1000	11.6 mv/MPa		Back Wall of Chamber	Chamber Pressure	6890. kPa	10
AB1183T	HKS-1000	10.6 mv/MPa		Right Wall of Chamber (2/3 Height)	Chamber Pressure	6890. kPa	10
AB1184	----	----		----	----	----	--
AB1185	HKS-500	30.2 mv/MPa		Water Filled Cylinder	Chamber Pressure	3450. kPa	10
AB1186	HKS-500	34.1 mv/MPa		Water Filled Cylinder	Chamber Pressure	3450. kPa	5
AB1187	HKS-1000	19.3 mv/MPa		Water Filled Cylinder	Chamber Pressure	6890. kPa	5
AB1188	HKS-5000	9.67 mv/MPa		Water Filled Cylinder	Chamber Pressure	6890. kPa	5
THC190	K	0.040 mv/°C		Chamber Hatch Cover	Chamber Temperature	1000°C	1
TF191	64-250S8-17	0.461 mv/[cal/m ² -sec]		Vent Tube, 1.6 m from Portal	Thermal Flux	36.6 cal/m ² -sec	10
TF192	64-250S8-17	0.461 mv/[cal/m ² -sec]		Vent Tube, 0.3 m from Portal	Thermal Flux	36.6 cal/m ² -sec	10

Table 5 Test C-4 (Loading Density 50 kg/m³): Pre-Test Gage Location and Digital System Set-up Data.

Designation	Transducer			Measurement Type	Digital Channel Set-Up	
	Model	Sensitivity	Location		Predicted Full-Scale	Excitation Voltage Volts
ABE171	XT-190-200	77.5 mv/MPa	Vent Tube, 1.6 m from Portal	Side-on Pressure	1380 kPa	10
ABE172	XT-190-100	181. mv/MPa	Vent Tube, 0.3 m from Portal	Side-on Pressure	689 kPa	10
ABE173	XT-190-200	94.9 mv/MPa	Free-Field, 0.3 m from Portal	Side-on Pressure	1380 kPa	10
ABE174	XT-190-100	142. mv/MPa	Free-Field, 0.9 m from Portal	Side-on Pressure	689 kPa	10
ABE175	XT-190-25	560. mv/MPa	Free-Field, 2.1 m from Portal	Side-on Pressure	172 kPa	10
ABE176	XT-190-10	930. mv/MPa	Free-Field, 4.5 m from Portal	Side-on Pressure	68.9 kPa	10
ABE177	HKS-1000	10.0 mv/MPa	Free-Field, 0.9 m from Portal	Total Pressure	6890. kPa	10
ABE178	HKS-500	54.1 mv/MPa	Free-Field, 2.1 m from Portal	Total Pressure	3450. kPa	10
AB1180	HKS-1000	10.3 mv/MPa	Front Wall of Chamber	Chamber Pressure	6890. kPa	10
AB1181B	HKS-500	49.0 mv/MPa	Right Wall of Chamber (1/3 Height)	Chamber Pressure	3450. kPa	10
AB1182	HKS-500	45.4 mv/MPa	Back Wall of Chamber	Chamber Pressure	6890. kPa	10
AB1183T	HKS-1000	11.5 mv/MPa	Right Wall of Chamber (2/3 Height)	Chamber Pressure	6890. kPa	10
AB1184	----	----	----	----	----	--
AB1185	HKS-500	31.5 mv/MPa	Water Filled Cylinder	Chamber Pressure	3450. kPa	10
AB1186	HKS-500	34.1 mv/MPa	Water Filled Cylinder	Chamber Pressure	3450. kPa	5
AB1187	HKS-1000	42.4 mv/MPa	Water Filled Cylinder	Chamber Pressure	6890. kPa	5
AB1188	HKS-5000	4.35 mv/MPa	Water Filled Cylinder	Chamber Pressure	6890. kPa	5
THC190	K	0.040 mv/°C	Chamber Hatch Cover	Chamber Temperature	1000°C	1
TF191	64-250SB-17	0.461 mv/[cal/m ² -sec]	Vent Tube, 1.6 m from Portal	Thermal Flux	36.6 cal/m ² -sec	10
TF192	64-250SB-17	0.461 mv/[cal/m ² -sec]	Vent Tube, 0.3 m from Portal	Thermal Flux	36.6 cal/m ² -sec	10

Table 6 Test C-1 (Loading Density 2 kg/m³): Gage Location and Peak Measured Data.

Transducer			
Designation	Location	Measurement Type	Measured Peak Data
ABE171	Vent Tube, 1.6 m from Portal	Side-on Pressure	<0.9 kPa
ABE172	Vent Tube, 0.3 m from Portal	Side-on Pressure	<0.3 kPa
ABE173	Free-Field, 0.3 m from Portal	Side-on Pressure	5.6 kPa
ABE174	Free-Field, 0.9 m from Portal	Side-on Pressure	4.3 kPa
ABE175	Free-Field, 2.1 m from Portal	Side-on Pressure	2.1 kPa
ABE176	Free-Field, 4.5 m from Portal	Side-on Pressure	1.3 Kpa
ABE177	Free-Field, 0.9 m from Portal	Total Pressure	<0.7 kPa
ABE178	Free-Field, 2.1 m from Portal	Total Pressure	<1.0 kPa
ABI180	Front Wall of Chamber	Chamber Pressure	<1.4 kPa
ABI181B	Right Wall of Chamber (1/3 Height)	Chamber Pressure	----
ABI182	Back Wall of Chamber	Chamber Pressure	<1.5 kPa
ABI183T	Right Wall of Chamber (2/3 Height)	Chamber Pressure	----
ABI184	Water Filled Cylinder	Chamber Pressure	<1.0 kPa
ABI185	Water Filled Cylinder	Chamber Pressure	<1.0 kPa
ABI186	Water Filled Cylinder	Chamber Pressure	----
1BI187	Water Filled Cylinder	Chamber Pressure	290. kPa
ABI188	Water Filled Cylinder	Chamber Pressure	----
THV190	Chamber Hatch Cover	Chamber Temperature	630. °C
TF191	Vent Tube, 1.6 m from Portal	Thermal Flux	34. cal ² -sec
TF192	Vent Tube, 0.3 m from Portal	Thermal Flux	27. cal ² -sec

Note: The digitizer sample rate was one sample per 220 micro-sec, for a total record length of 60 sec.

Table 7 Test C-2 (Loading Density 5 kg/m³): Gage Location and Peak Measured Data.

Transducer			
Designation	Location	Measurement Type	Measured Peak Data
ABE171	Vent Tube, 1.6 m from Portal	Side-on Pressure	<1.3 kPa
ABE172	Vent Tube, 0.3 m from Portal	Side-on Pressure	<0.5 kPa
ABE173	Free-Field, 0.3 m from Portal	Side-on Pressure	6.4 kPa
ABE174	Free-Field, 0.9 m from Portal	Side-on Pressure	7.1 kPa
ABE175	Free-Field, 2.1 m from Portal	Side-on Pressure	3.5 kPa
ABE176	Free-Field, 4.5 m from Portal	Side-on Pressure	6.4 Kpa
ABE177	Free-Field, 0.9 m from Portal	Total Pressure	<2.2 kPa
ABE178	Free-Field, 2.1 m from Portal	Total Pressure	<1.9 kPa
ABI180	Front Wall of Chamber	Chamber Pressure	<4.0 kPa
ABI181B	Right Wall of Chamber (1/3 Height)	Chamber Pressure	<3.4 kPa
ABI182	Back Wall of Chamber	Chamber Pressure	<4.0 kPa
ABI183T	Right Wall of Chamber (2/3 Height)	Chamber Pressure	<2.7 kPa
ABI184	Water Filled Cylinder	Chamber Pressure	----
ABI185	Water Filled Cylinder	Chamber Pressure	<6.7 kPa
ABI186	Water Filled Cylinder	Chamber Pressure	----
lBI187	Water Filled Cylinder	Chamber Pressure	<13.5 kPa
ABI188	Water Filled Cylinder	Chamber Pressure	----
THV190	Chamber Hatch Cover	Chamber Temperature	604.°C
TF191	Vent Tube, 1.6 m from Portal	Thermal Flux	42. cal ² -sec
TF192	Vent Tube, 0.3 m from Portal	Thermal Flux	34. cal ² -sec

Note: The digitizer sample rate was one sample per 220 micro-sec, for a total record length of 60 sec.

Table 8 Test C-3 (Loading Density 20 kg/m³): Gage Location and Peak Measured Data.

Transducer			
Designation	Location	Measurement Type	Measured Peak Data
ABE171	Vent Tube, 1.6 m from Portal	Side-on Pressure	335.kPa
ABE172	Vent Tube, 0.3 m from Portal	Side-on Pressure	56.1kPa
ABE173	Free-Field, 0.3 m from Portal	Side-on Pressure	----
ABE174	Free-Field, 0.9 m from Portal	Side-on Pressure	89.0 kPa
ABE175	Free-Field, 2.1 m from Portal	Side-on Pressure	>70.0 kPa
ABE176	Free-Field, 4.5 m from Portal	Side-on Pressure	11.2 Kpa
ABE177	Free-Field, 0.9 m from Portal	Total Pressure	----
ABE178	Free-Field, 2.1 m from Portal	Total Pressure	104. kPa
ABI180	Front Wall of Chamber	Chamber Pressure	235. kPa
ABI181B	Right Wall of Chamber (1/3 Height)	Chamber Pressure	196.kPa
ABI182	Back Wall of Chamber	Chamber Pressure	155. kPa
ABI183T	Right Wall of Chamber (2/3 Height)	Chamber Pressure	----
ABI184	Water Filled Cylinder	Chamber Pressure	----
ABI185	Water Filled Cylinder	Chamber Pressure	155. kPa
ABI186	Water Filled Cylinder	Chamber Pressure	135. kPa
ABI187	Water Filled Cylinder	Chamber Pressure	145. kPa
ABI188	Water Filled Cylinder	Chamber Pressure	69.0 kPa
THC190	Chamber Hatch Cover	Chamber Temperature	616. °C
TF191	Vent Tube, 1.6 m from Portal	Thermal Flux	220. cal/m ² -sec
TF192	Vent Tube, 0.3 m from Portal	Thermal Flux	166. cal/m ² -sec

Note: The digitizer sample rate was one sample per 220 micro-sec, for a total record length of 60 sec.

Table 9. Test C-4 (Loading Density 50 kg/m³): Gage Location and Peak Measured Data

Transducer			
Designation	Location	Measurement Type	Measured Peak Data
ABE171	Vent Tube, 1.6 m from Portal	Side-on Pressure	>1400. kPa
ABE172	Vent Tube, 0.3 m from Portal	Side-on Pressure	350. kPa
ABE173	Free-Field, 0.3 m from Portal	Side-on Pressure	382. kPa
ABE174	Free-Field, 0.9 m from Portal	Side-on Pressure	34.5 kPa
ABE175	Free-Field, 2.1 m from Portal	Side-on Pressure	----
ABE176	Free-Field, 4.5 m from Portal	Side-on Pressure	----
ABE177	Free-Field, 0.9 m from Portal	Total Pressure	285. kPa
ABE178	Free-Field, 2.1 m from Portal	Total Pressure	----
ABI180	Front Wall of Chamber	Chamber Pressure	----
ABI181B	Right Wall of Chamber (1/3 Height)	Chamber Pressure	889. kPa
ABI182	Back Wall of Chamber	Chamber Pressure	587. kPa
ABI183T	Right Wall of Chamber (2/3 Height)	Chamber Pressure	1833. kPa
ABI184	Water Filled Cylinder	Chamber Pressure	----
ABI185	Water Filled Cylinder	Chamber Pressure	840. kPa
ABI186	Water Filled Cylinder	Chamber Pressure	722. kPa
1BI187	Water Filled Cylinder	Chamber Pressure	545. kPa
ABI188	Water Filled Cylinder	Chamber Pressure	298. kPa
THC190	Chamber Hatch Cover	Chamber Temperature	----
TF191	Vent Tube, 1.6 m from Portal	Thermal Flux	>372. cal/m ² -sec
TF192	Vent Tube, 0.3 m from Portal	Thermal Flux	>372. cal/m ² -sec

Note: The digitizer sample rate was one sample per 220 micro-sec, for a total record length of 60 sec.

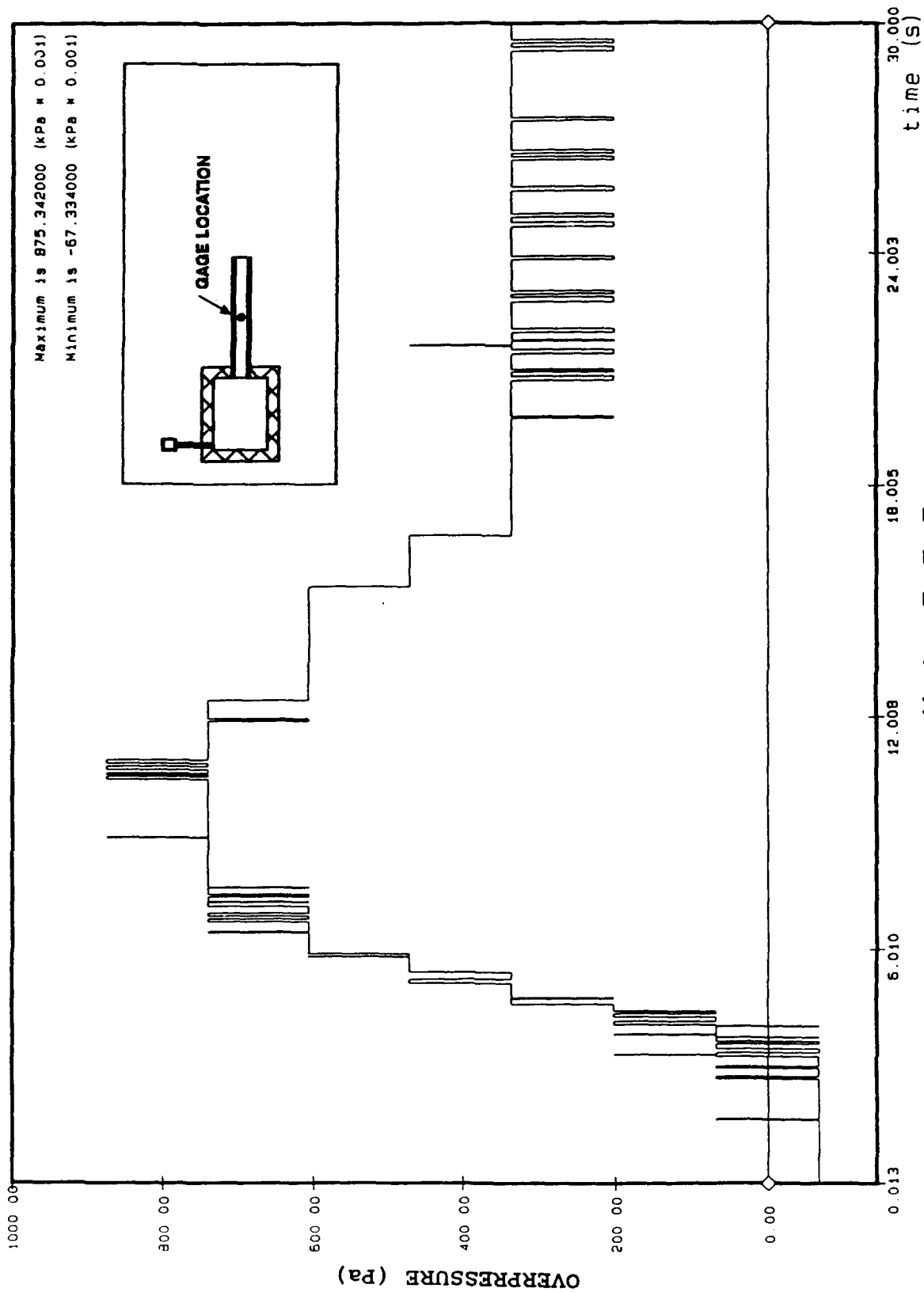
APPENDIX A1

KA-III, PHASE C

TEST C-1

10 kg M-1 PROPELLANT BURN

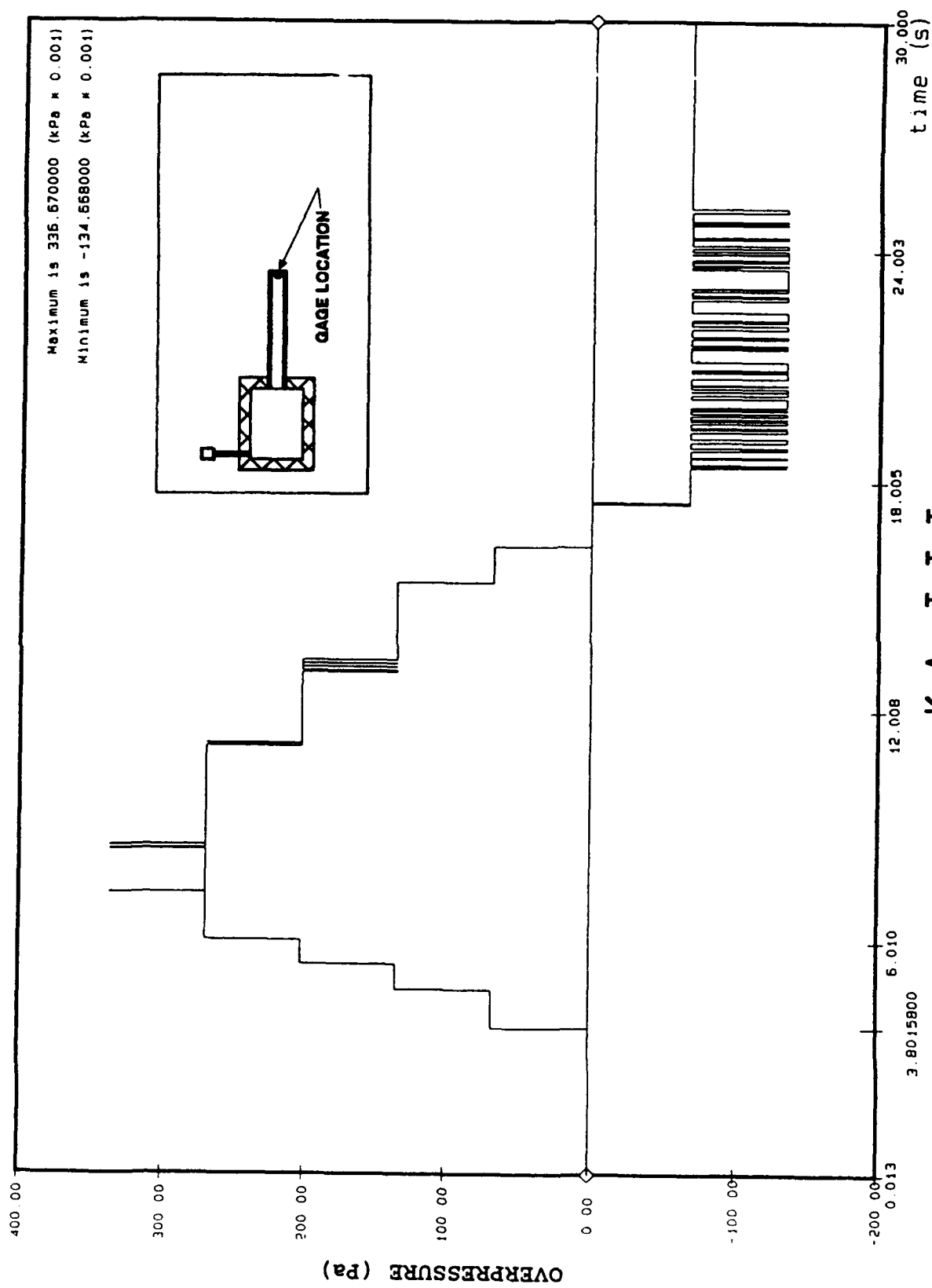
DATA-TIME HISTORIES



K A I I I
Air Blast External Event C1
Pressure Gauge # ABE171

Figure: A1-1

Filter 0 11.20 n2



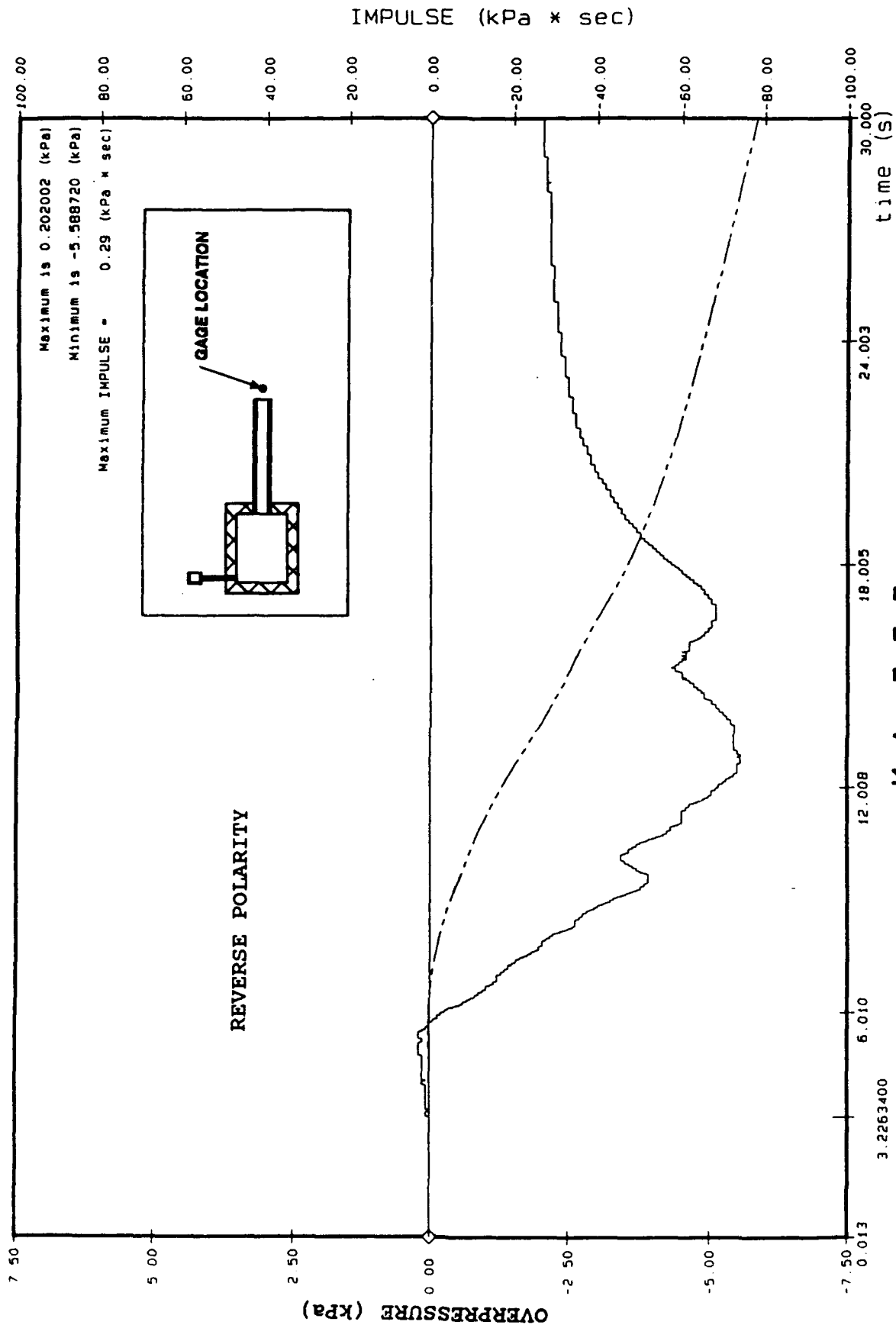
K A I I I

Air Blast External Event C1

Pressure Gauge # ABE172

Figure: A1-2

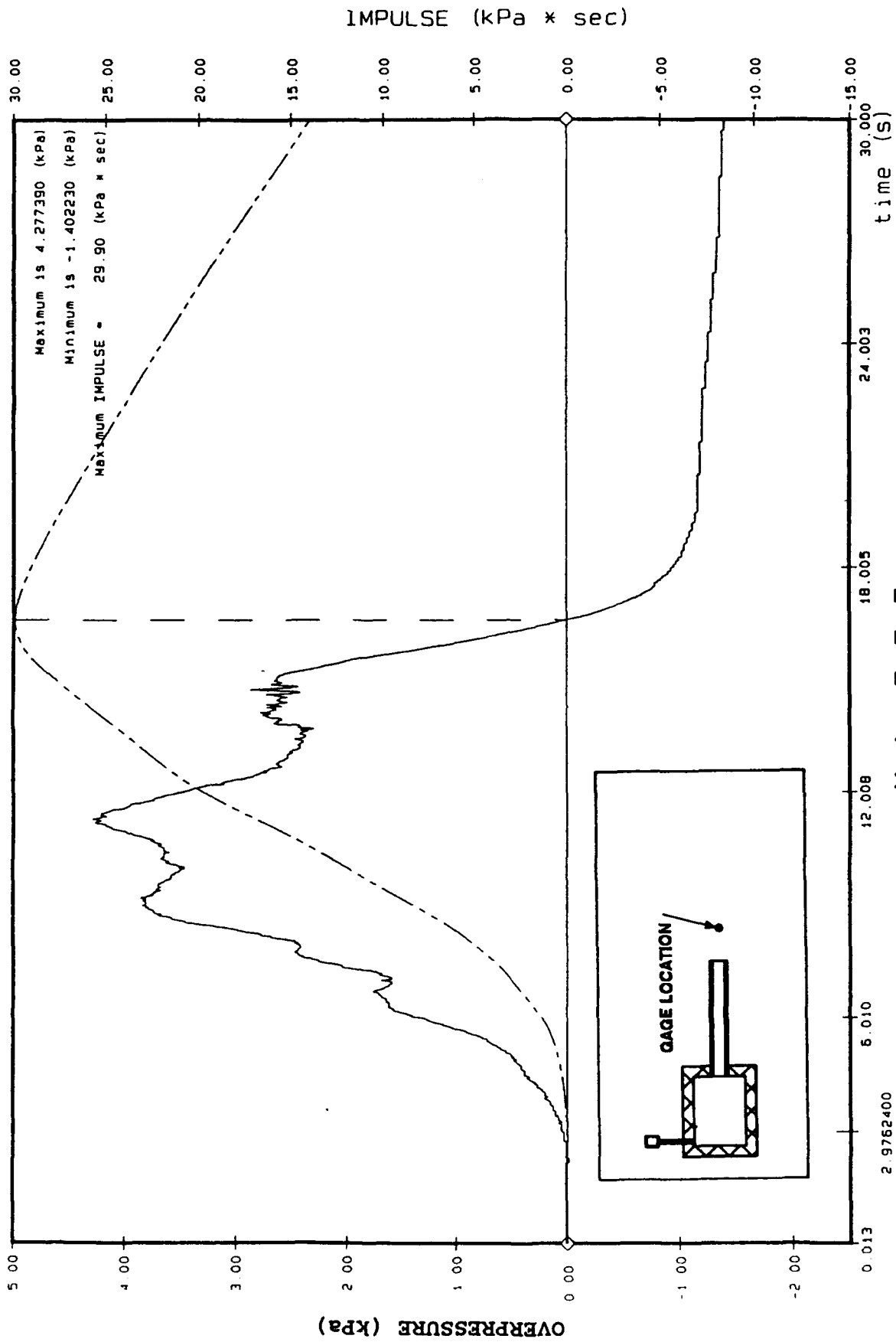
Filter # 11.20 Hz



K A I I I
Air Blast External Event C1
Pressure Gauge # ABE173

Figure: A1-3

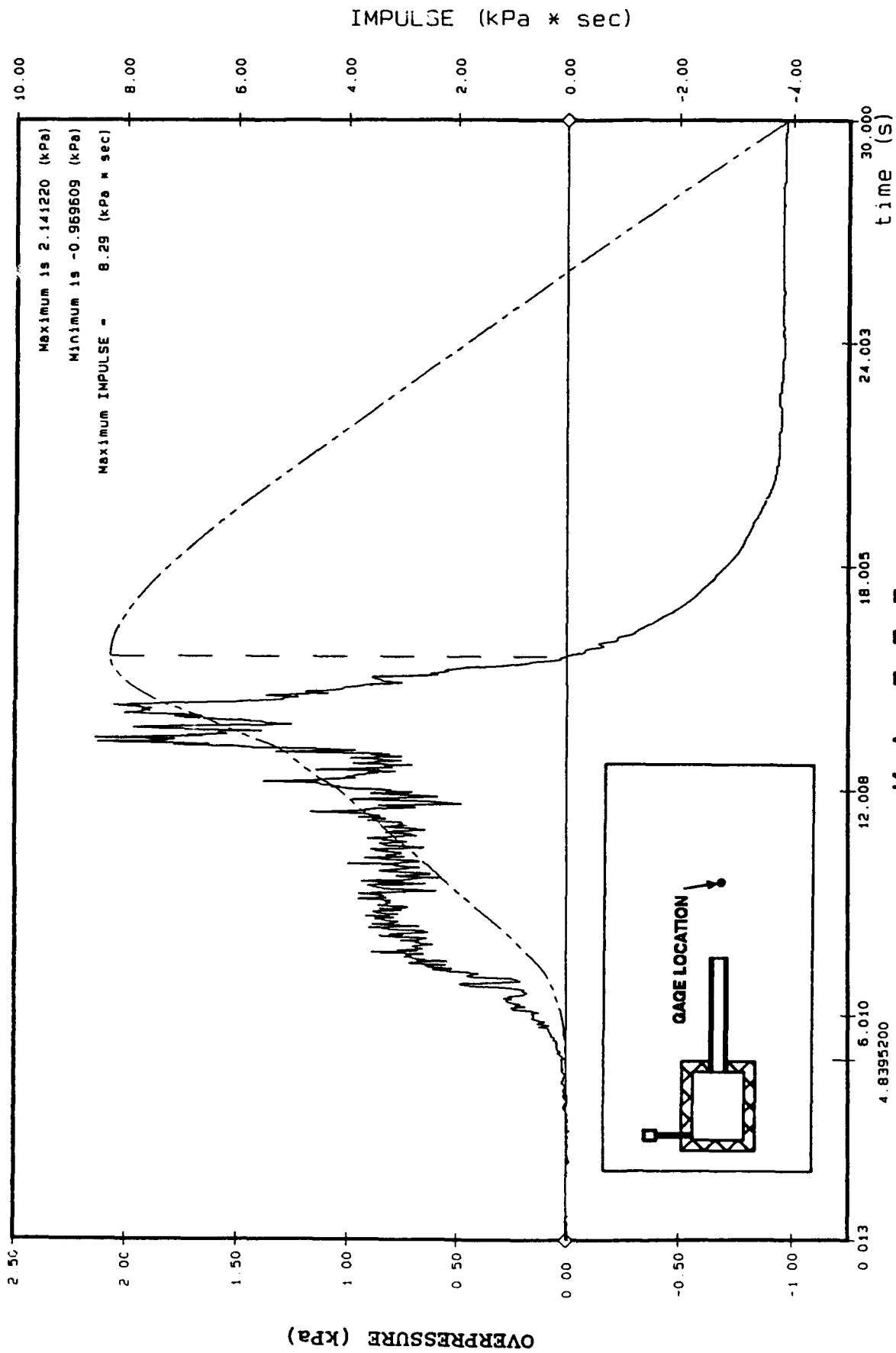
Filter @ 11.20 Hz



K A I I I
Air Blast External Event C1
Pressure Gauge # ABE174

Filter @ 11.20 Hz

Figure: A1-4



K A I I I
Air Blast External Event C1
Pressure Gauge # ABE175

Figure: A1-5

Filter @ 11.20 Hz

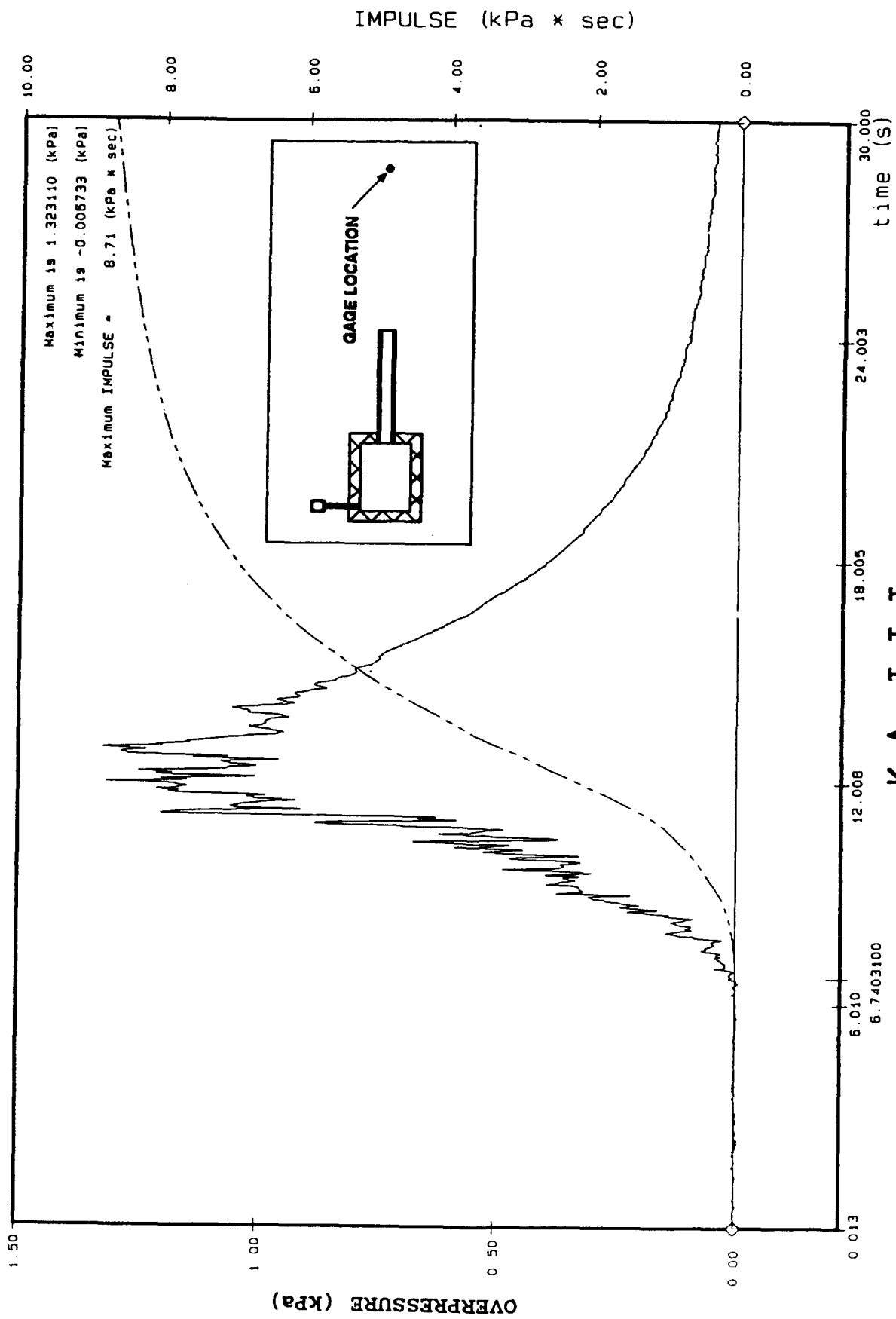
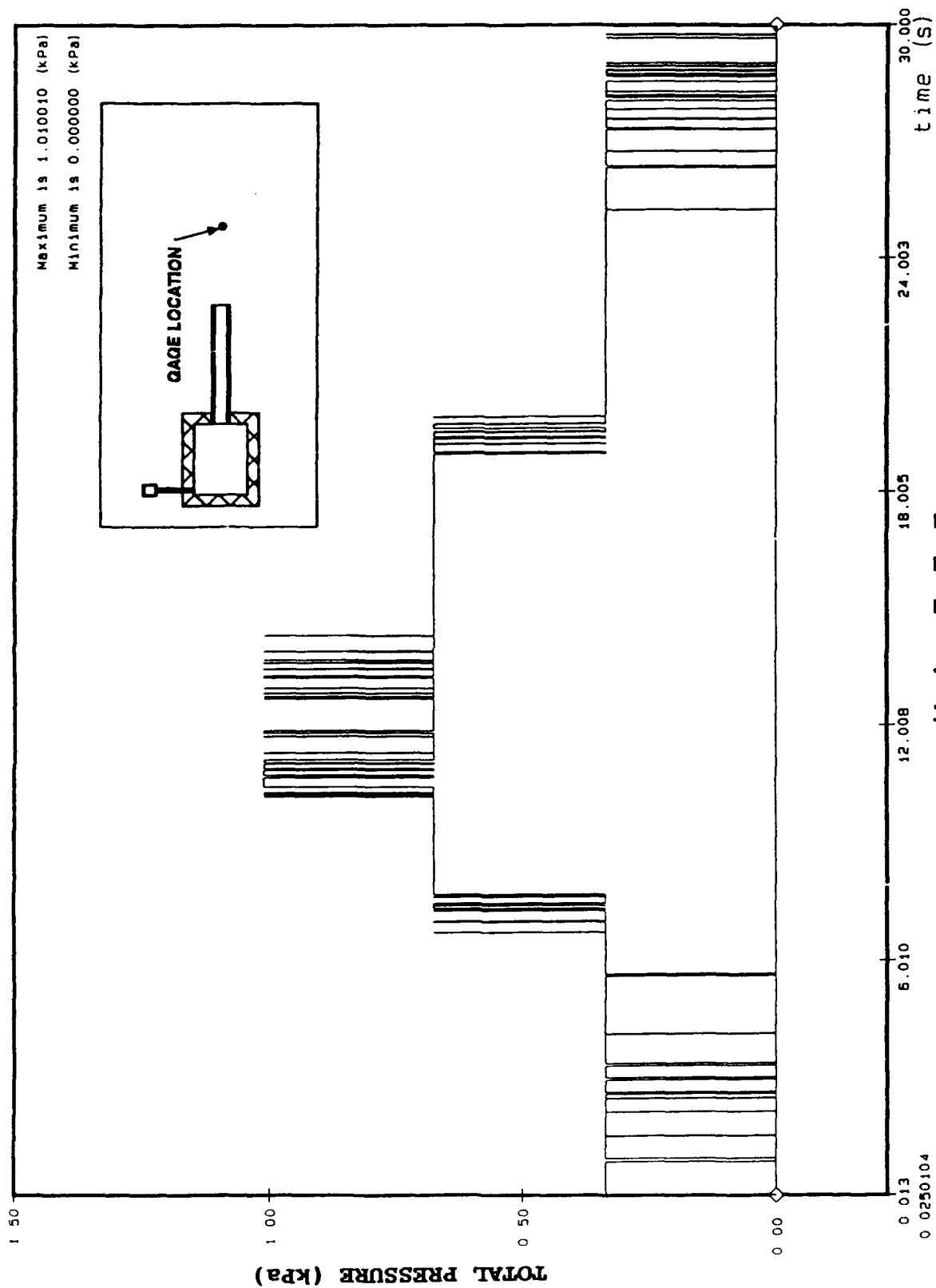


Figure: A1-6



Air Blast External Head Event C1
Pressure Gauge # ABEH178

Figure: A1-7

Filter @ 11.20 Hz

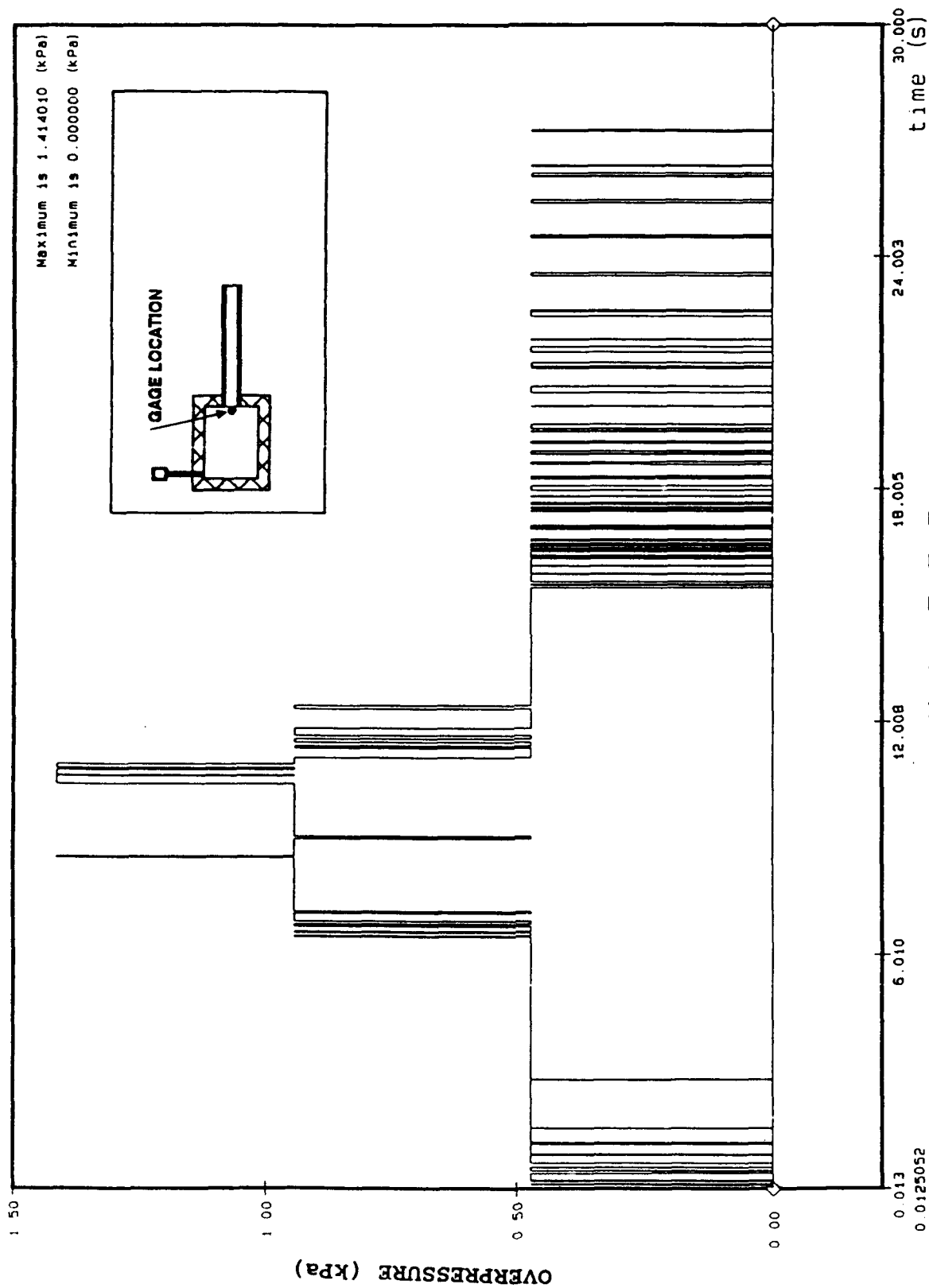


Figure: A1-8

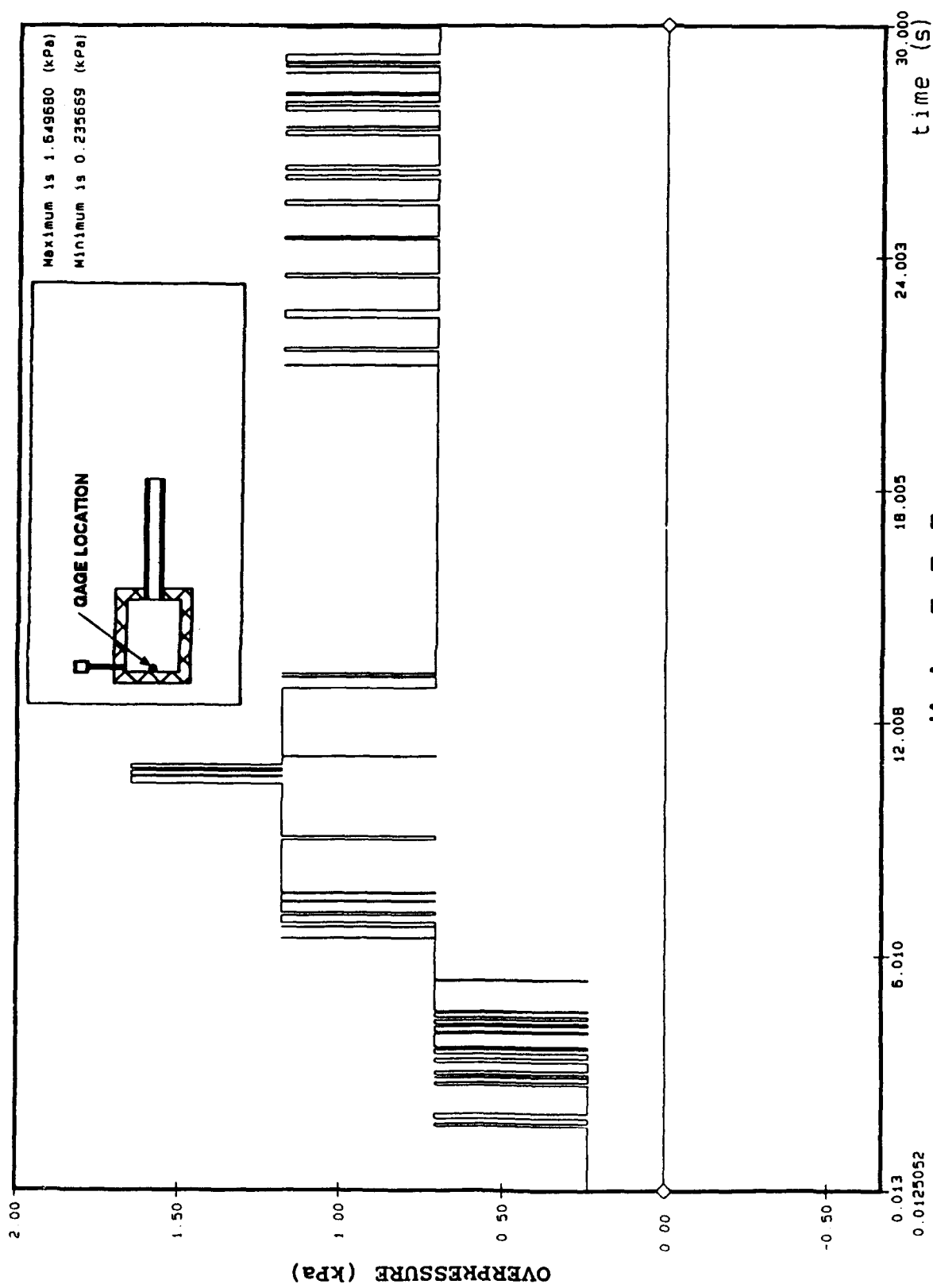
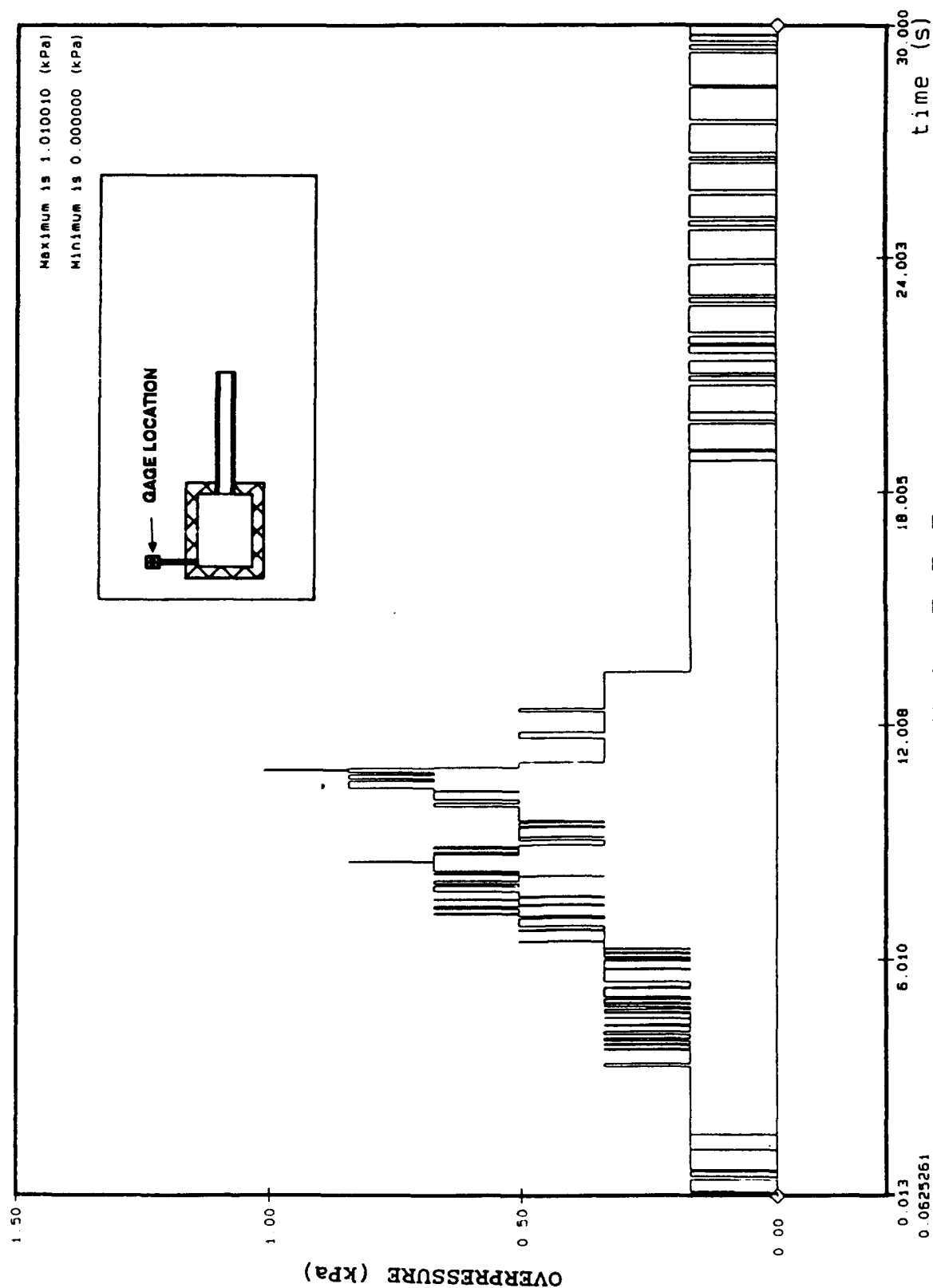


Figure: A1-9



K A I I I
Air Blast Internal Event C1
Pressure Gauge # ABI184

Figure: A1-10

Filter # 11.20 Hz

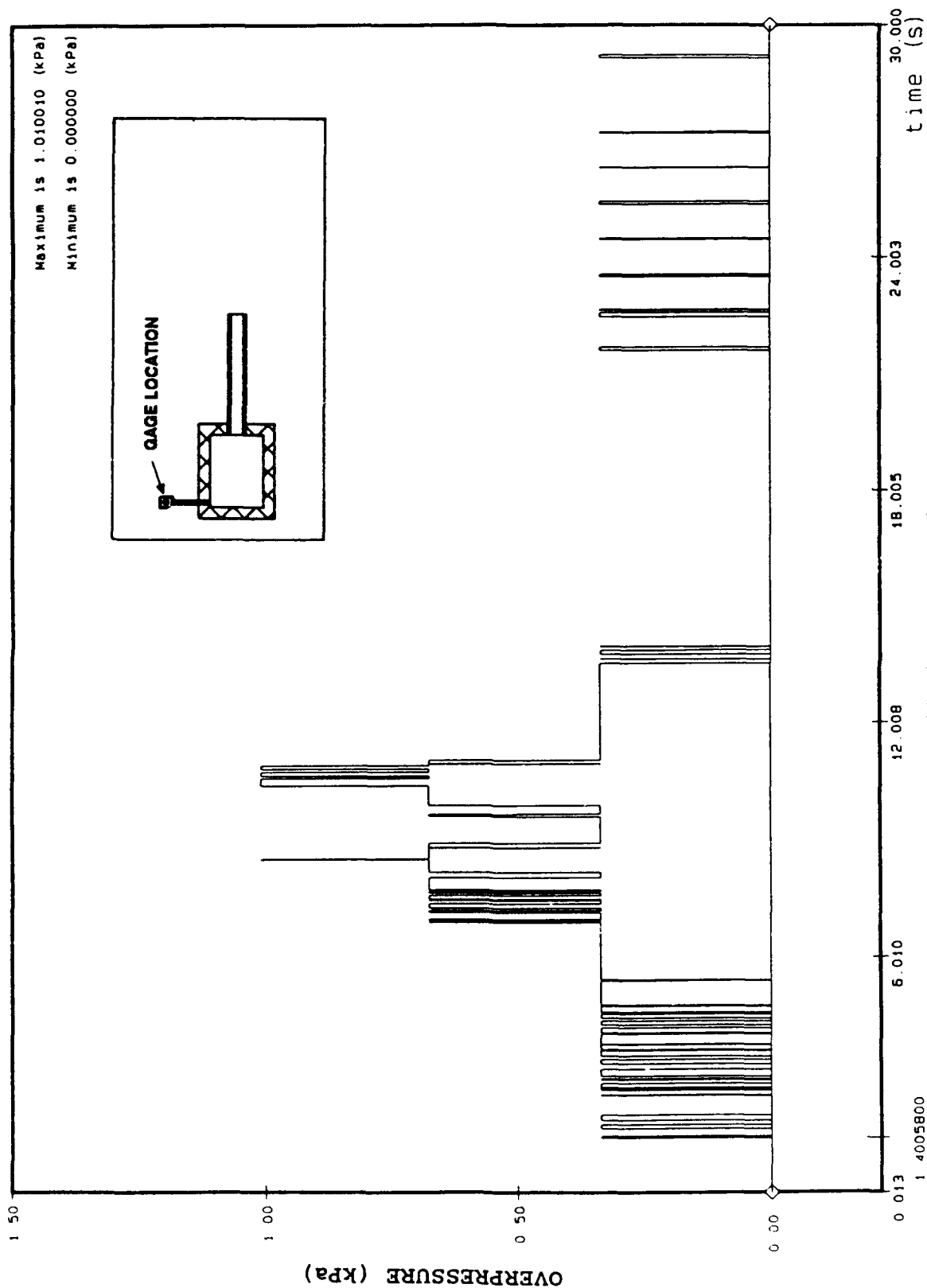
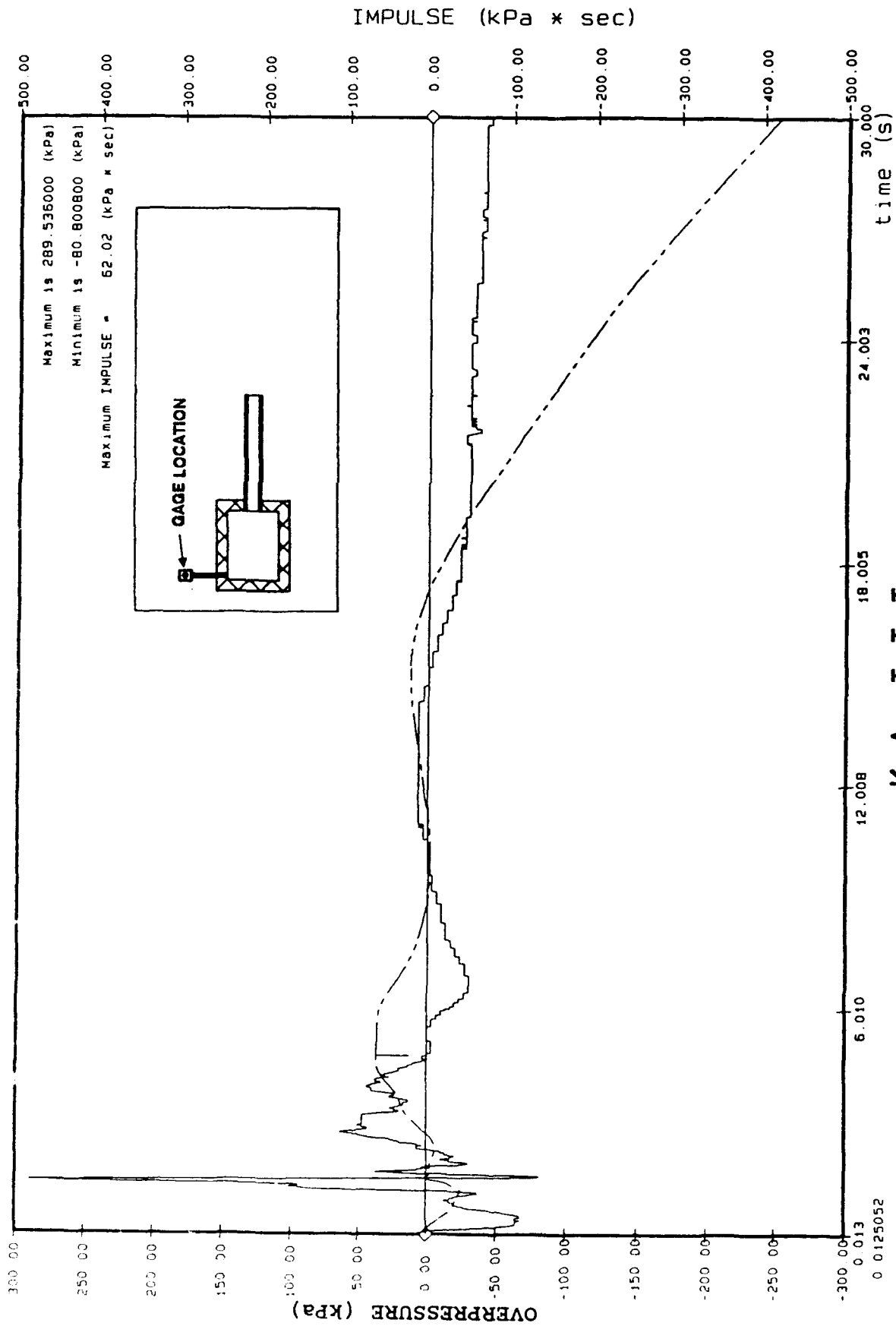


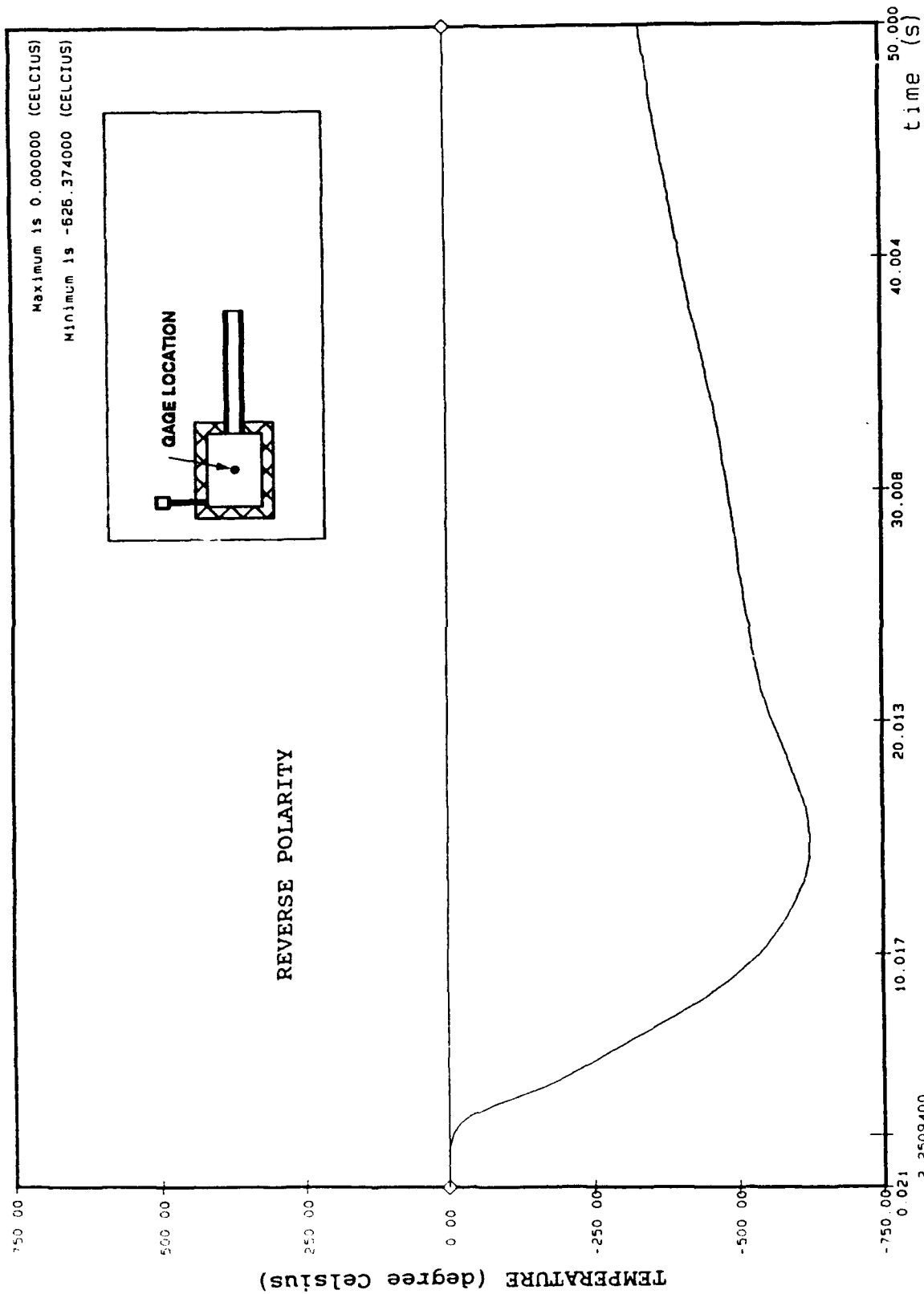
Figure: A1-11



K A I I I
 Air Blast Internal Event C1
 Pressure Gauge # ABI187

Figure: A1-12

Filter 0 11.20 Hz



K A I I I

Temperature Experiment C 1
Thermocouple Gauge # THC190

Filter # 6.70 Hz

Figure: A1-13

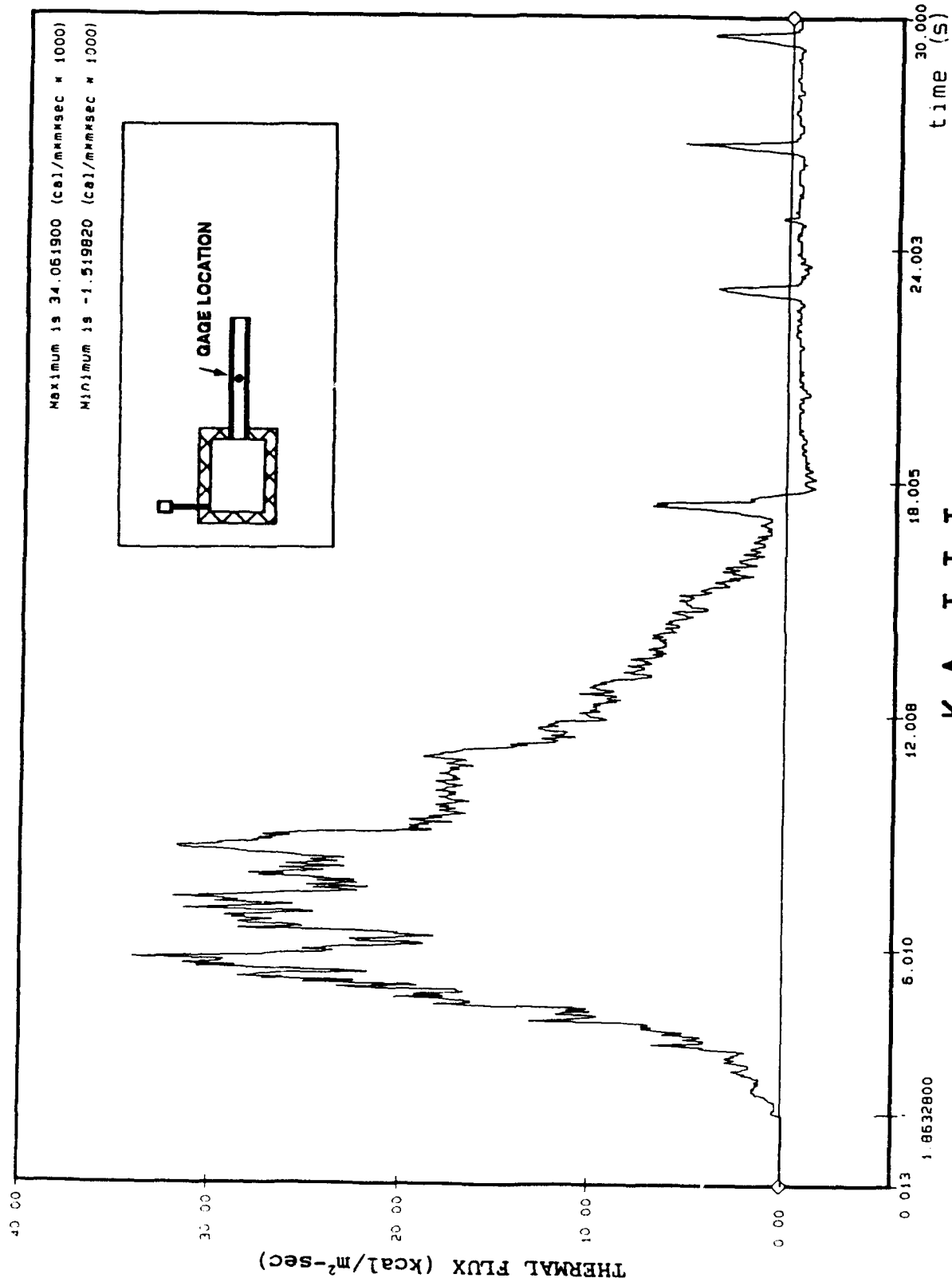


Figure: A1-14

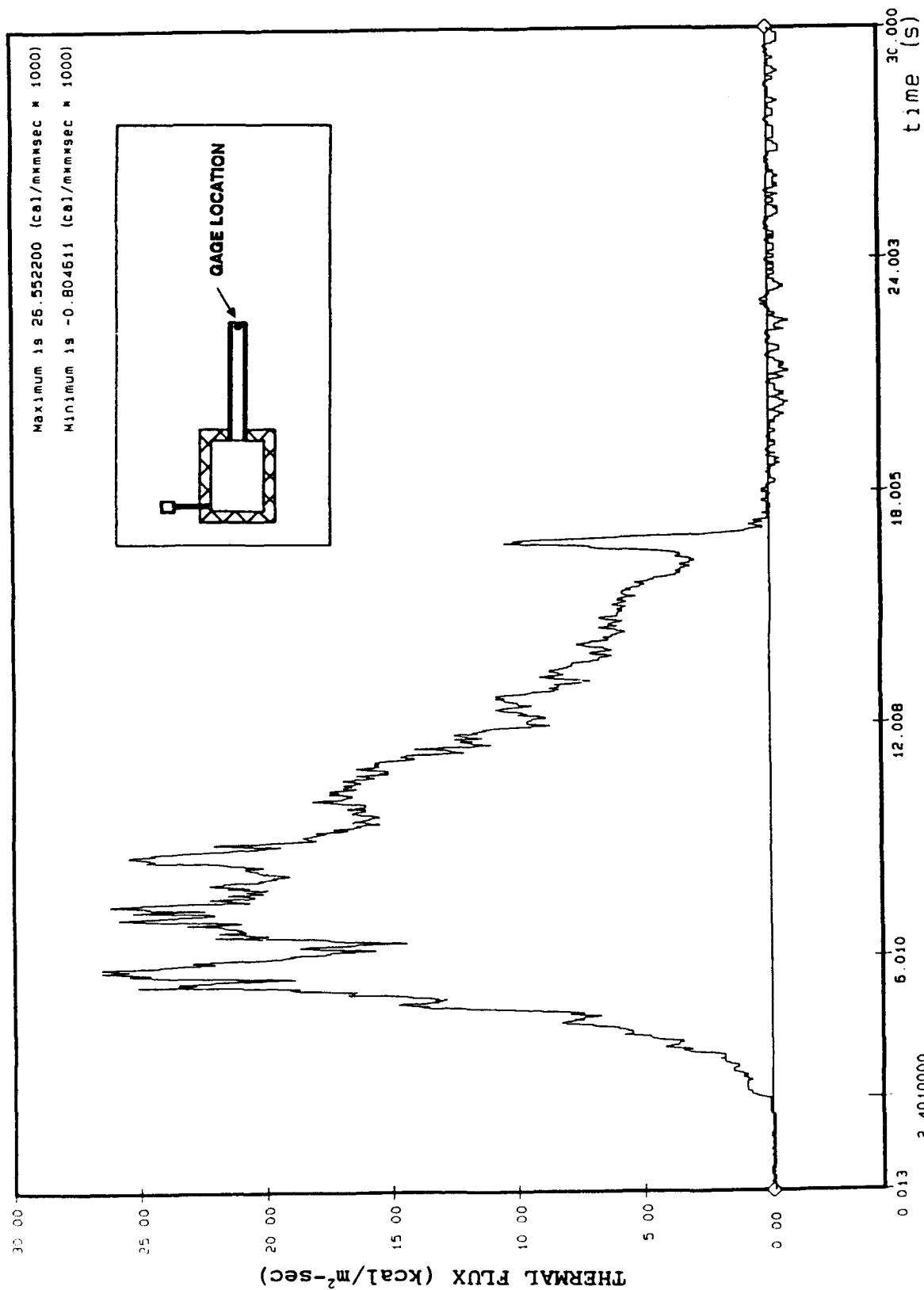


Figure: A1-15

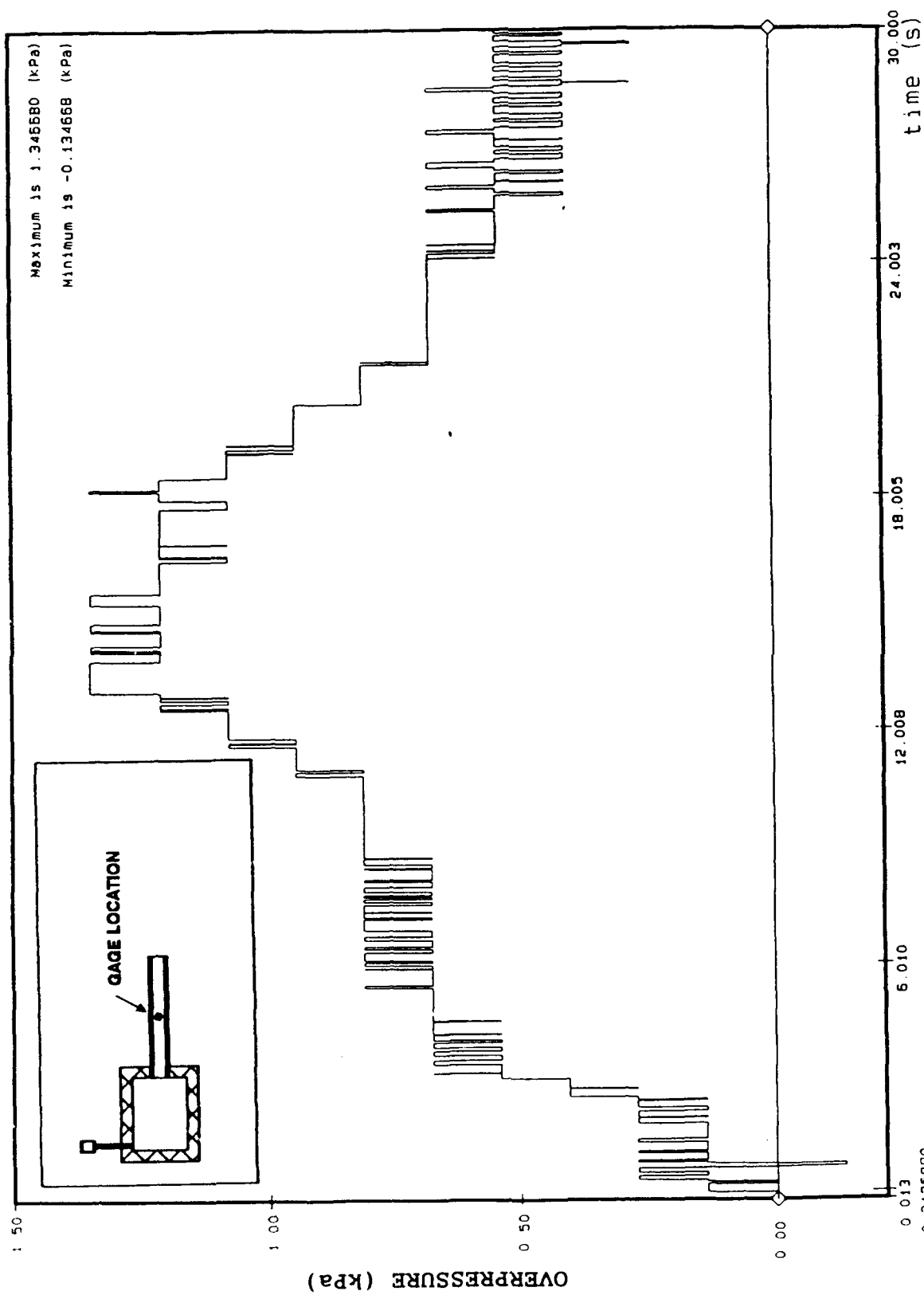
APPENDIX A2

KA-III, PHASE C

TEST C-2

25 kg M-1 PROPELLANT BURN

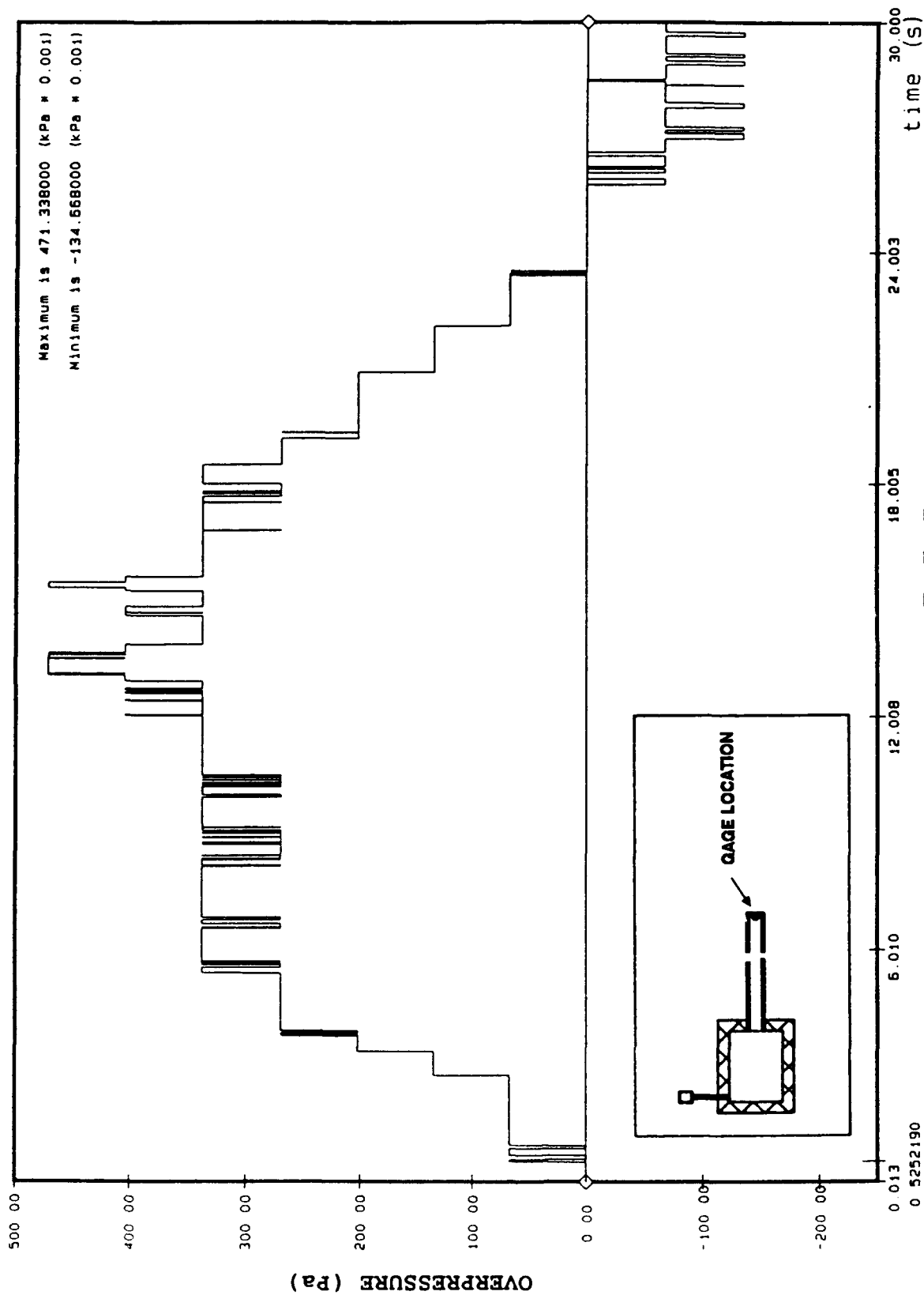
DATA-TIME HISTORIES



K A I I I
Air Blast External Event C2
Pressure Gauge # ABE171

Filter 11.20 Hz

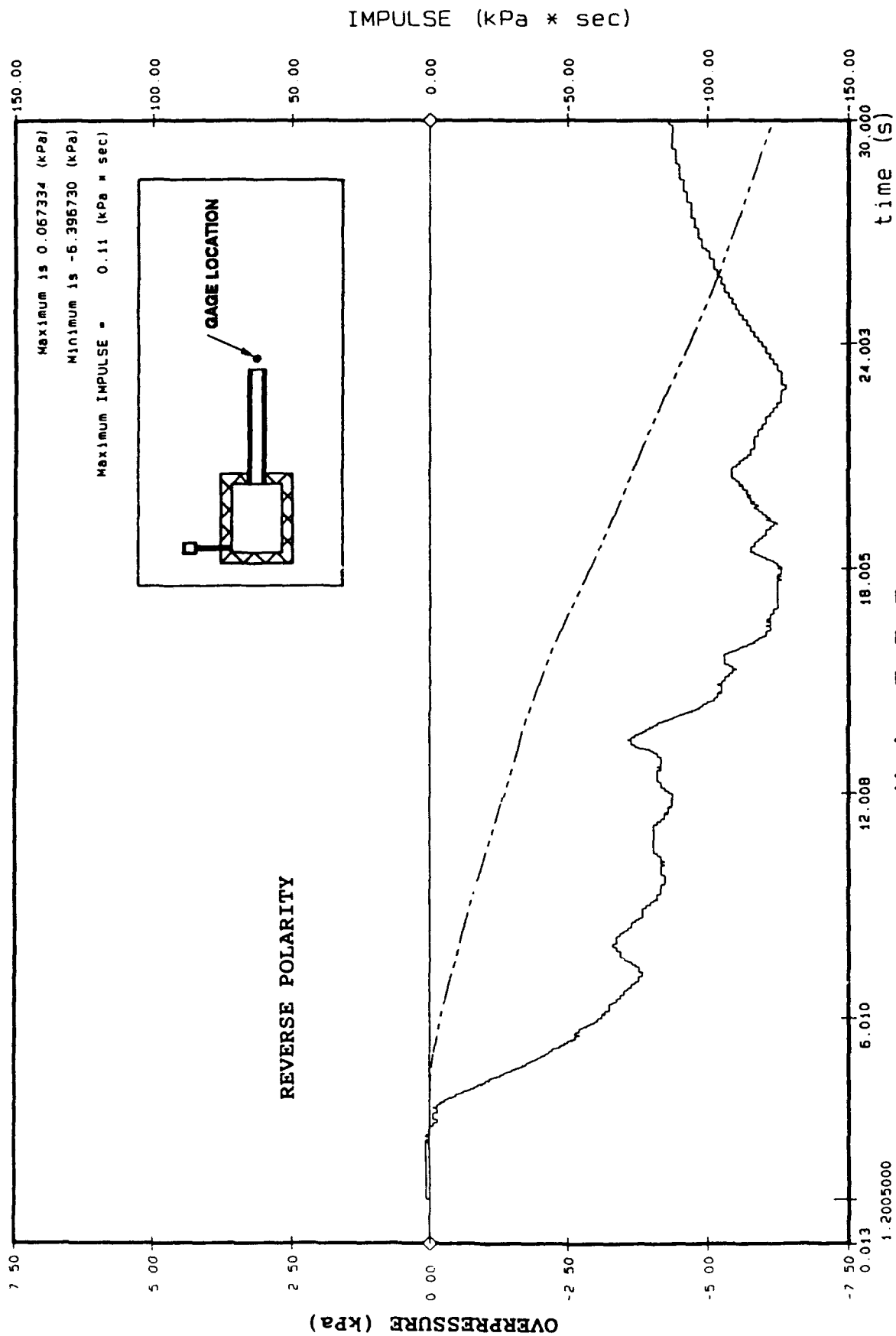
Figure: A2-1



K A I I I
Air Blast External Event C2
Pressure Gauge # ABE172

Figure: A2-2

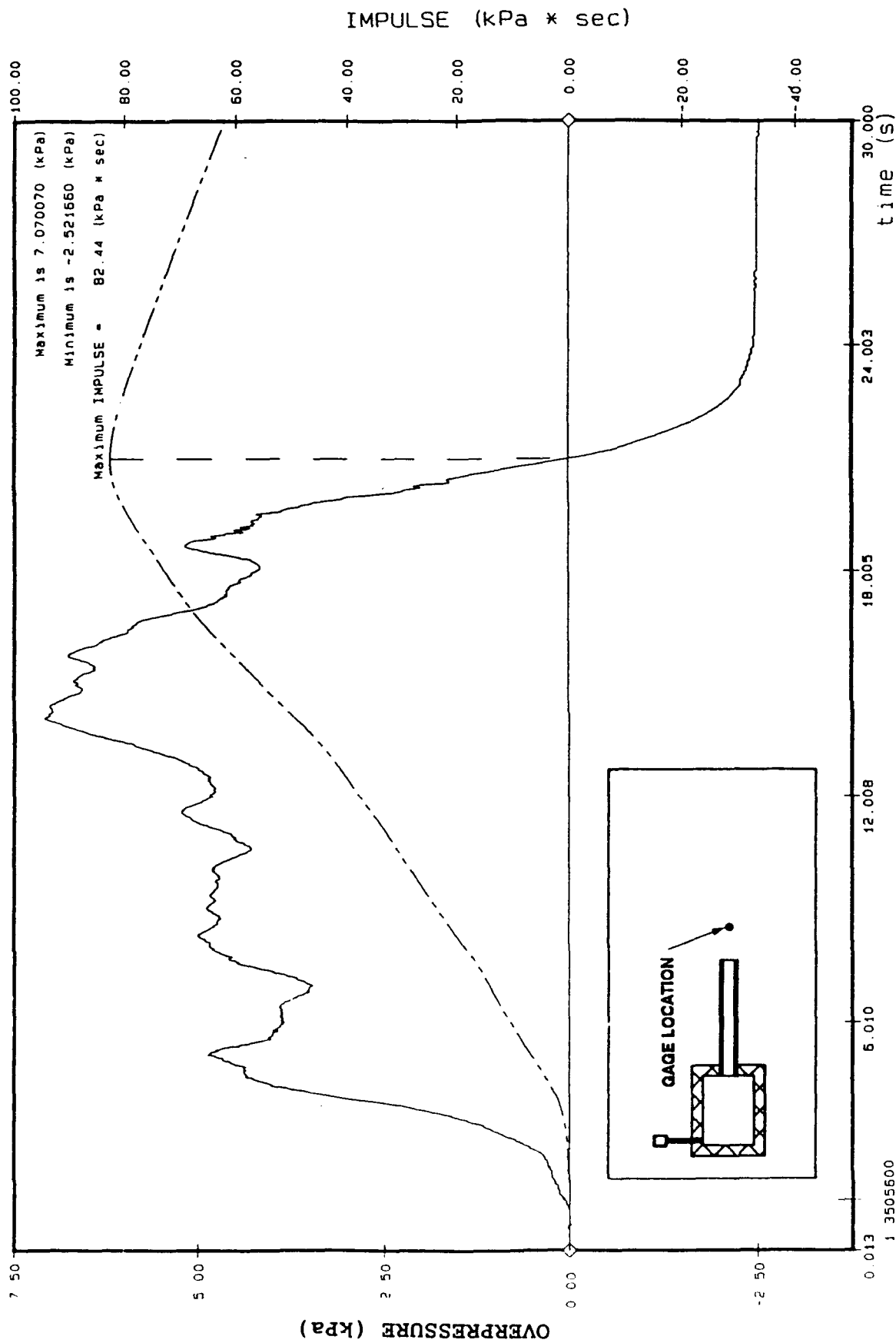
Filter 0 11.20 Hz



K A I I I
 Air Blast External Event C2
 Pressure Gauge # ABE173

Filter @ 11.20 Hz

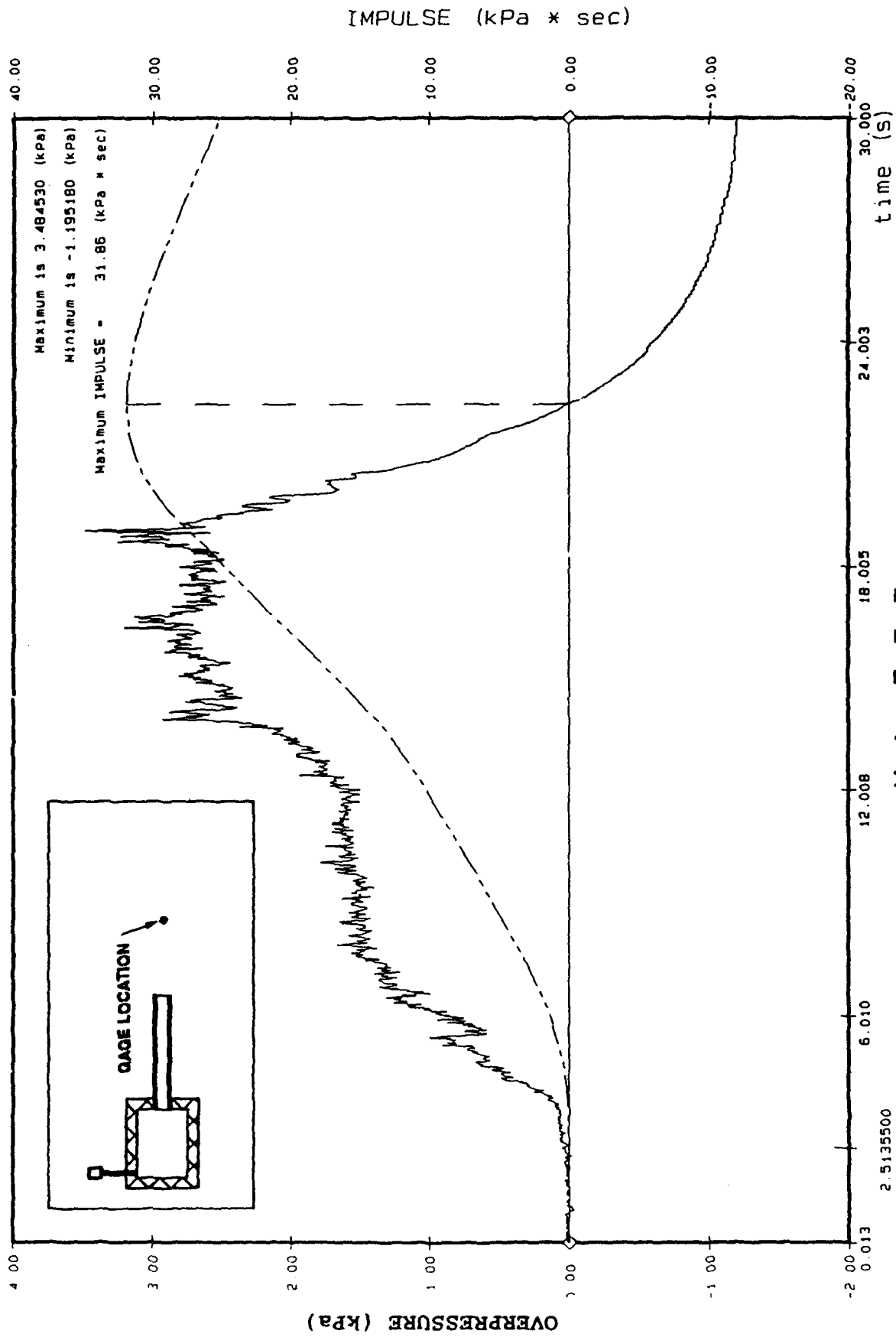
Figure: A2-3



K A I I I
Air Blast External Event C2
Pressure Gauge # ABE174

Filter @ 11.20 Hz

Figure: A2-4



K A I I I
Air Blast External Event C2
Pressure Gauge # ABE175

Filter @ 11.20 Hz

Figure: A2-5

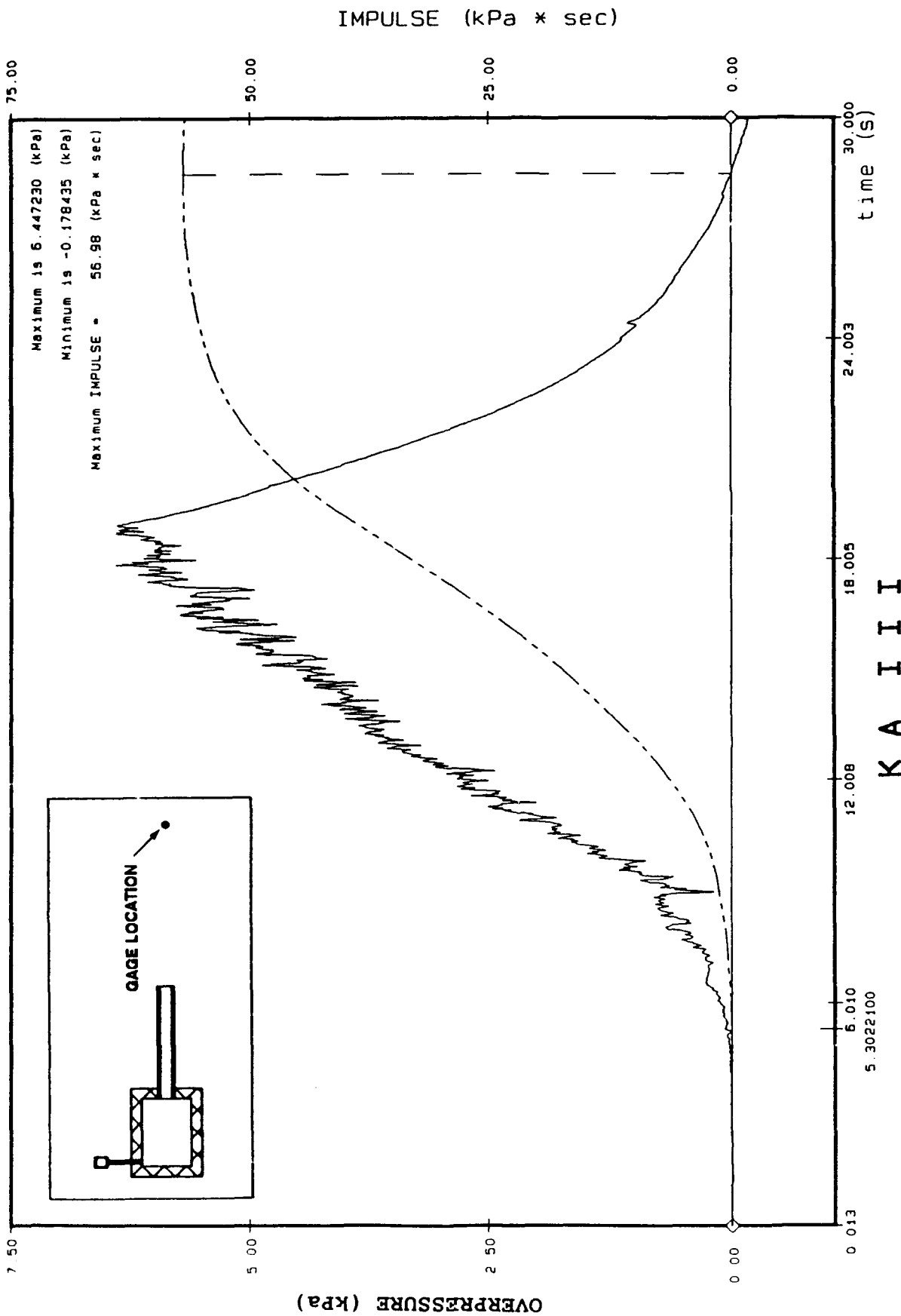
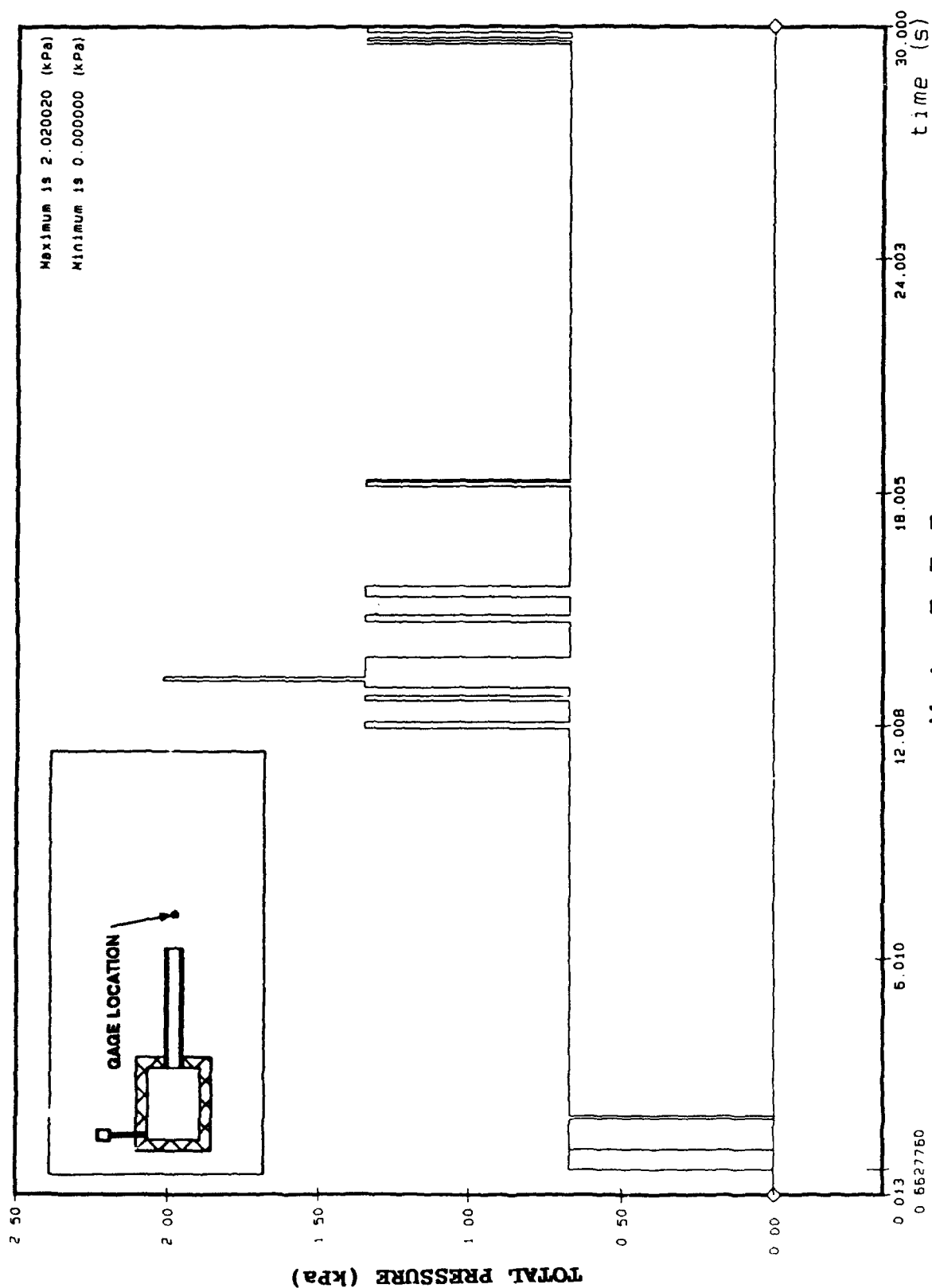


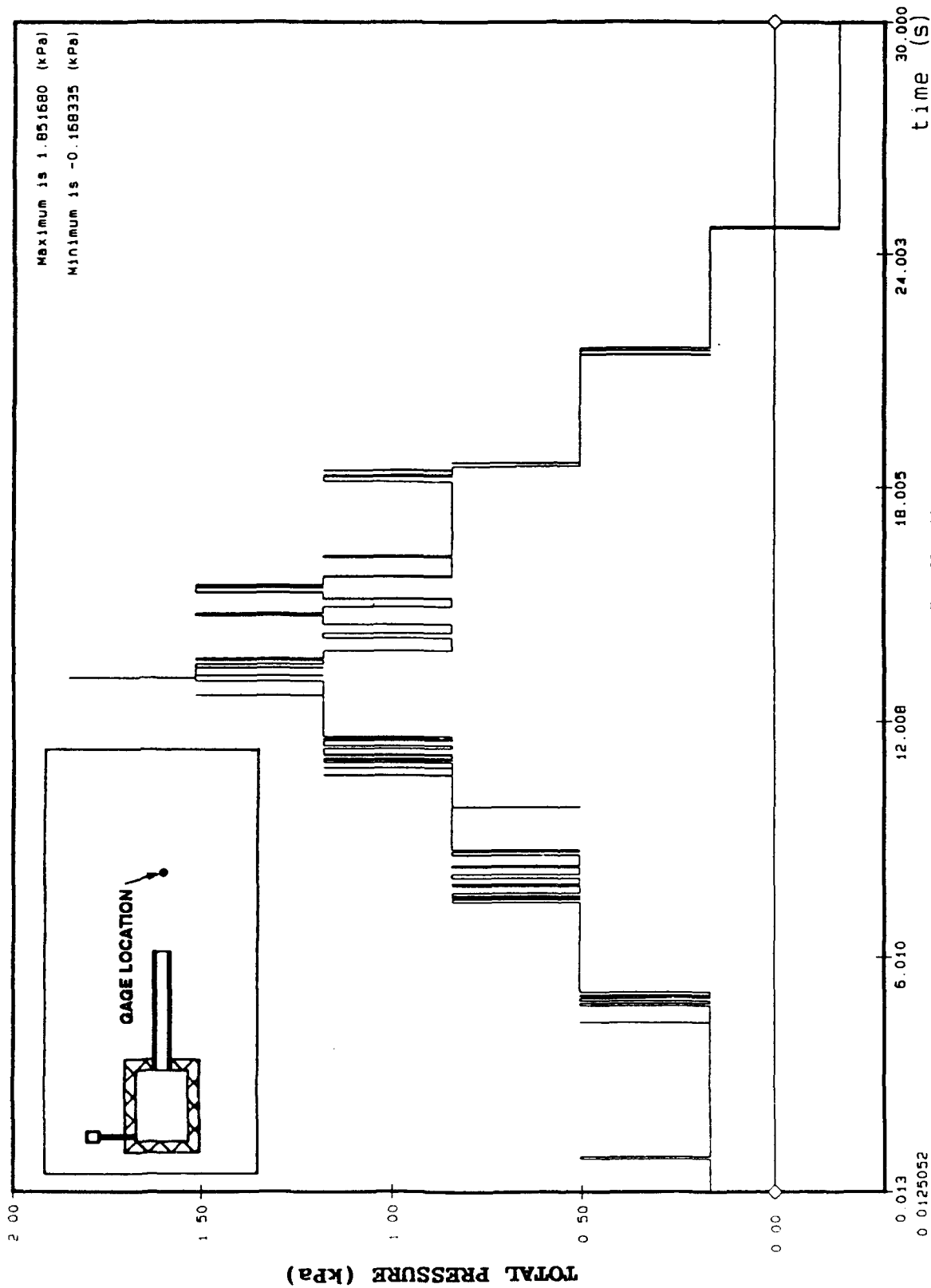
Figure: A2-6



Air Blast External Head Event C2
Pressure Gauge # ABEH177

Figure: A2-7

Filter # 11.20 hz



K A I I I
Air Blast External Head Event C2
Pressure Gauge # ABEH178
Filter @ 11.20 Hz

Figure: A2-8

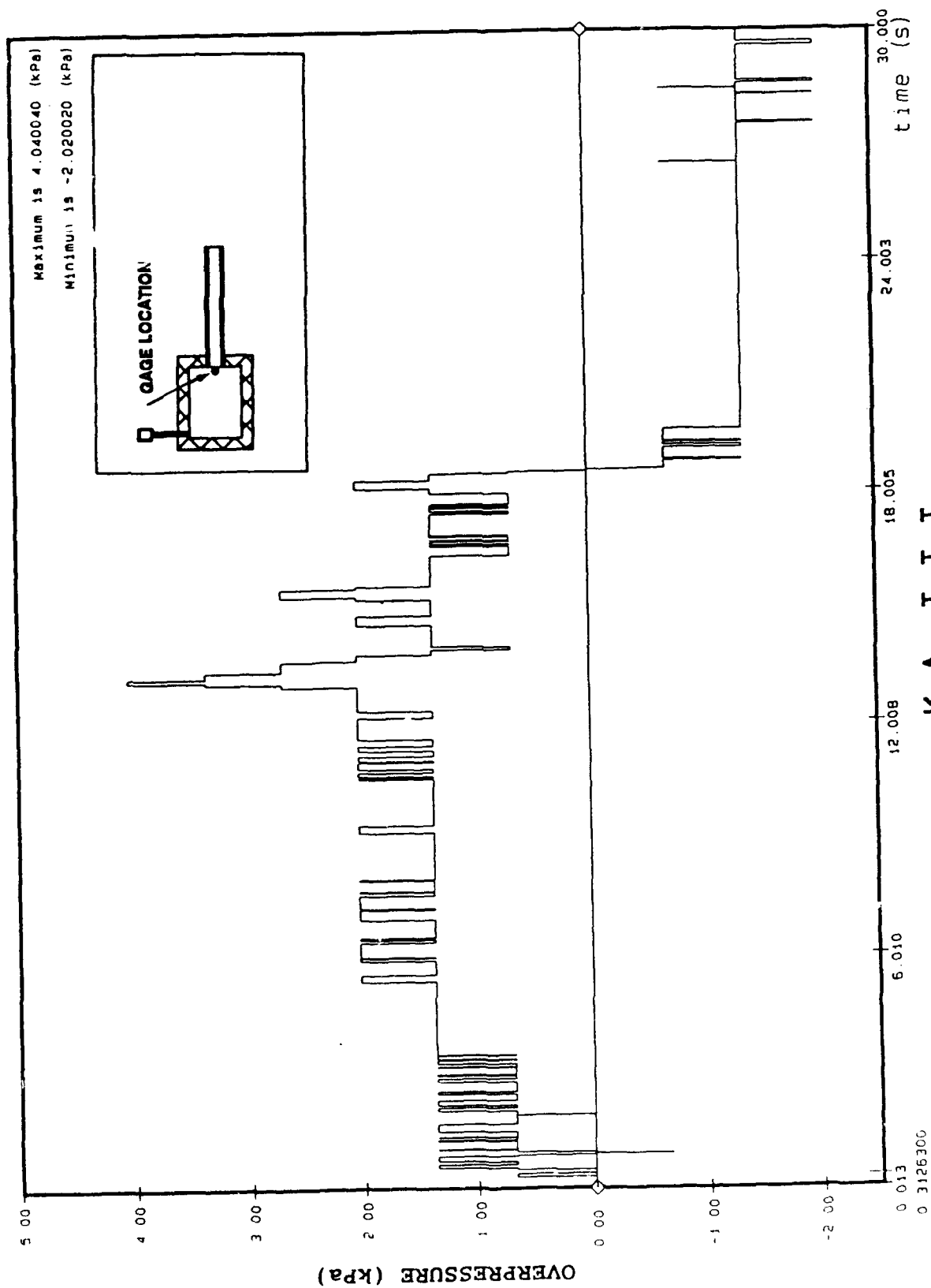
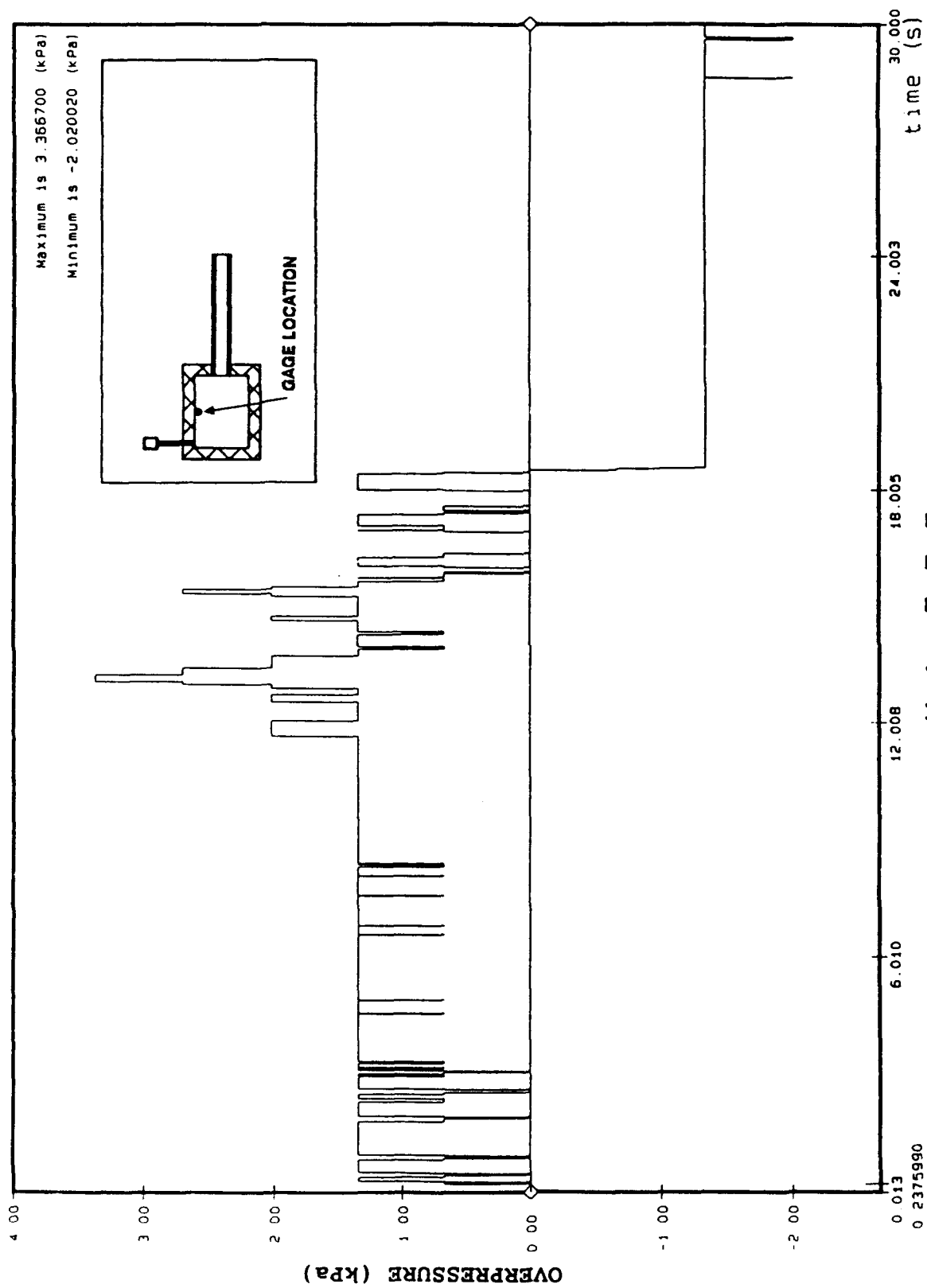


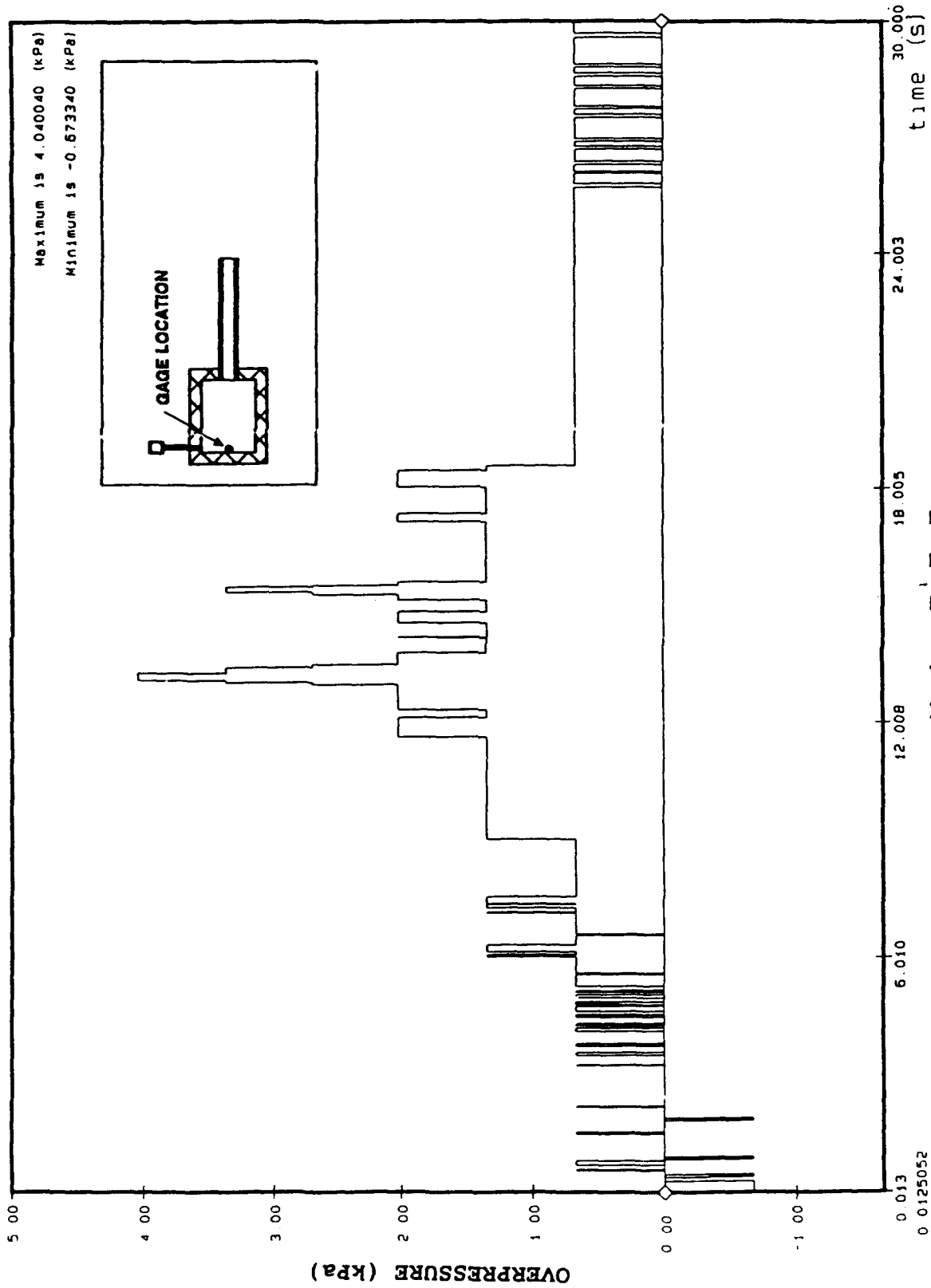
Figure: A2-9



Filter 0 13 20 Hz

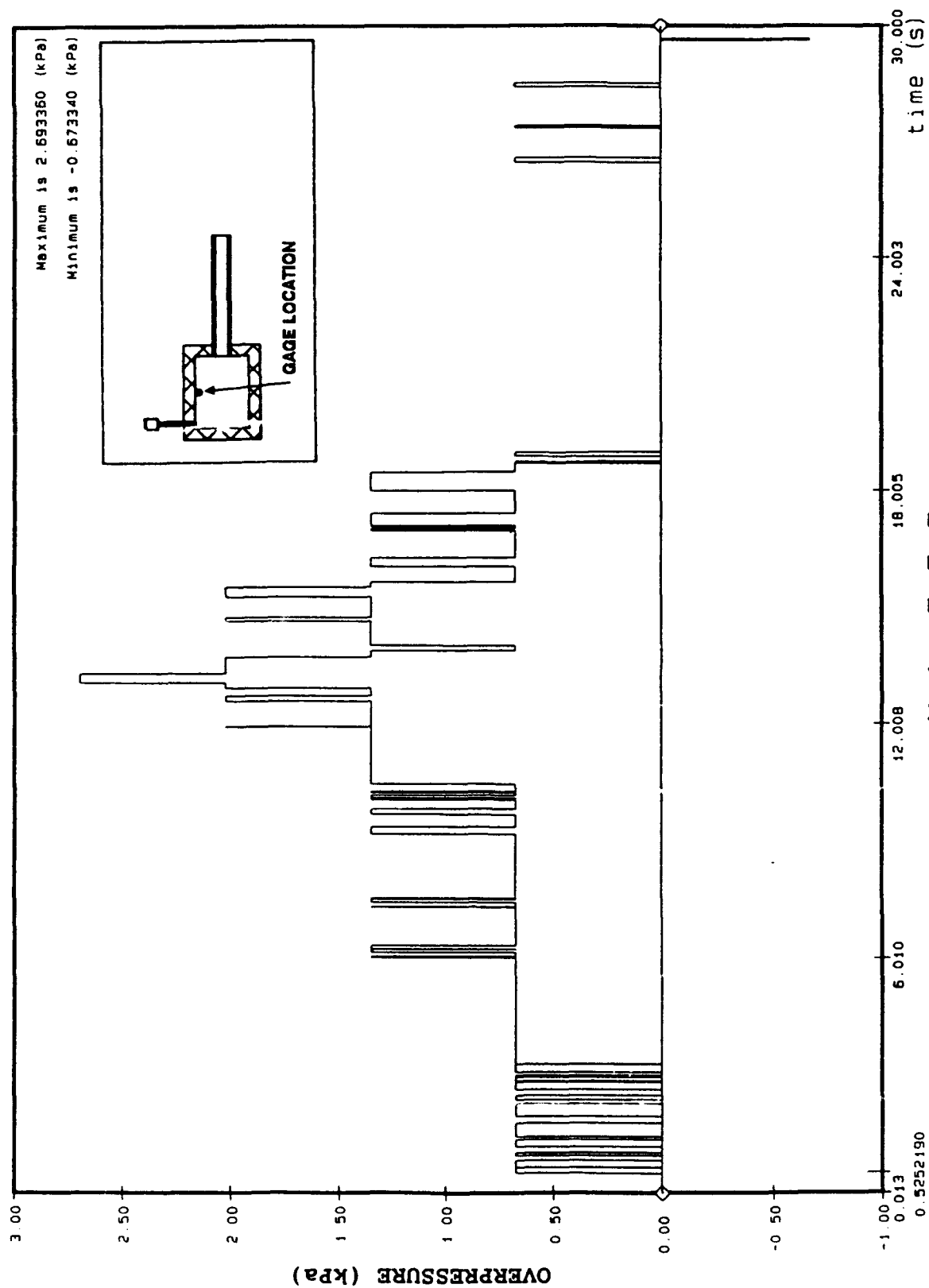
Figure: A2-10

K A I I I
Air Blast Internal Event C2
Pressure Gauge # ABI181B



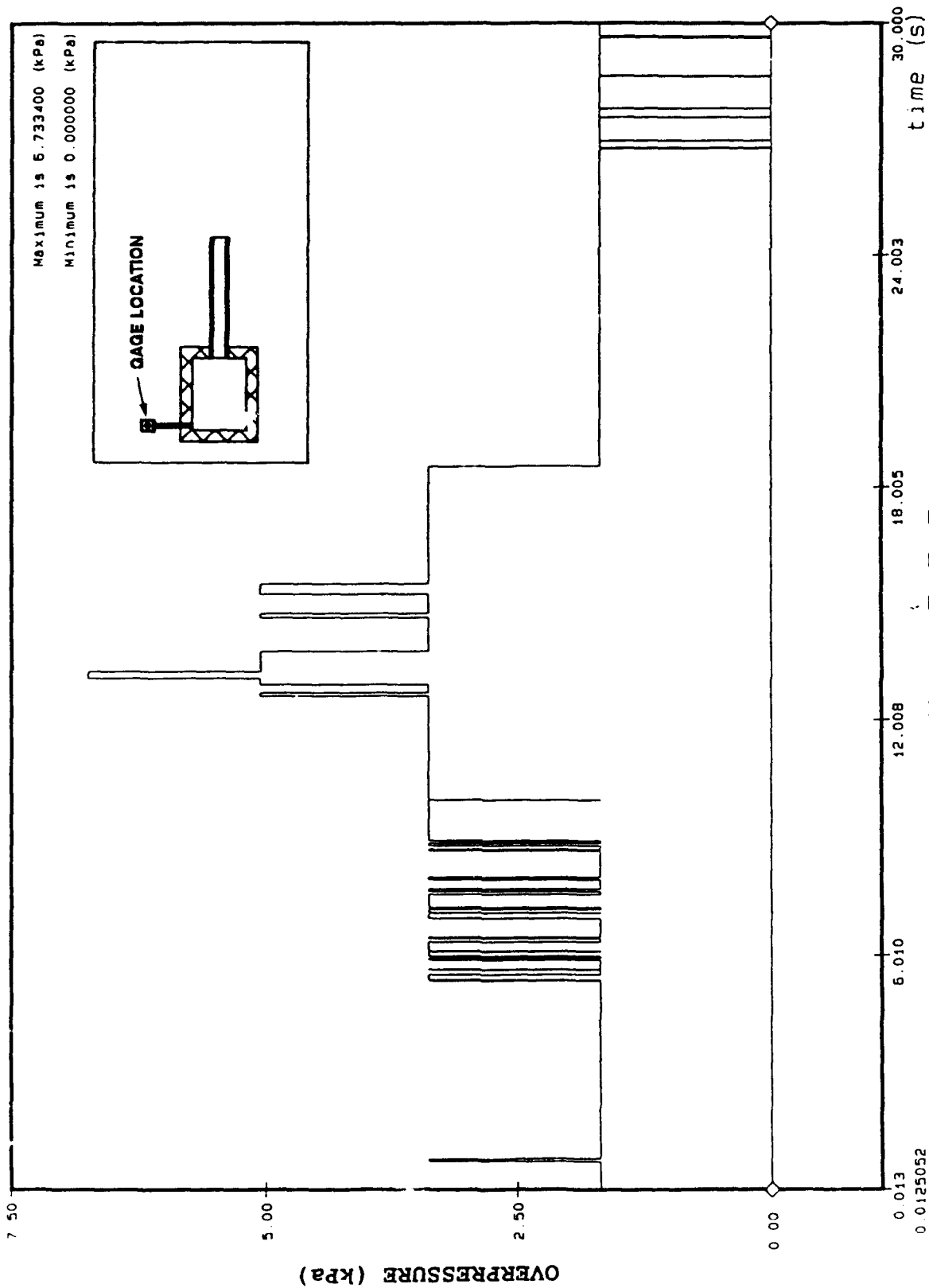
Filter 0 11 20 n2

Figure: A2-11



K A I I I
Air Blast Internal Event C2
Pressure Gauge # ABI183T

Filter @ 11.20 Hz

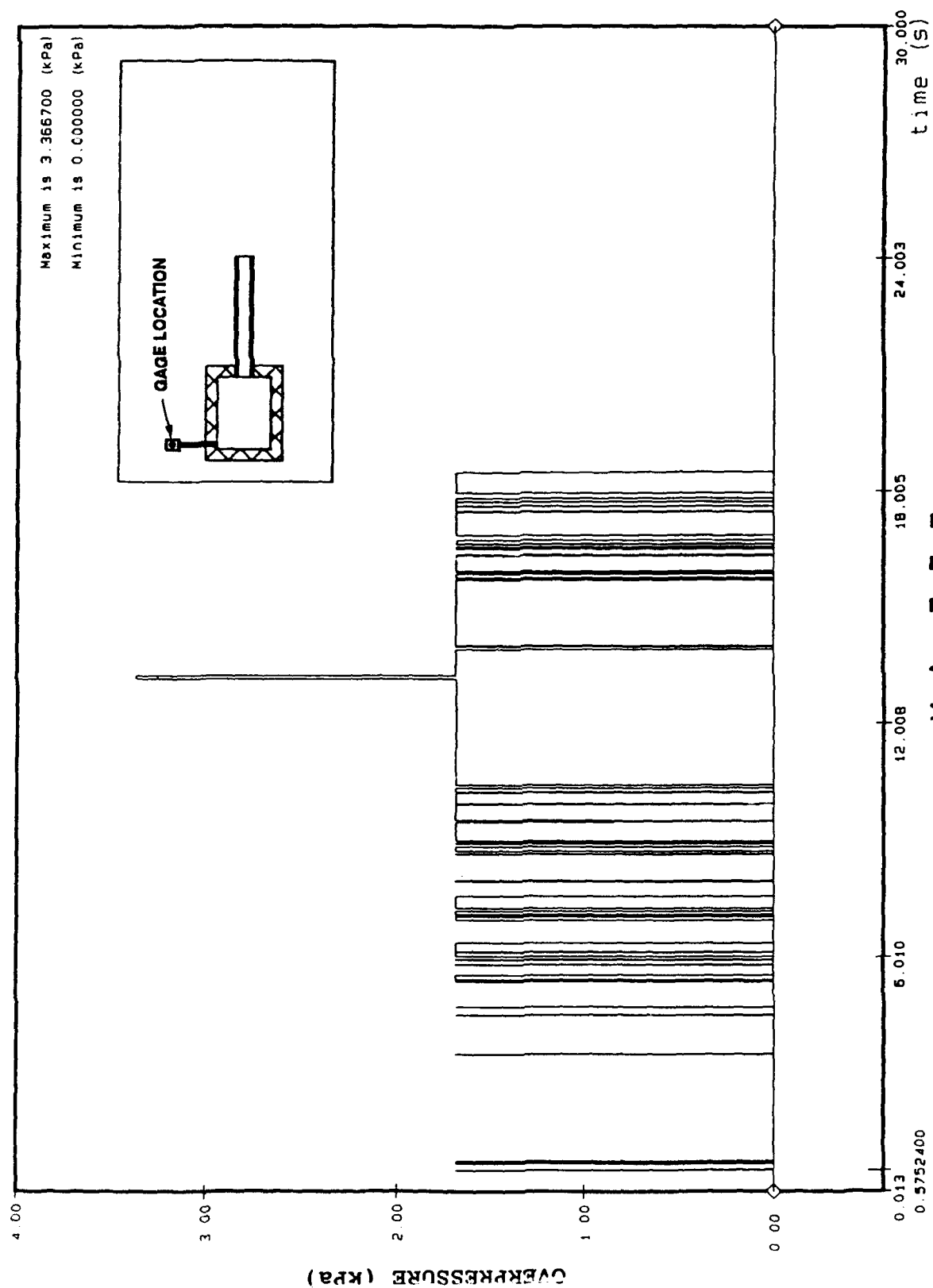


K A I I I

Air Blast Internal Event C2
Pressure Gauge # ABI185

Figure: A2-13

Filter 0.11.20 Hz



K A I I I
Air Blast Internal Event C2
Pressure Gauge # ABI186

Figure: A2-14

Filter @ 11.20 Hz

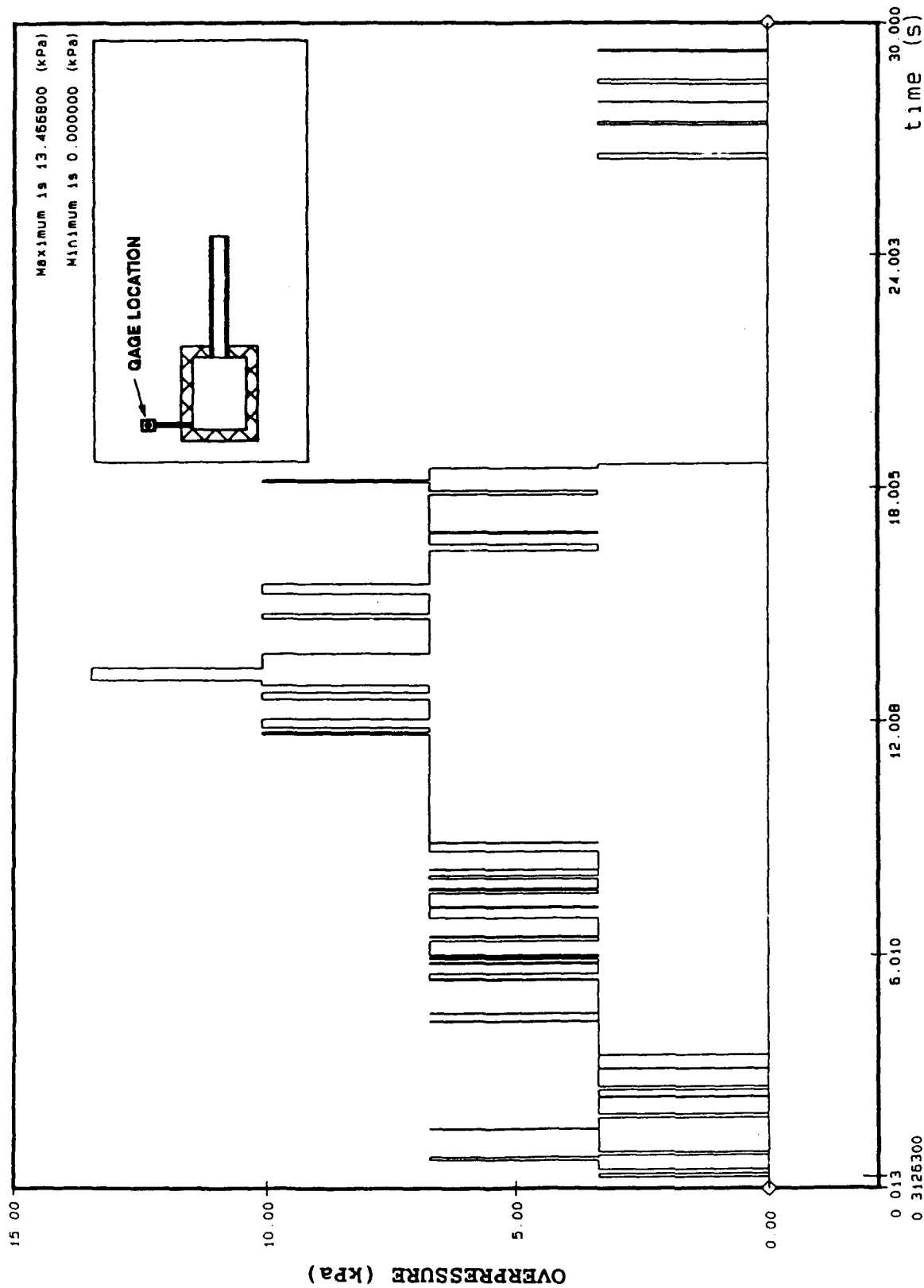
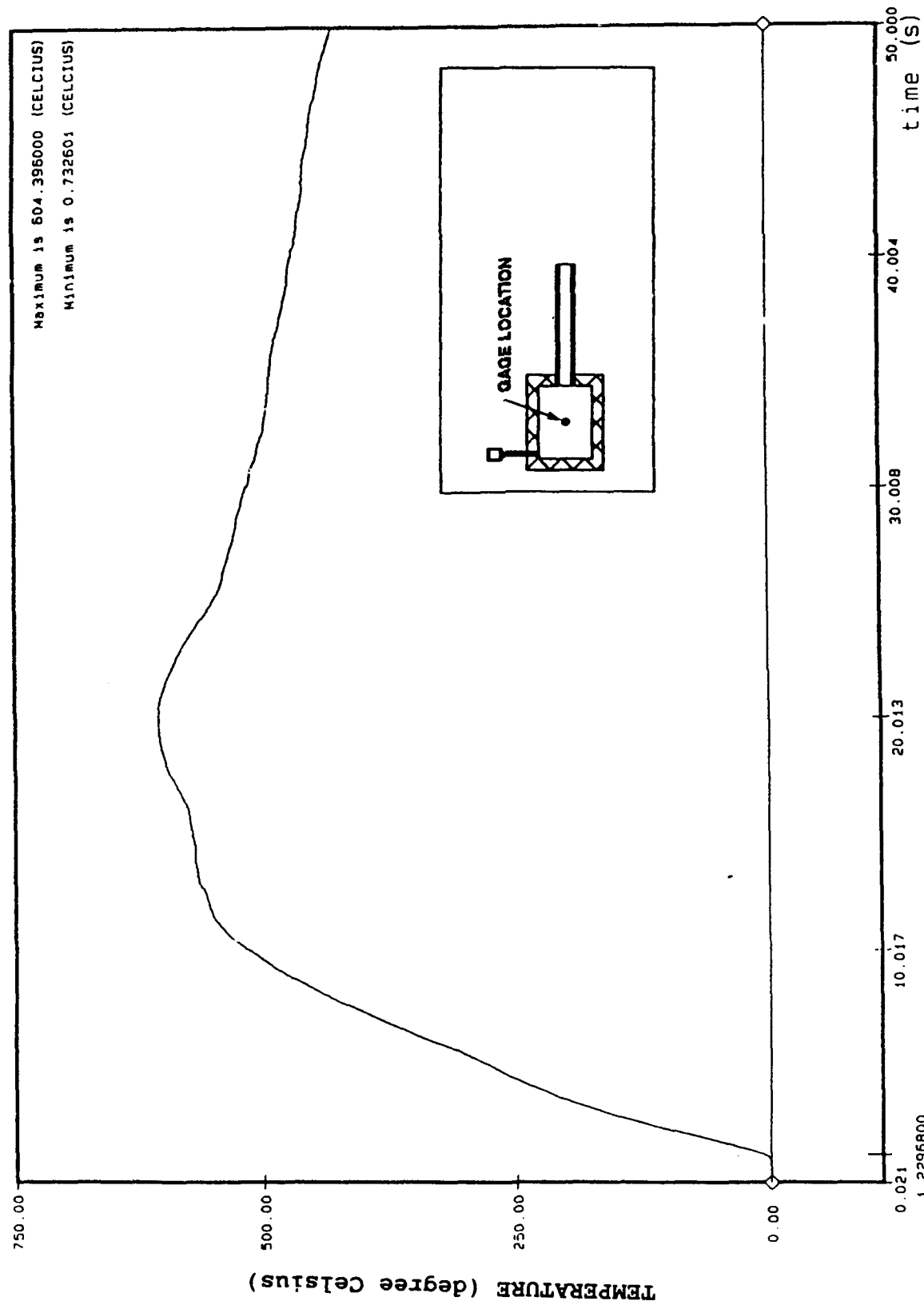


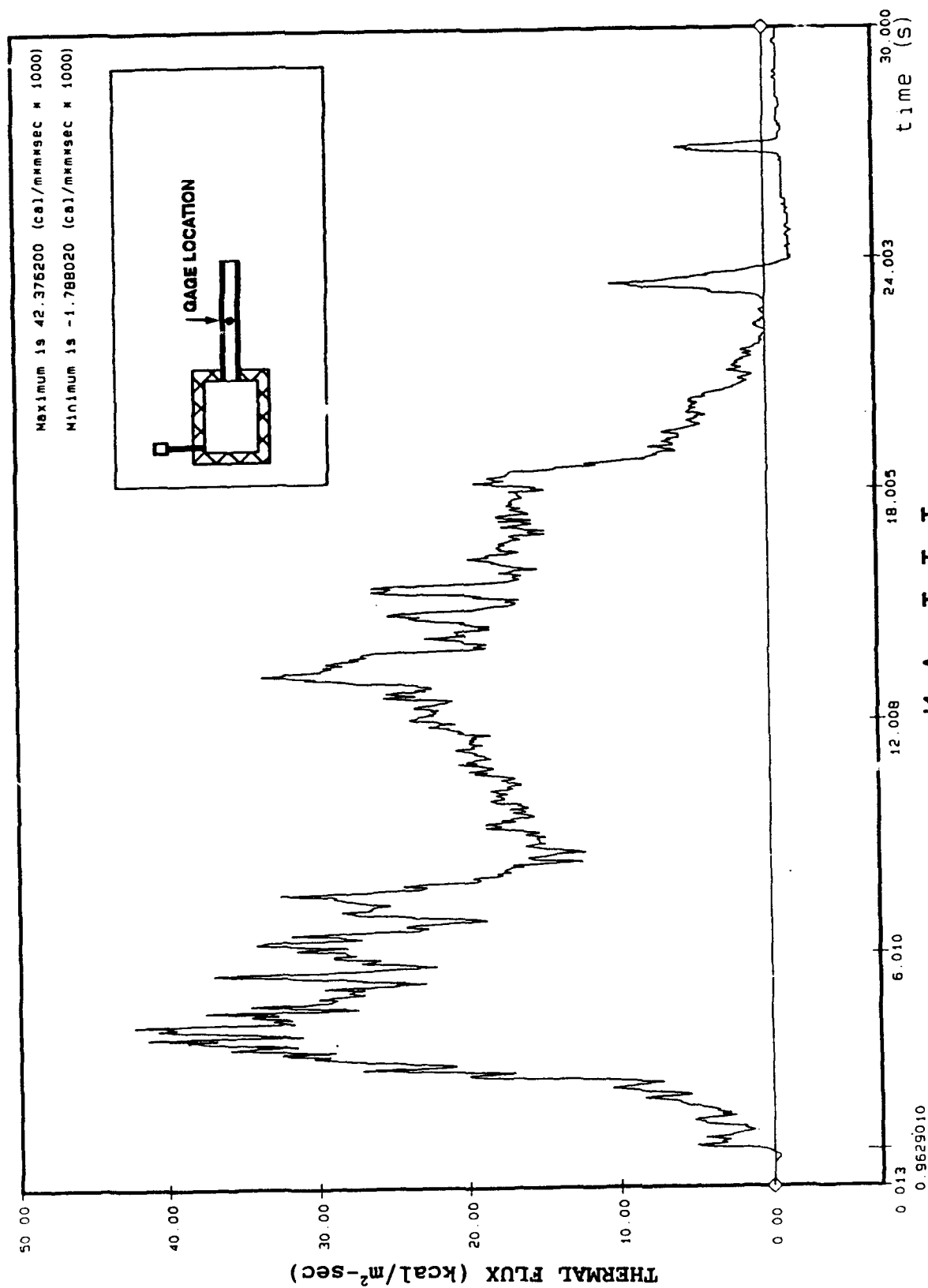
Figure: A2-15

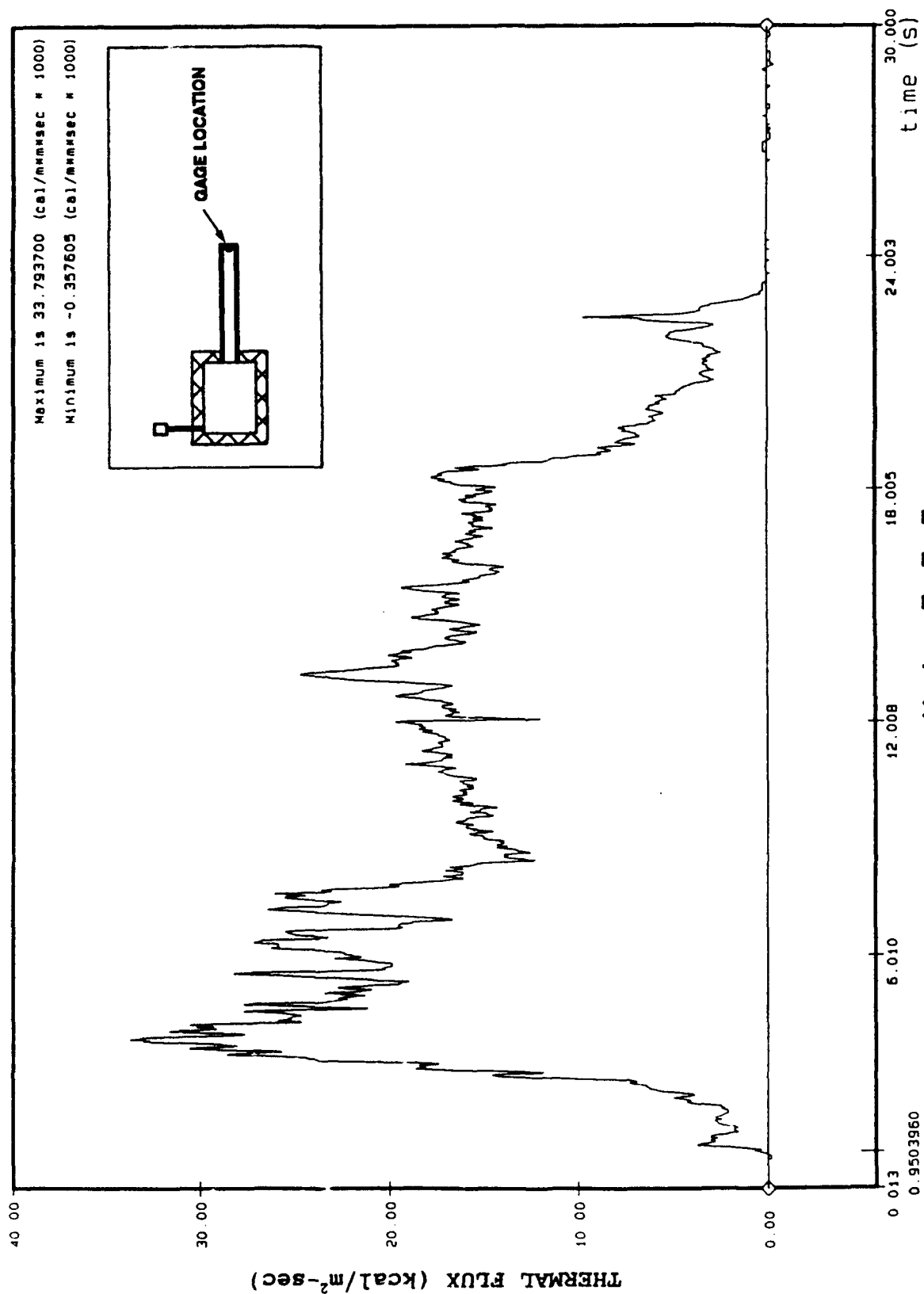


K A I I I
Temperature Experiment C 2
Thermocouple Gauge # THC190

Figure: A2-16

Filter # 5.72 Hz





K A I I I

Thermal Flux Event C2

Thermal Flux Gauge # TF192

Figure: A2-18

Filter 11.20 Hz

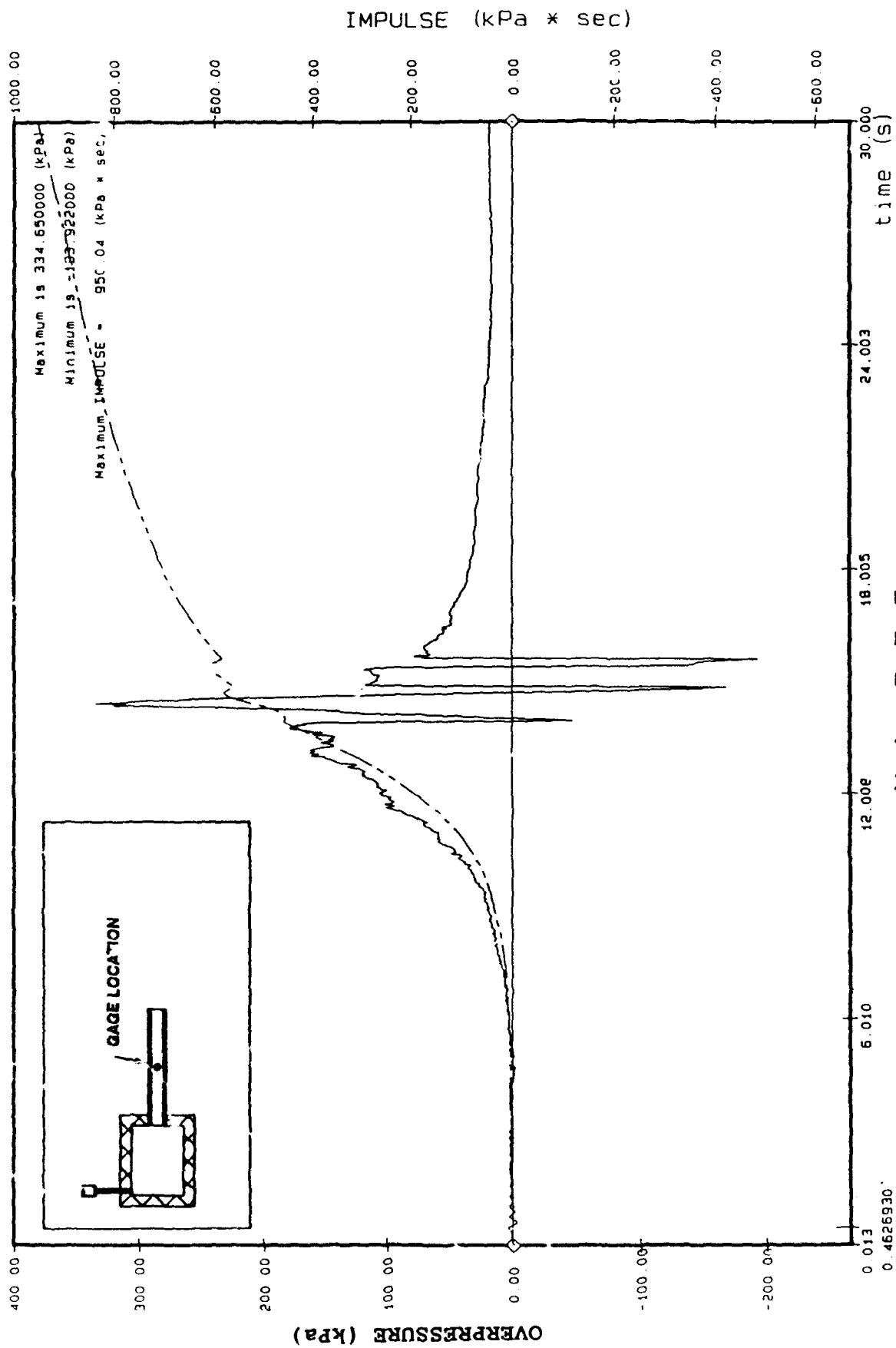
APPENDIX A3

KA-III, PHASE C

TEST C-3

100 kg M-1 PROPELLANT BURN

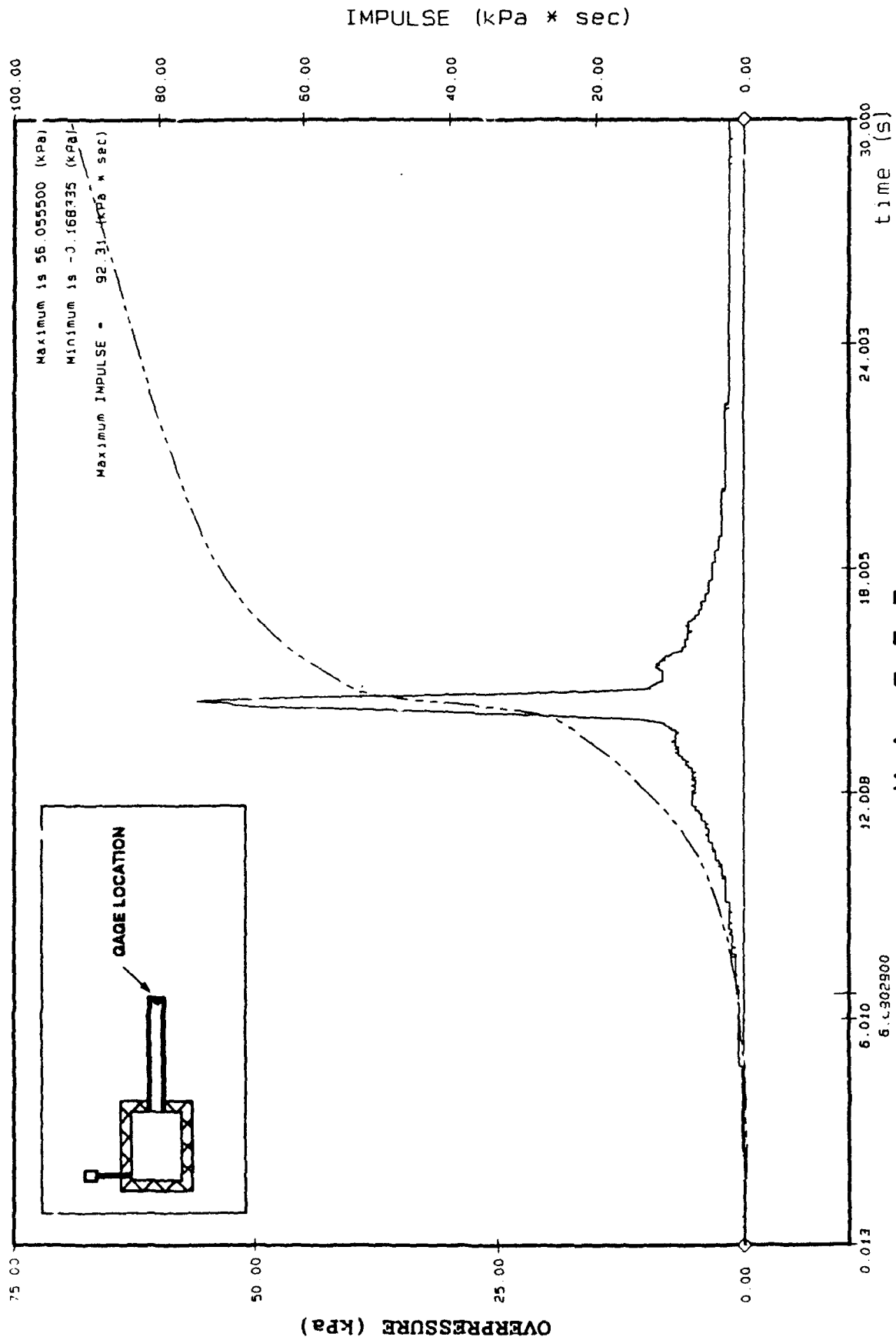
DATA-TIME HISTORIES



K A I I I
 Air Blast External Event C3
 Pressure Gauge # ABE171

Filter 15.20 Hz

Figure: A3-1



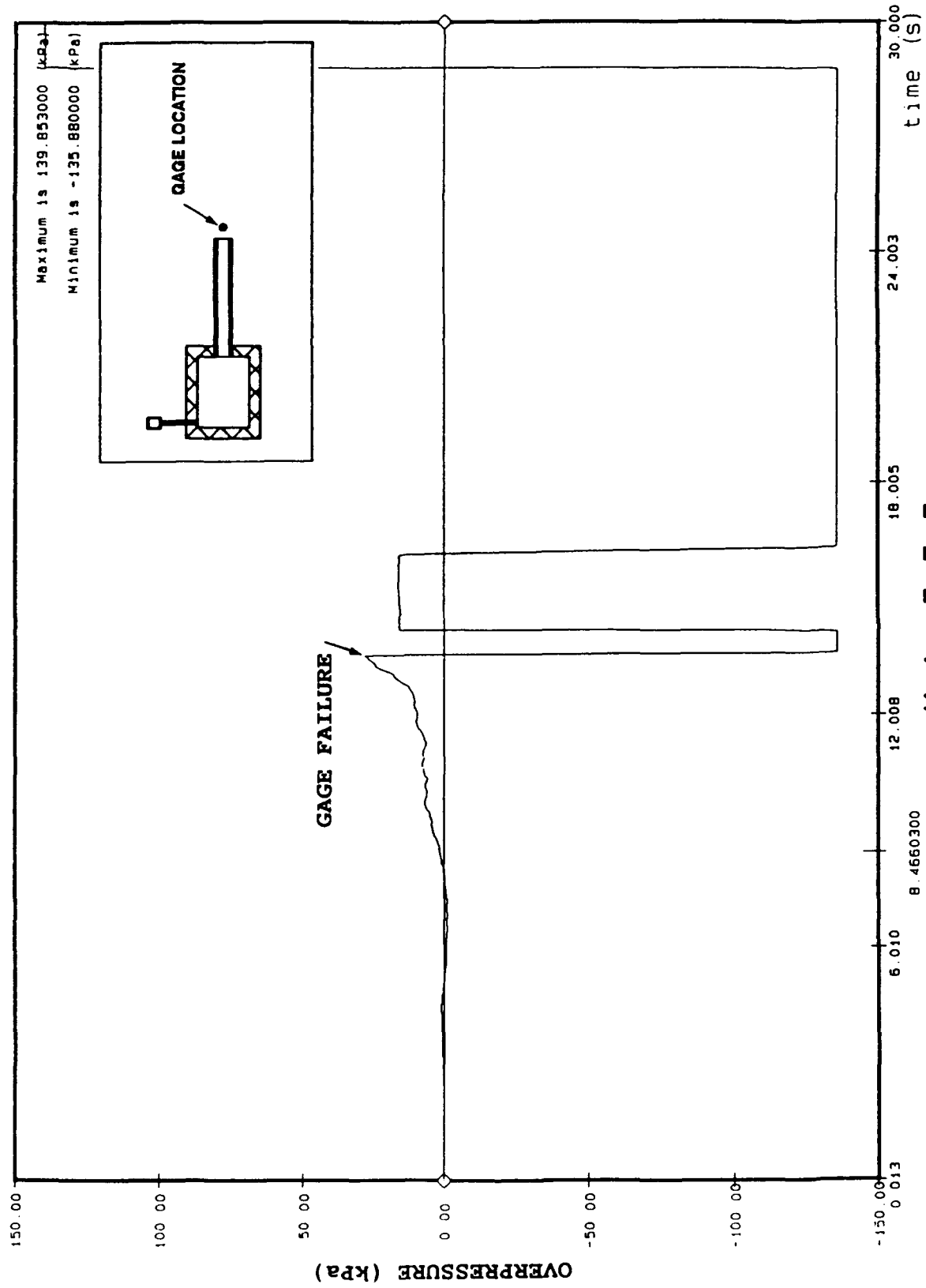
K A I I I

Air Blast External Event C3

Pressure Gauge # ABE172

Figure: A3-2

Filter # 11 20 n2



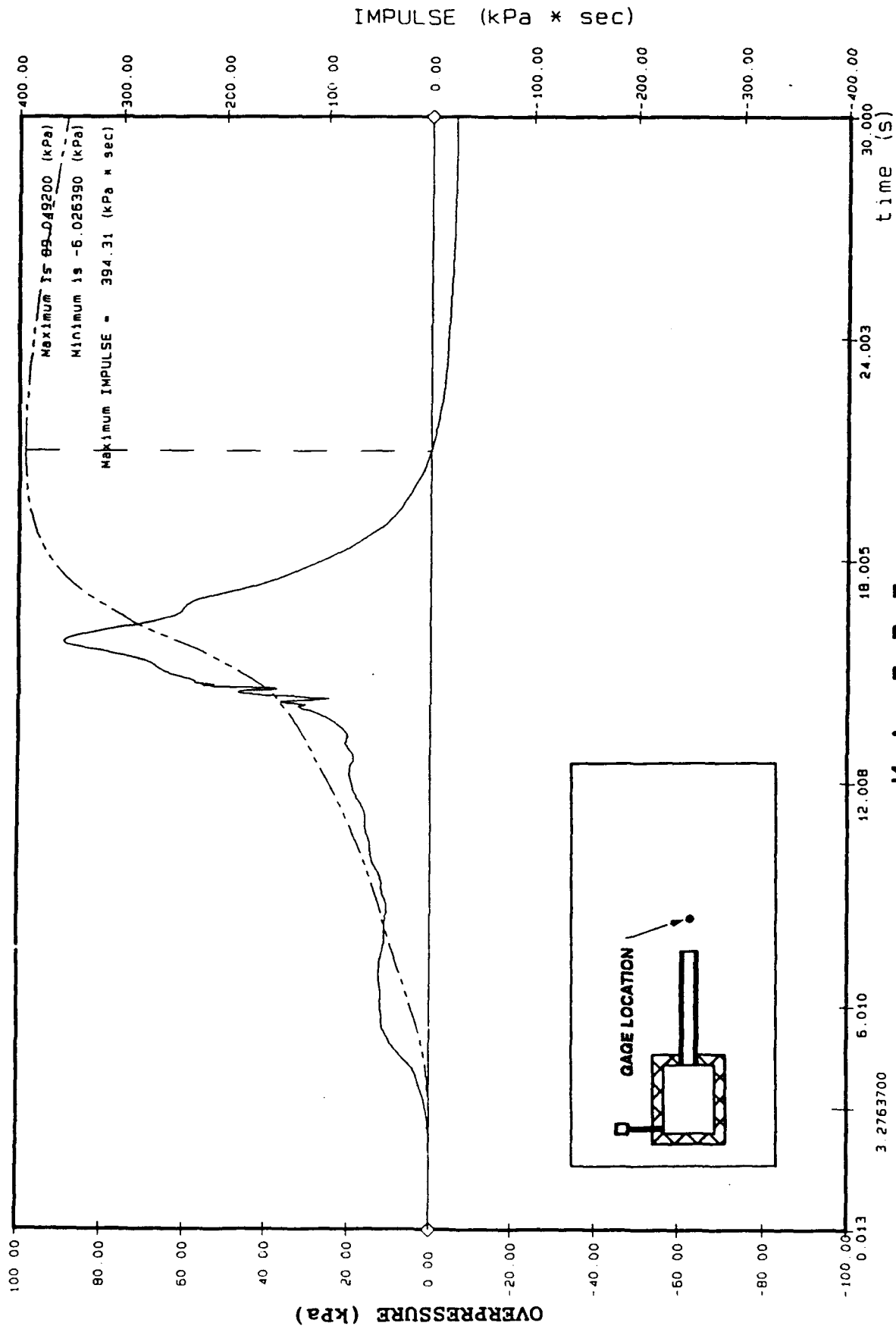
K A I I I

Air Blast External Event C3

Pressure Gauge # ABE173

Filter # 11 20 n2

Figure: A3-3



K A I I I
Air Blast External Event C3
Pressure Gauge # ABE174

Filter # 11.20 Hz

Figure: A3-4

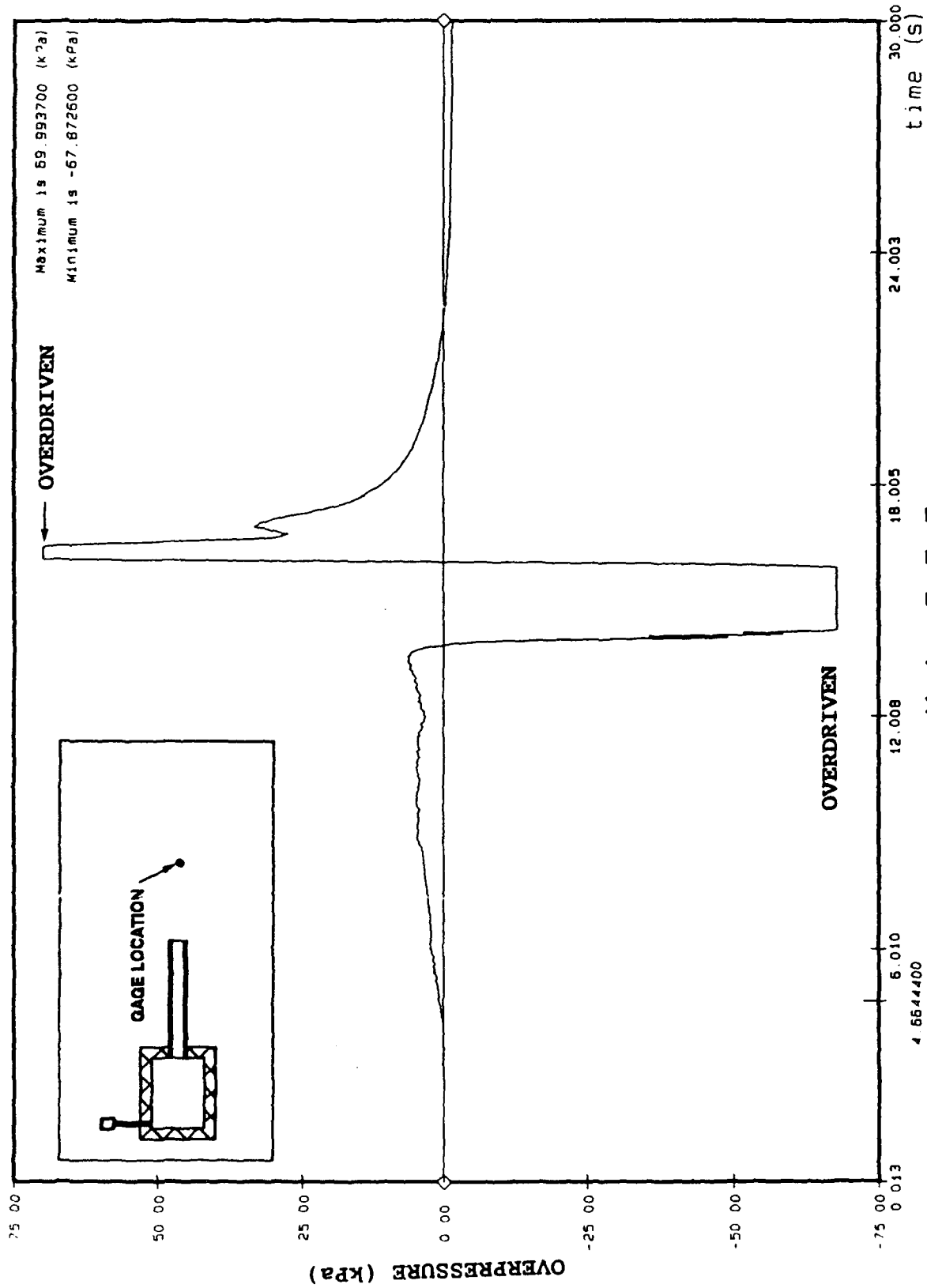
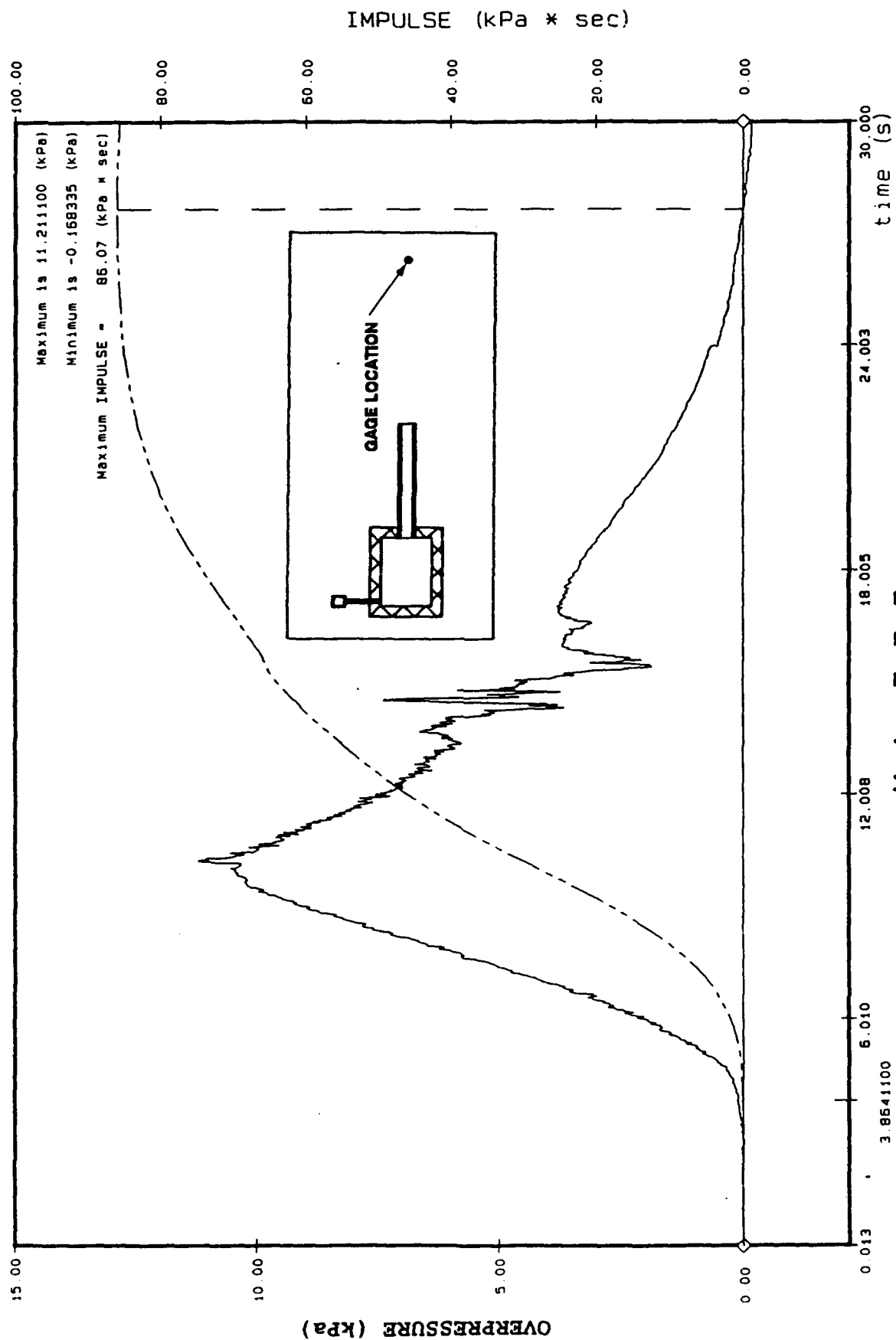


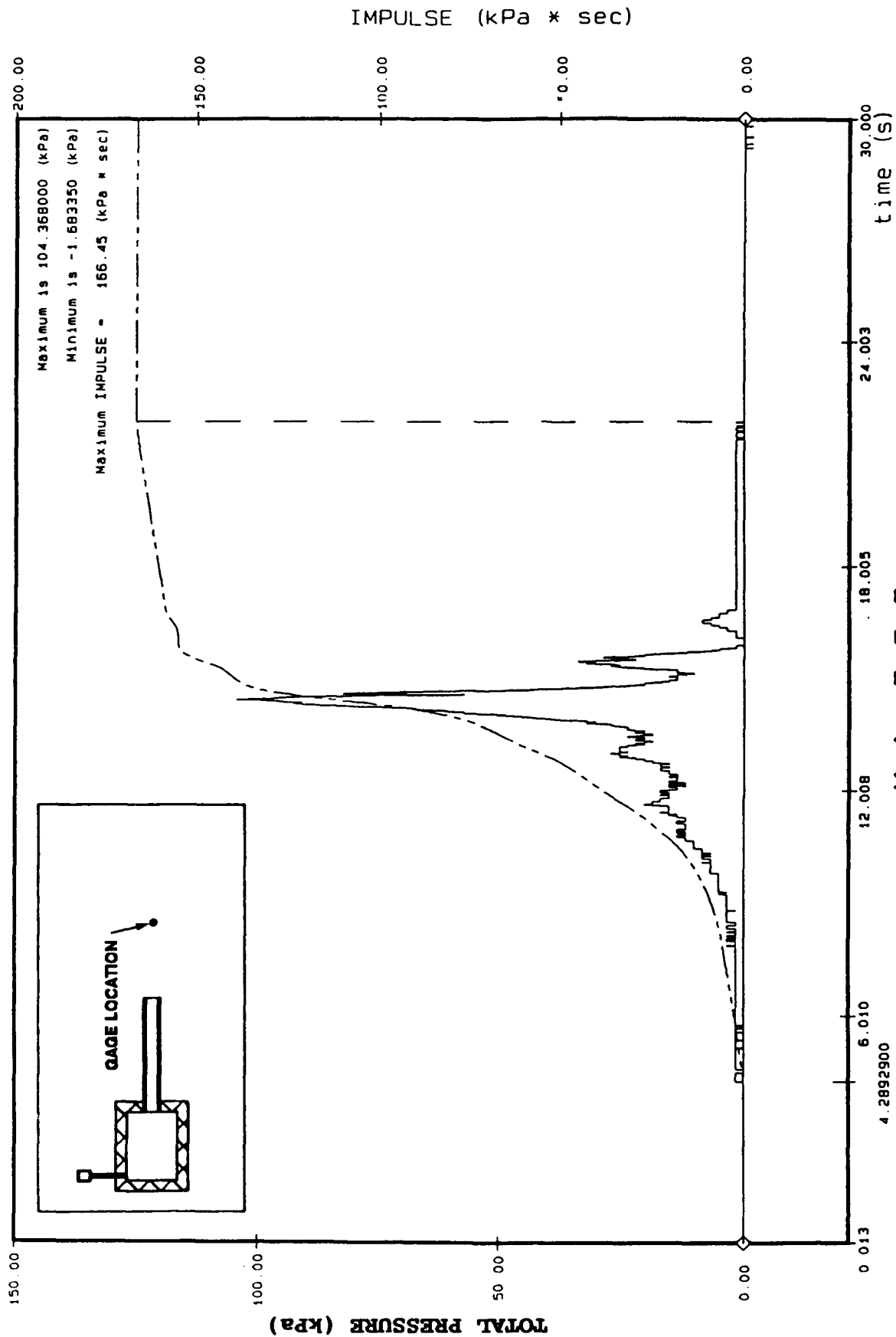
Figure: A3-5



K A I I I
Air Blast External Event C3
Pressure Gauge # ABE176

Figure: A3-6

Filter @ 11.20 Hz



K A I I I
Air Blast External Head Event C3
Pressure Gauge # ABEH178

Figure: A3-7

Filter 0 11 20 Hz

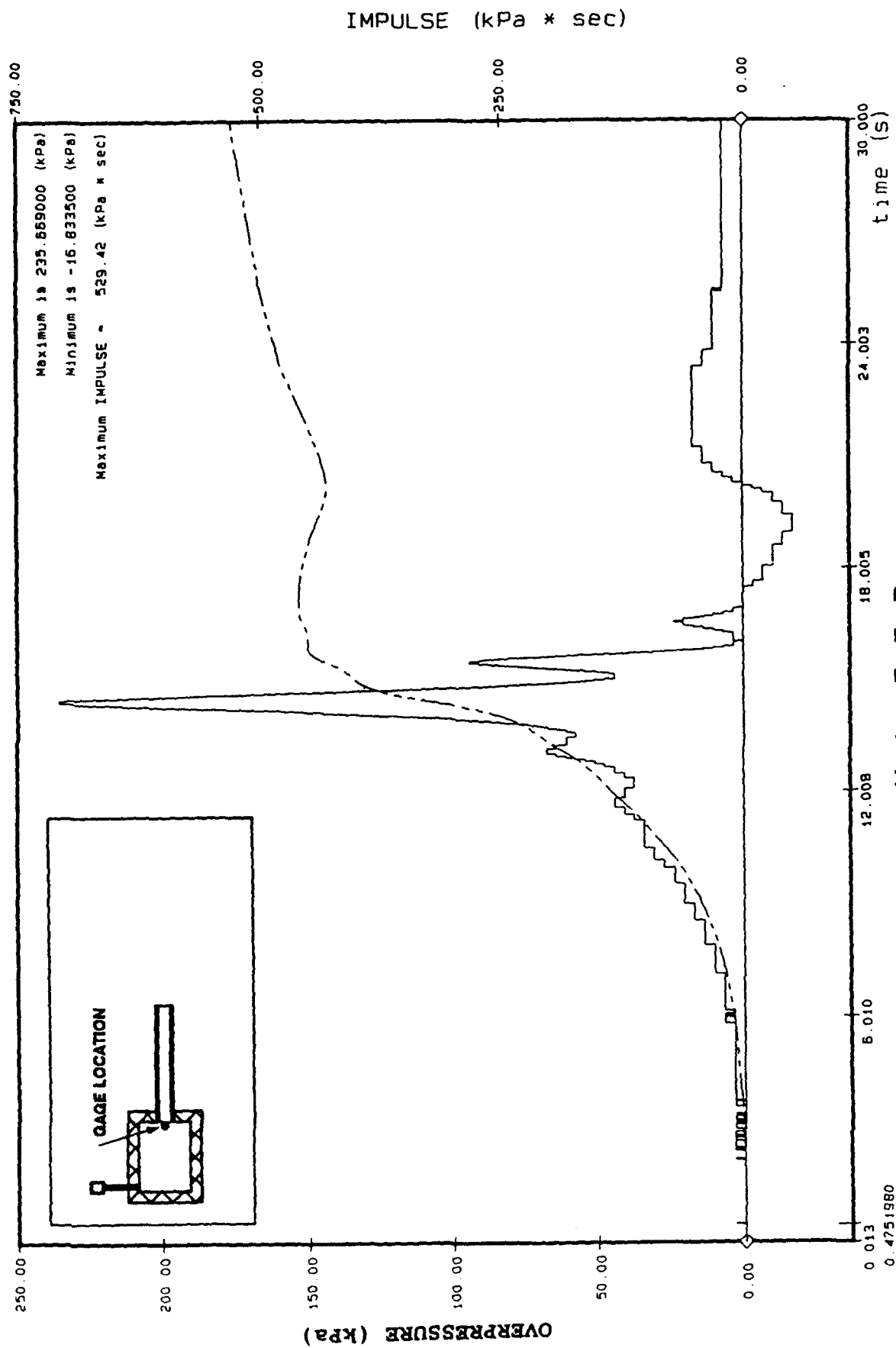
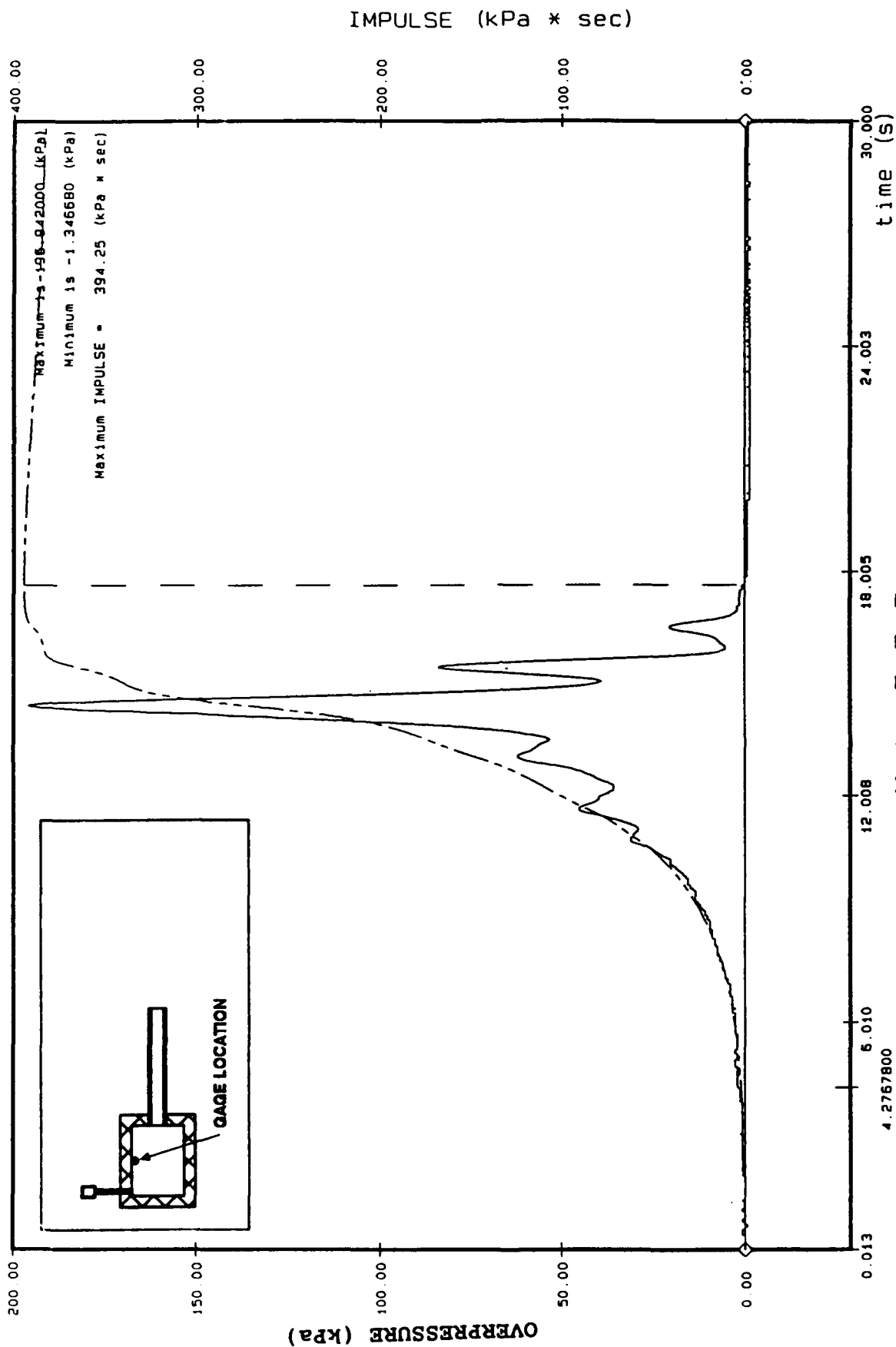


Figure: A3-8

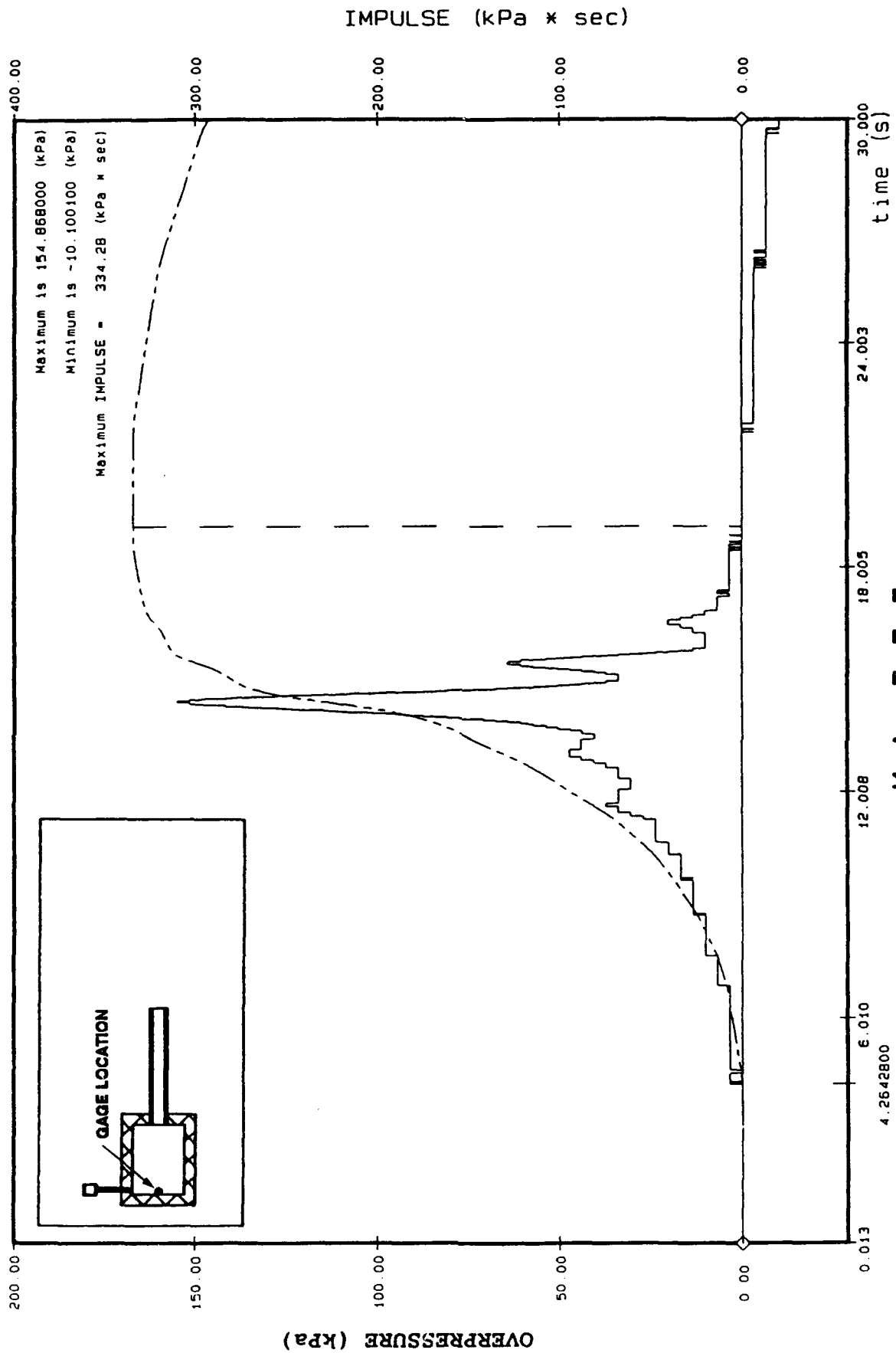
Filter 0 11 20 n2



K A I I I
 Air Blast Internal Event C3
 Pressure Gauge # ABI181B

Figure: A3-9

Filter # 11.20 n2



K A I I I
 Air Blast Internal Event C3
 Pressure Gauge # ABI182
 Filter @ 11.20 Hz

Figure: A3-10

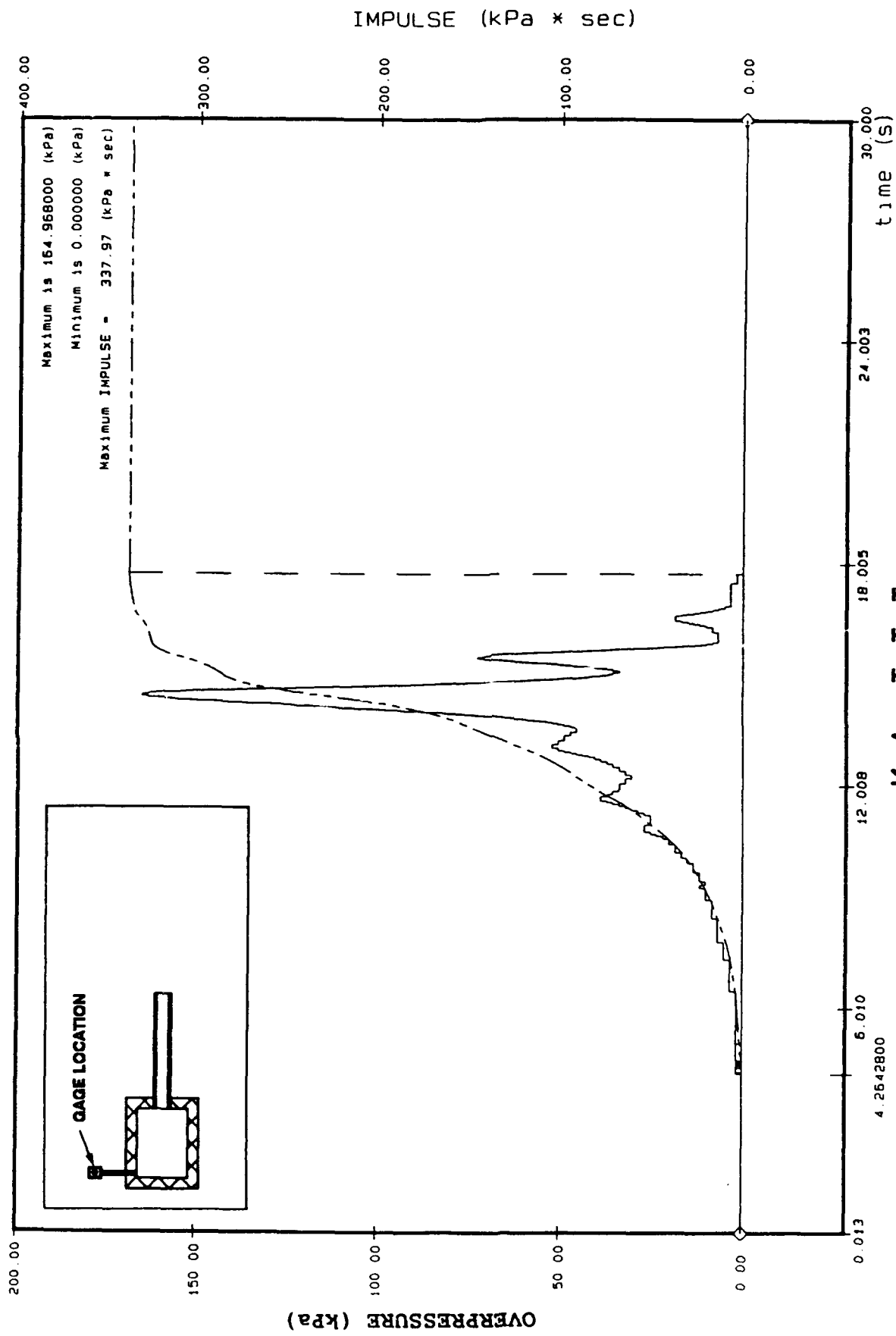


Figure: A3-11

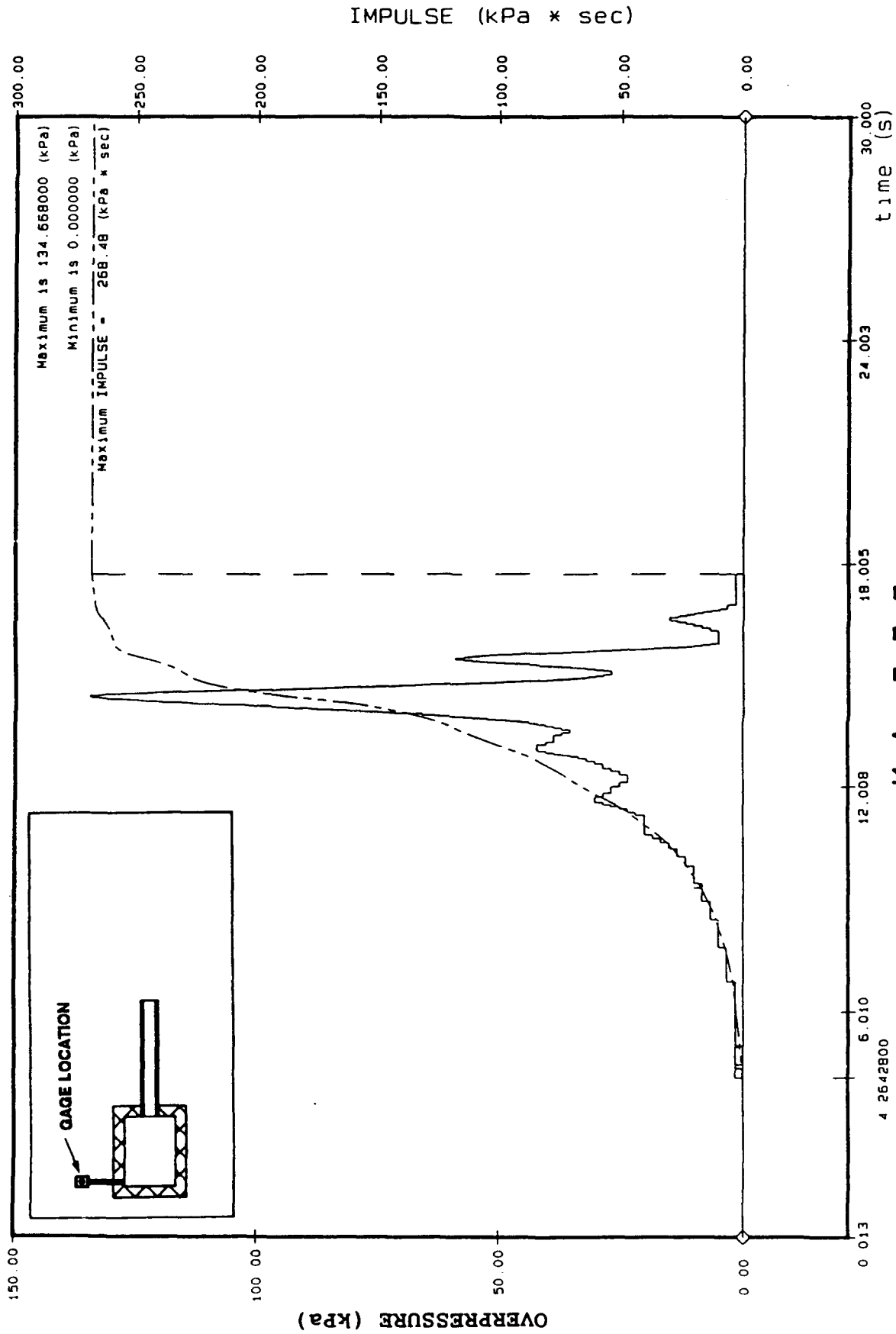


Figure: A3-12

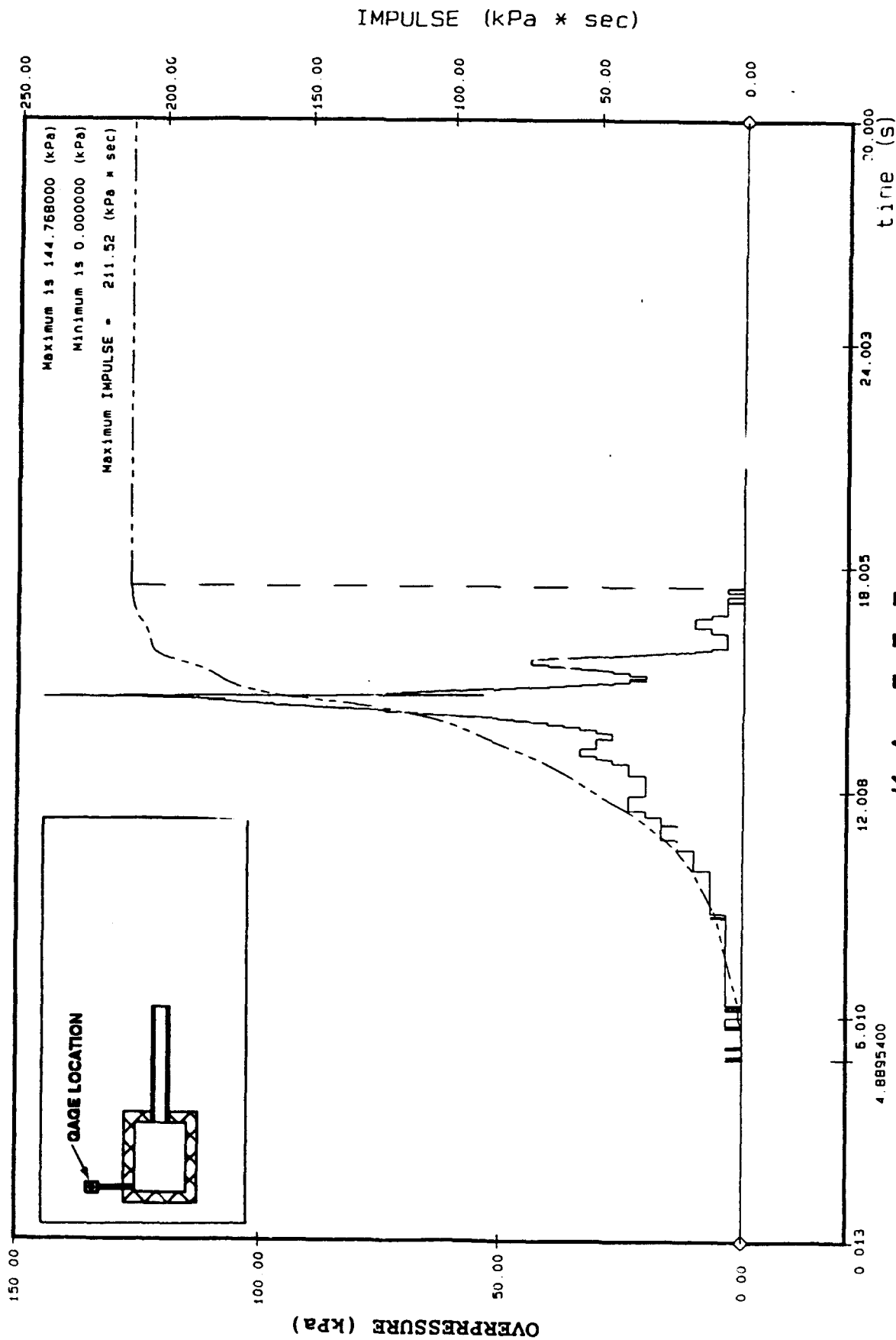
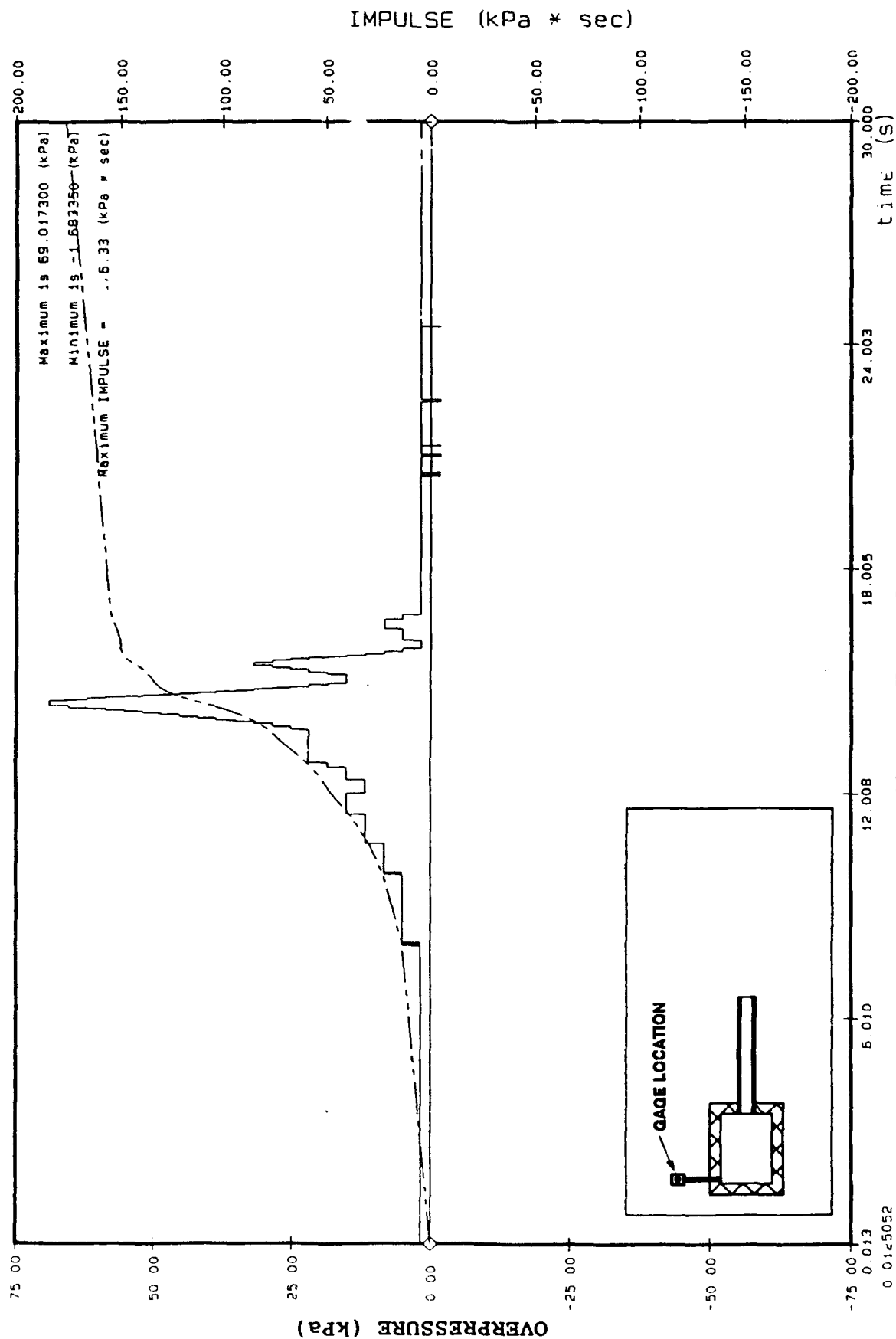


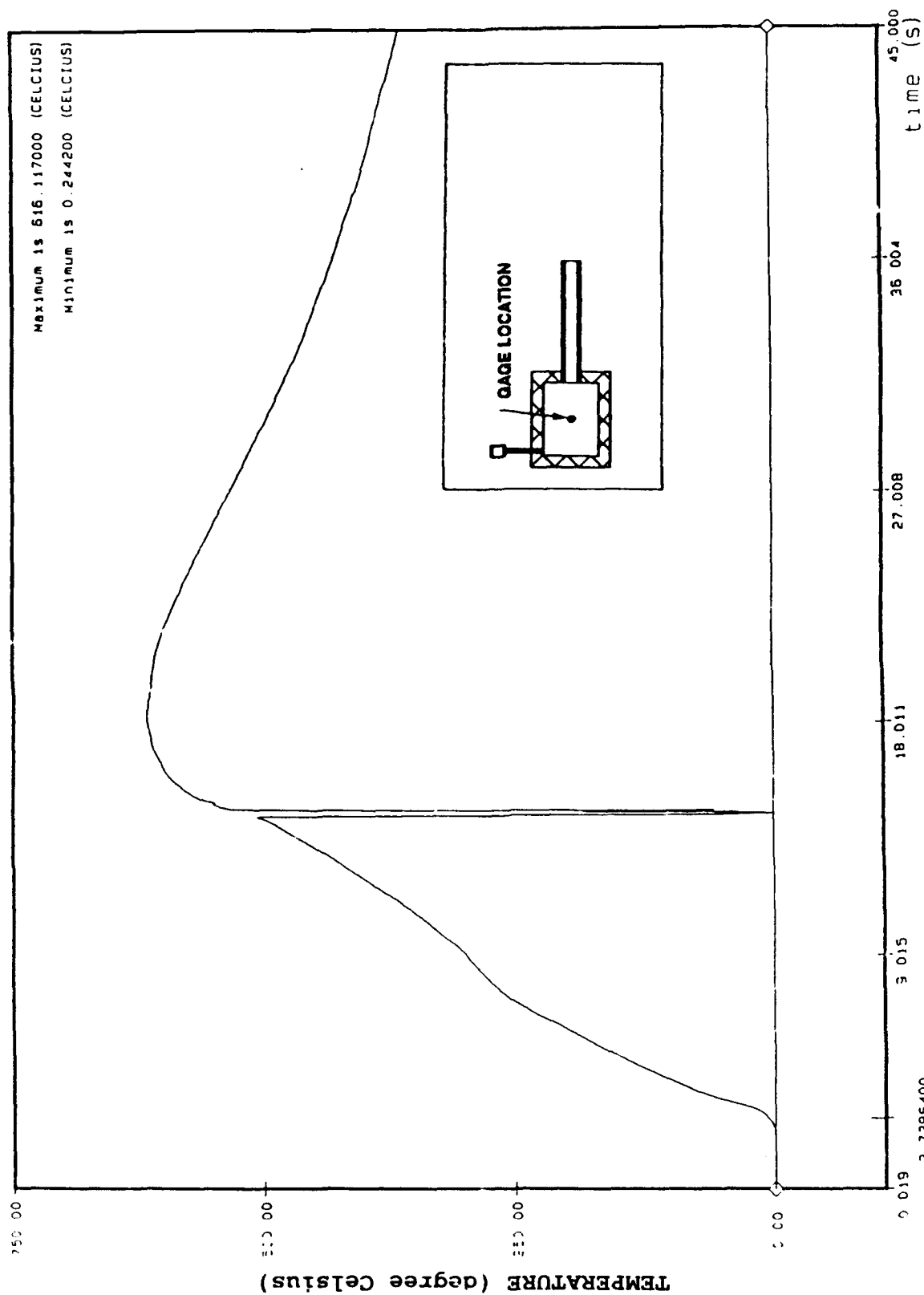
Figure: A3-13



K A I I I
Air Blast Internal Event C3
Pressure Gauge # ABI188

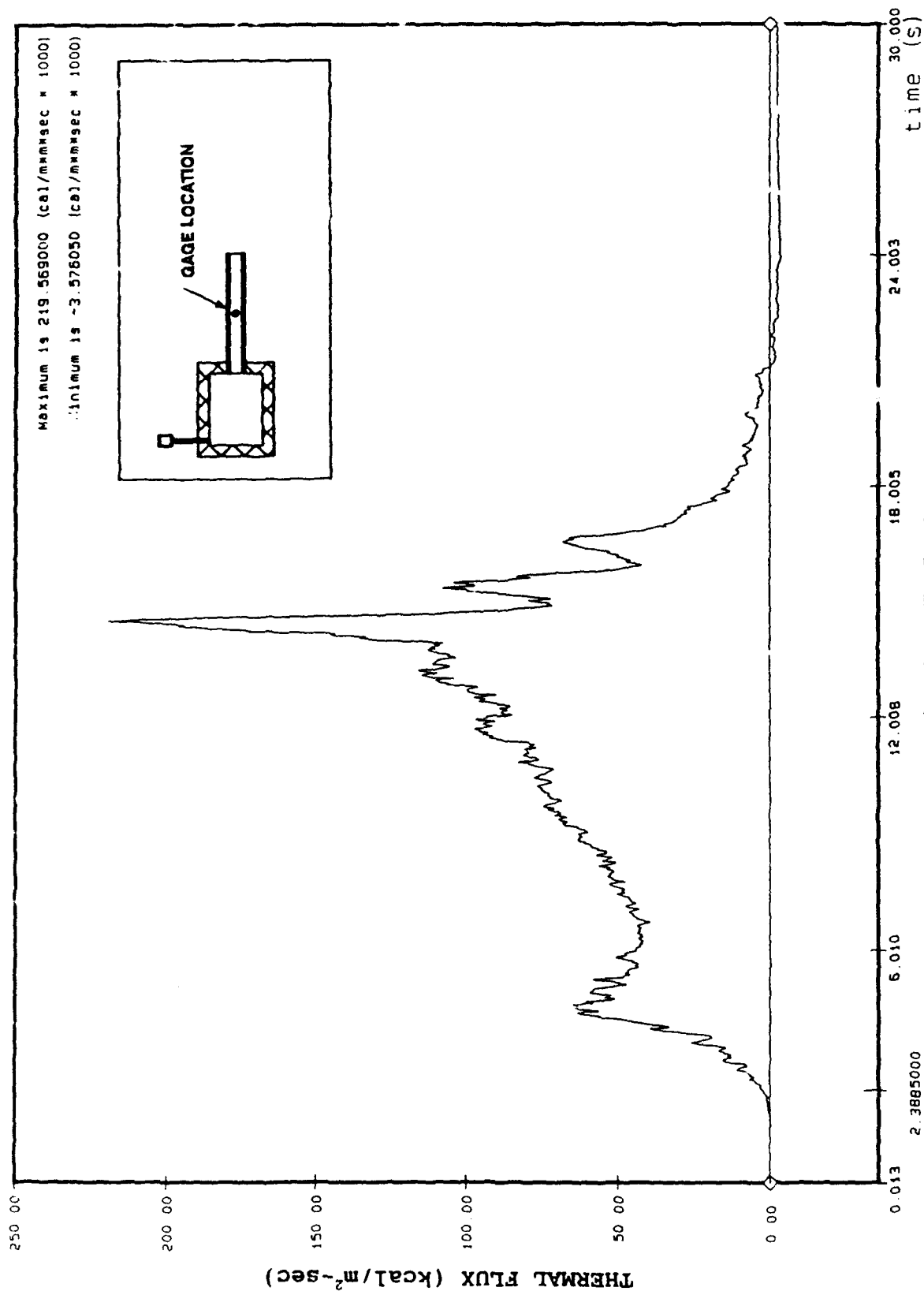
Figure: A3-14

Filter # 11 20 n2



K A I I I
Temperature Experiment C 3
Thermocouple Gauge # THC190

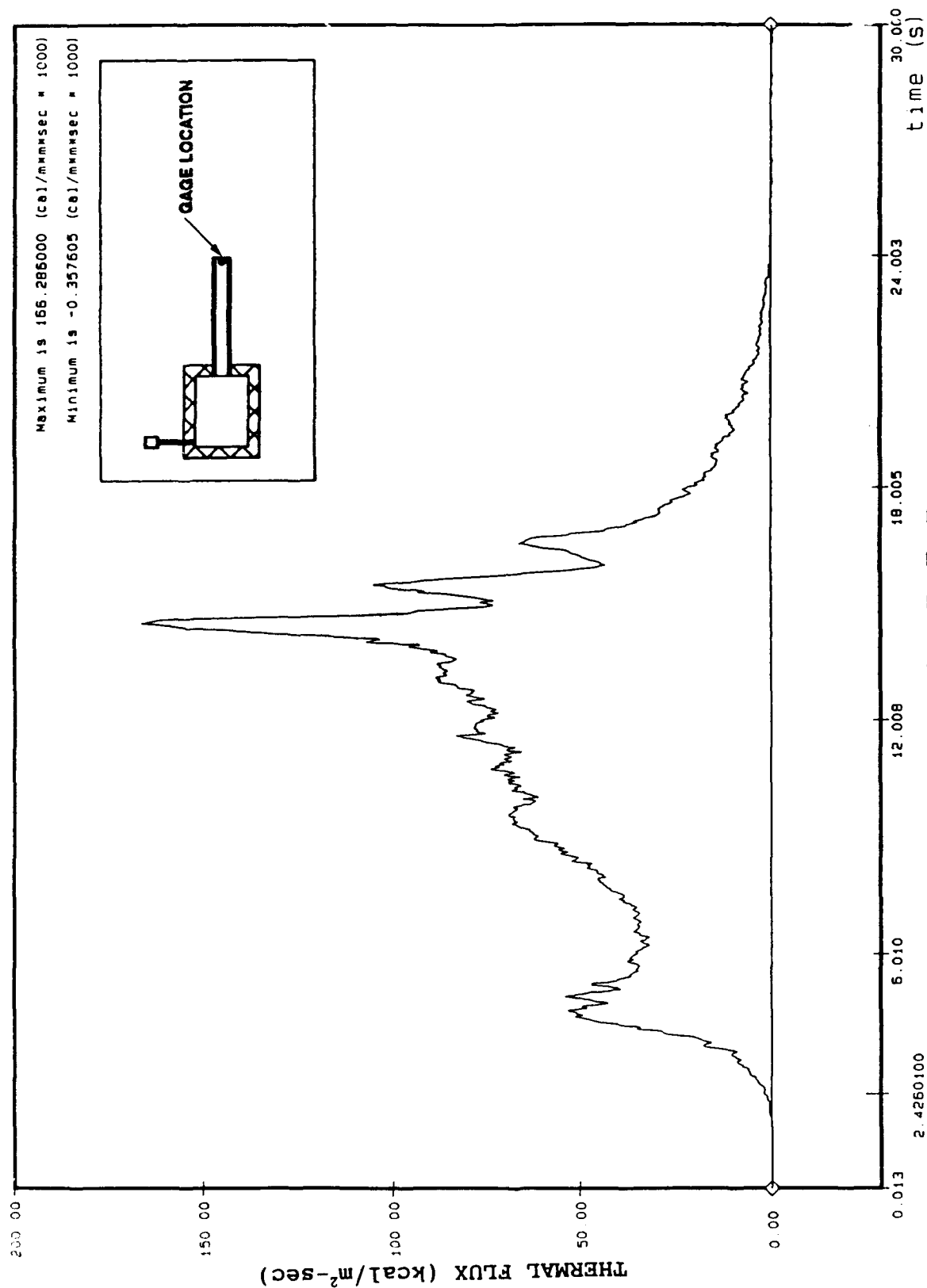
Figure: A3-15



Filter @ 11.20 Hz

Figure: A3-16

107



Thermal Flux Event C3
Thermal Flux Gauge # TF192

Filter @ 11.20 Hz

Figure: A3-17

APPENDIX A4

KA-III, PHASE C

TEST C-4

250 kg M-1 PROPELLANT BURN

DATA-TIME HISTORIES

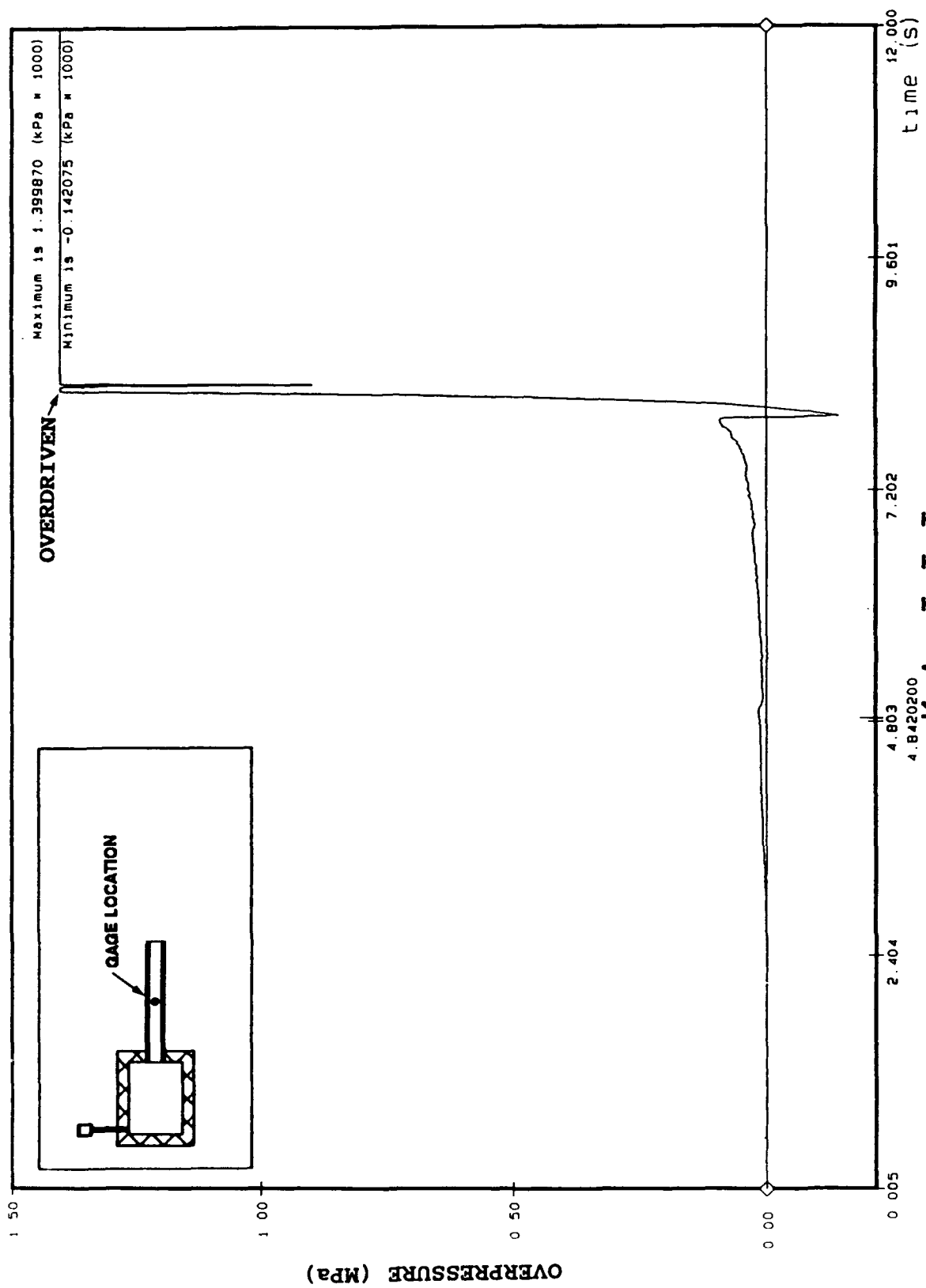
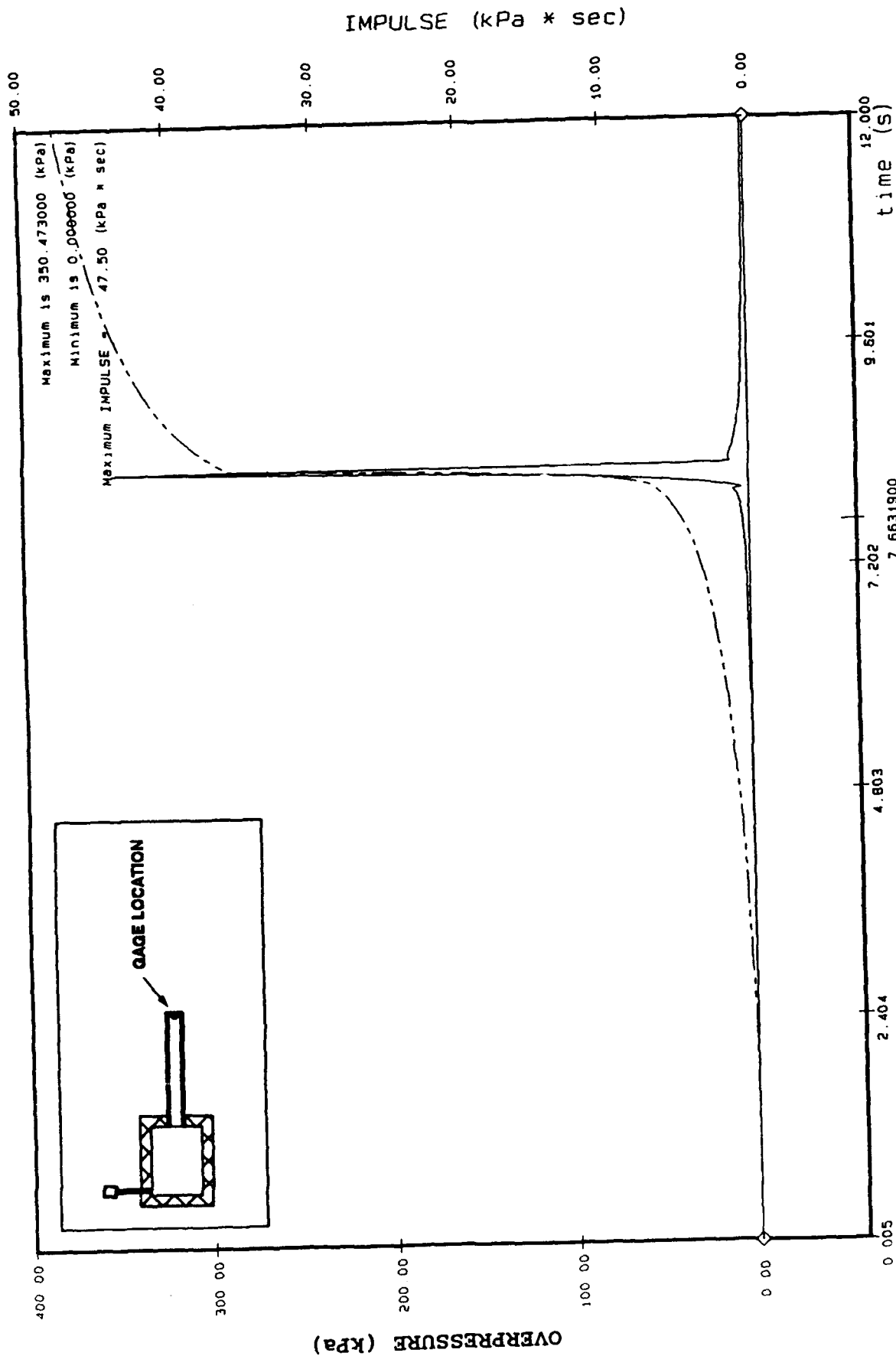


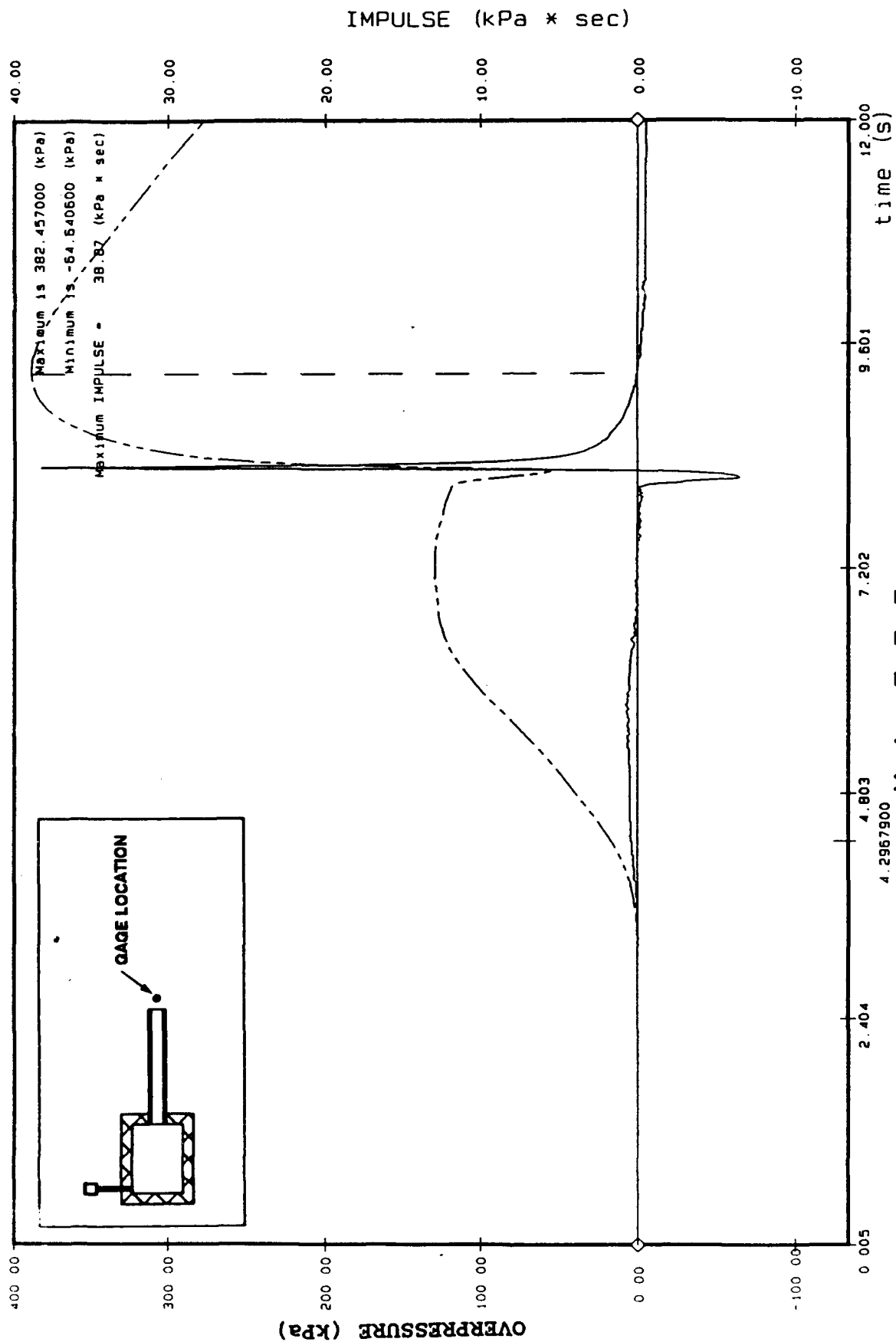
Figure: A4-1



K A I I I
Air Blast External Event C4
Pressure Gauge # ABE172

Figure: A4-2

Filter # 28.00 Hz



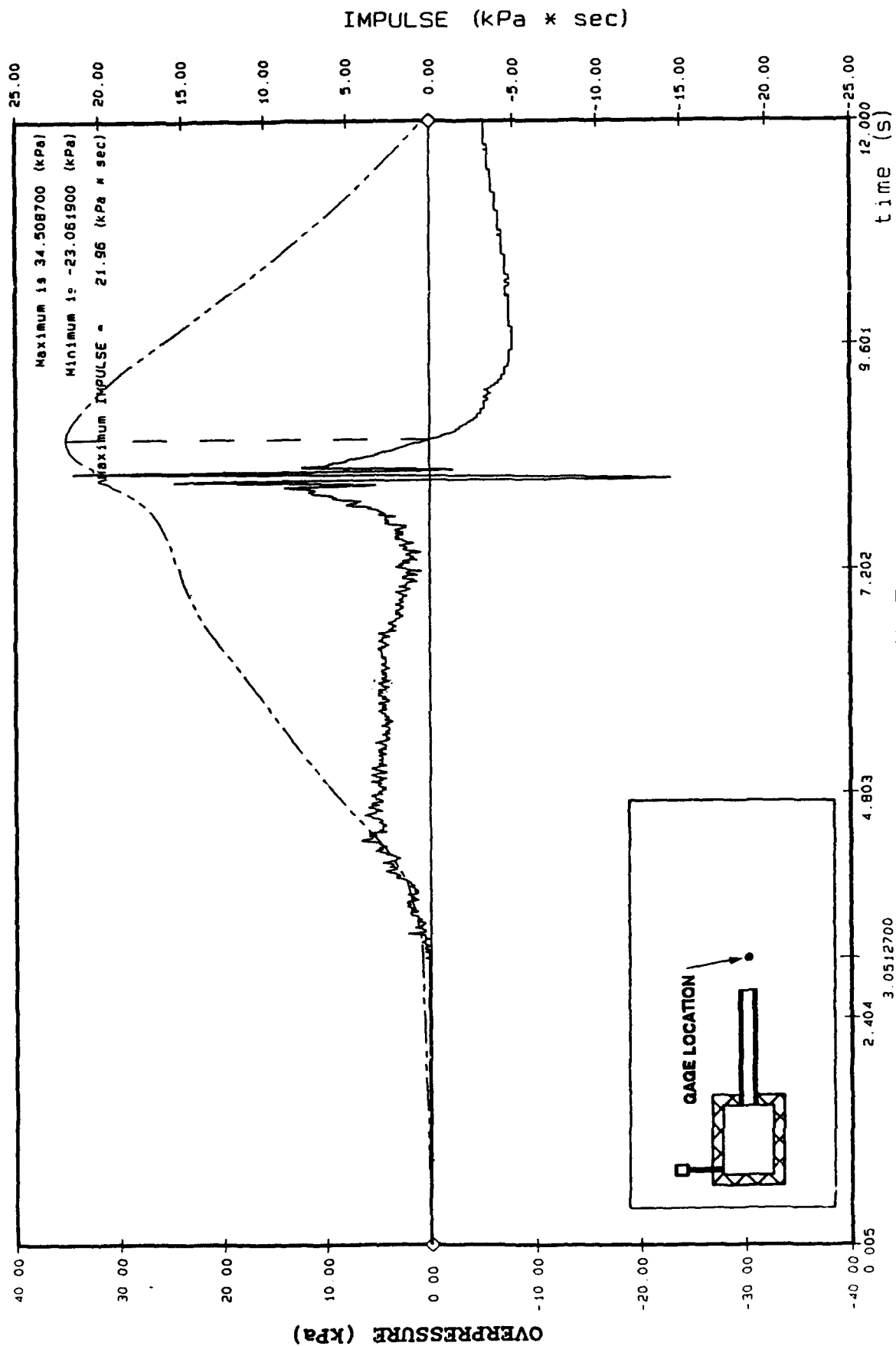
K A I I I

Air Blast External Event C4

Pressure Gauge # ABE173

Figure: A4-3

Filter @ 28.00 Hz



K A I I I
Air Blast External Event C4
Pressure Gauge # ABE174

Figure: A4-4

Filter @ 28.00 Hz

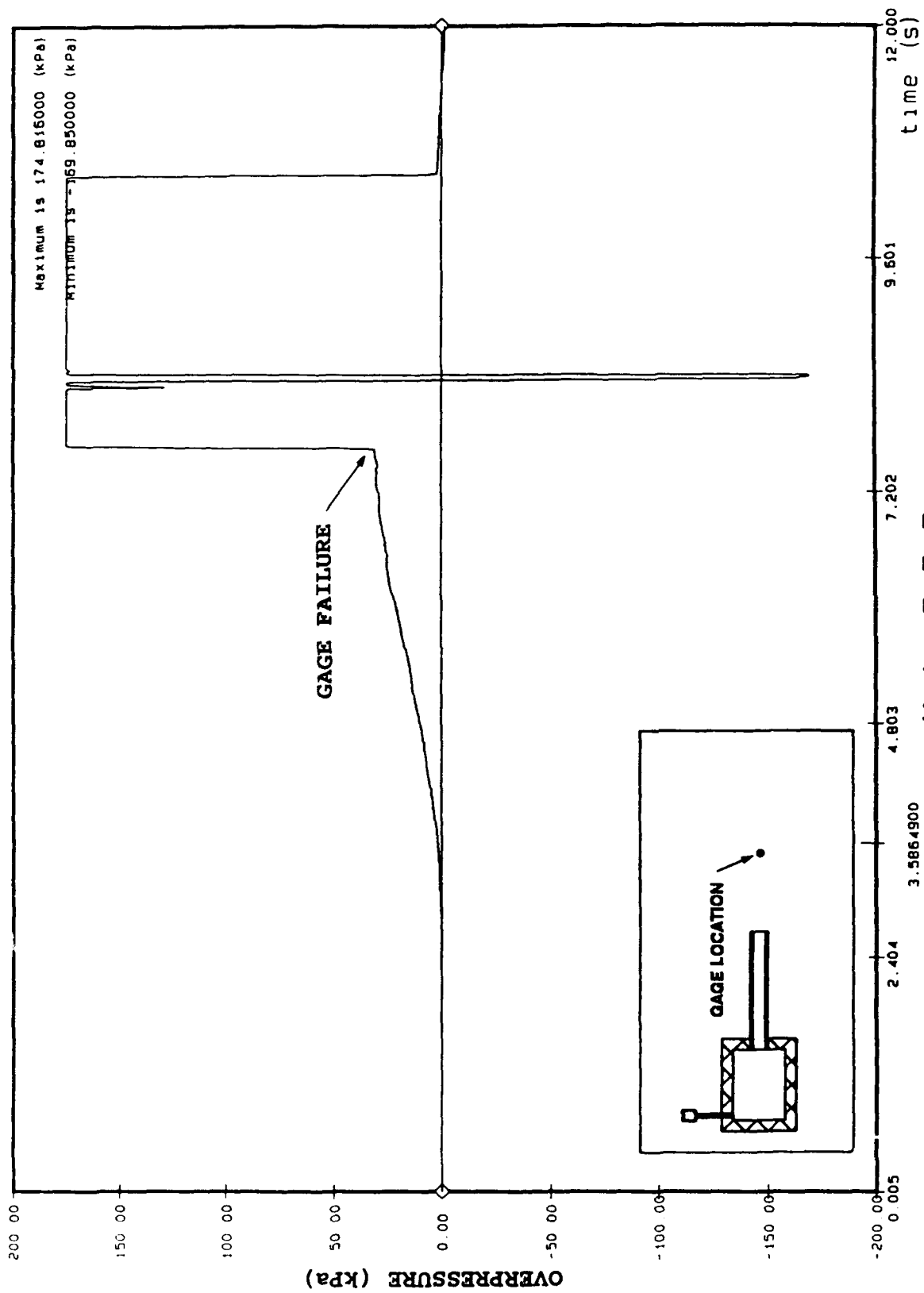
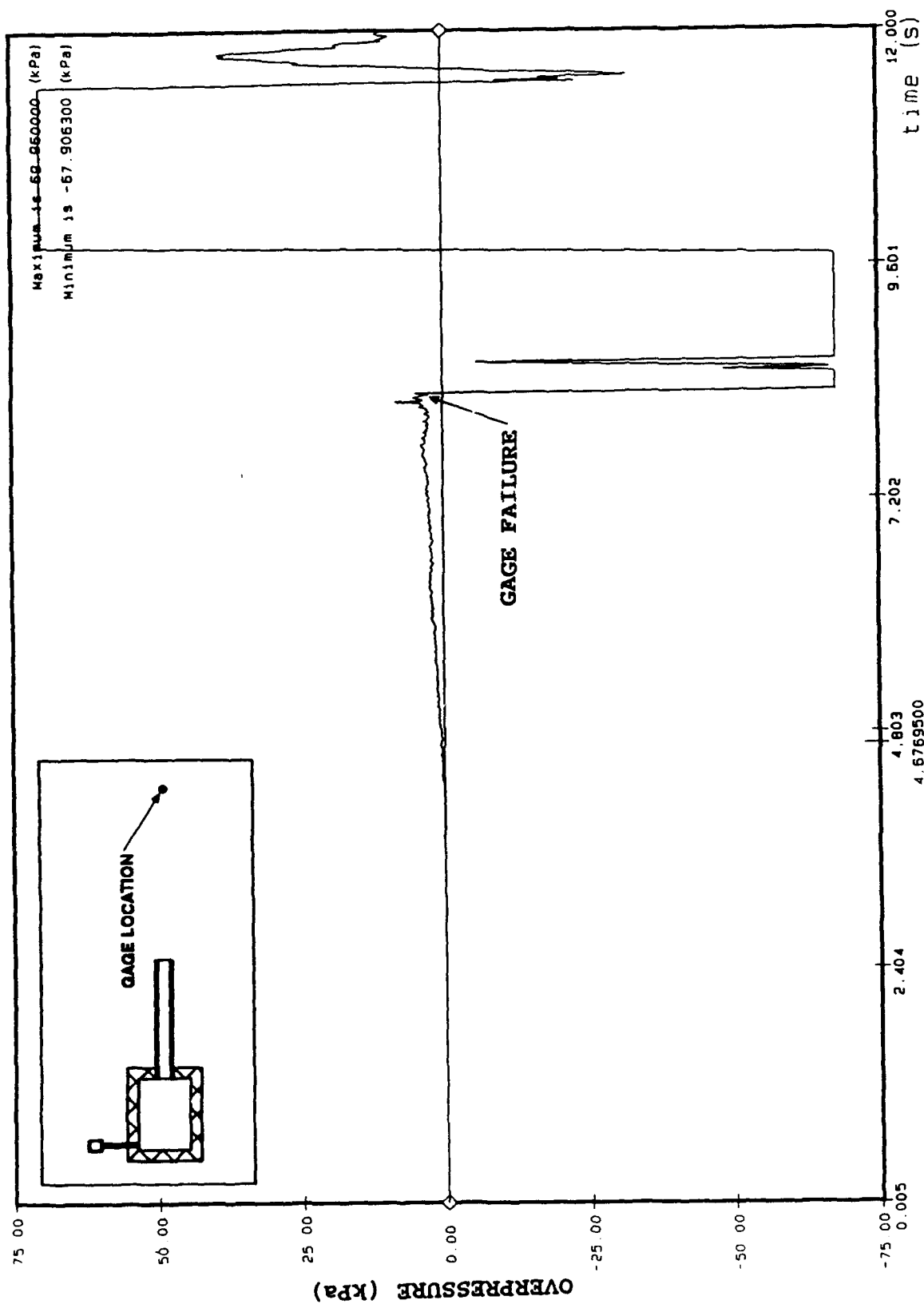


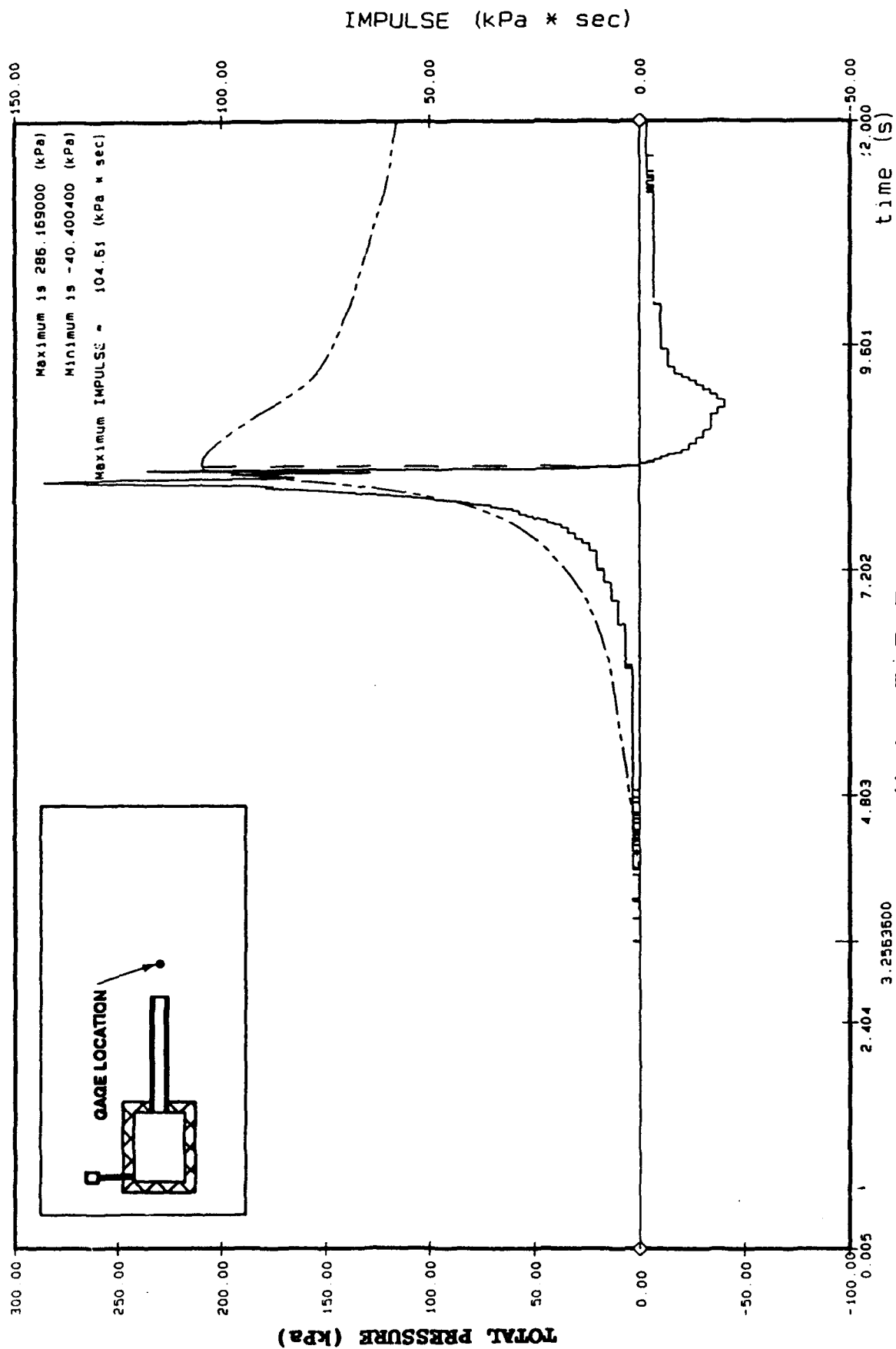
Figure: A4-5



Air Blast External Event C4
Pressure Gauge # ABE176

Filter @ 28.00 Hz

Figure: A4-6



K A I I I
Air Blast External Head Event C4
Pressure Gauge # ABEH177

Figure: A4-7

Filter @ 28.00 Hz

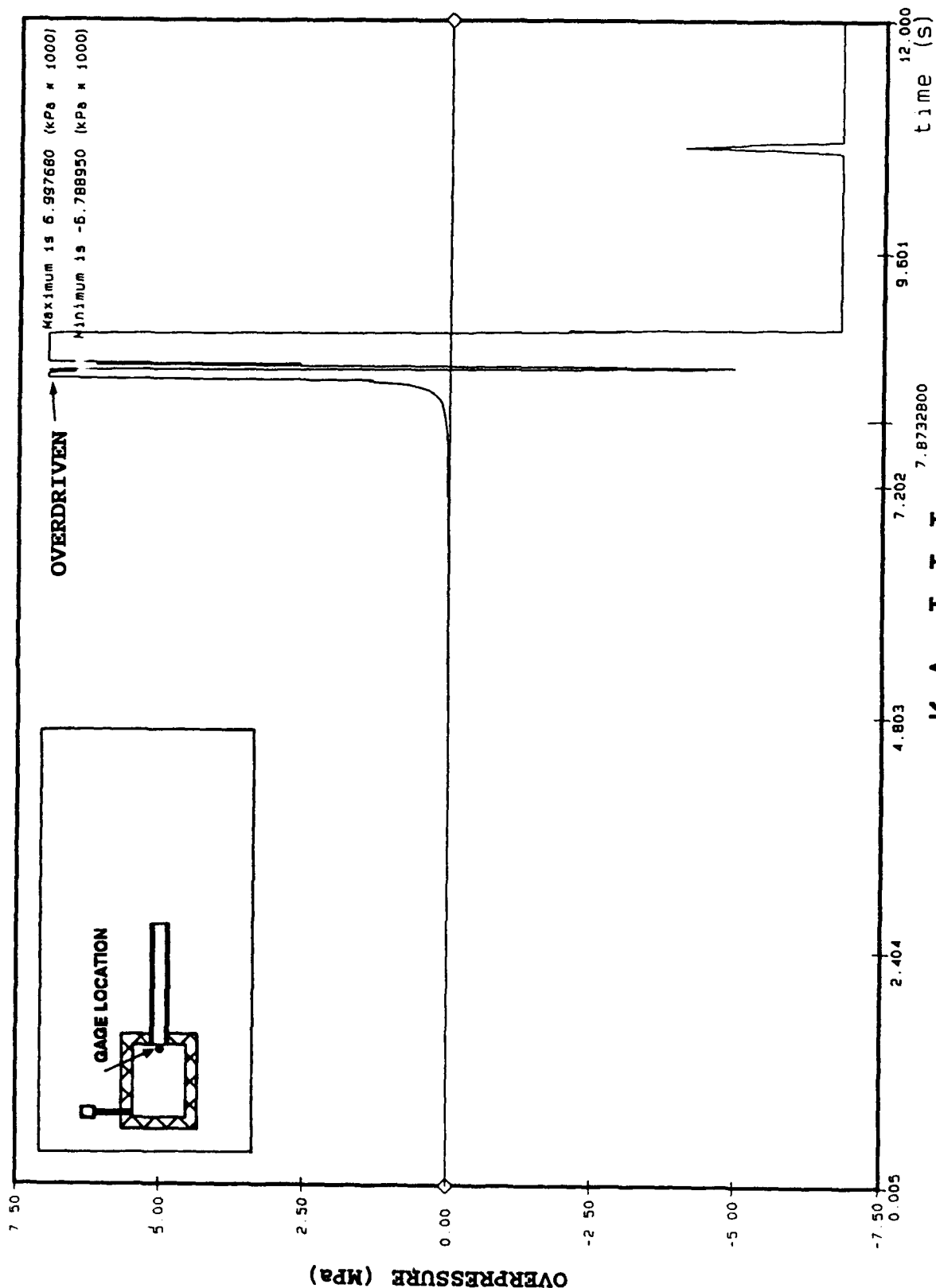


Figure: A4-8

Filter @ 28.00 Hz

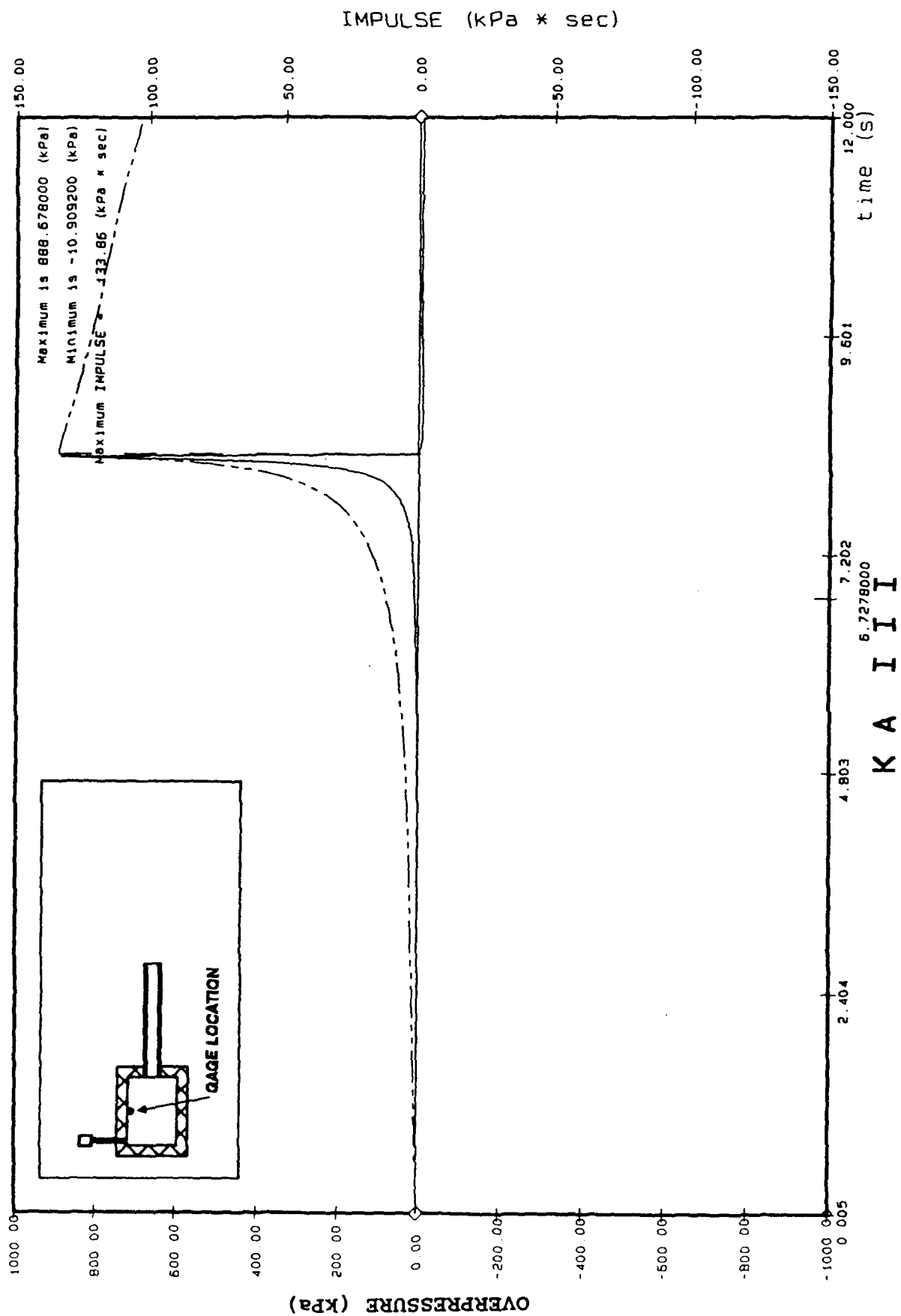


Figure: A4-9

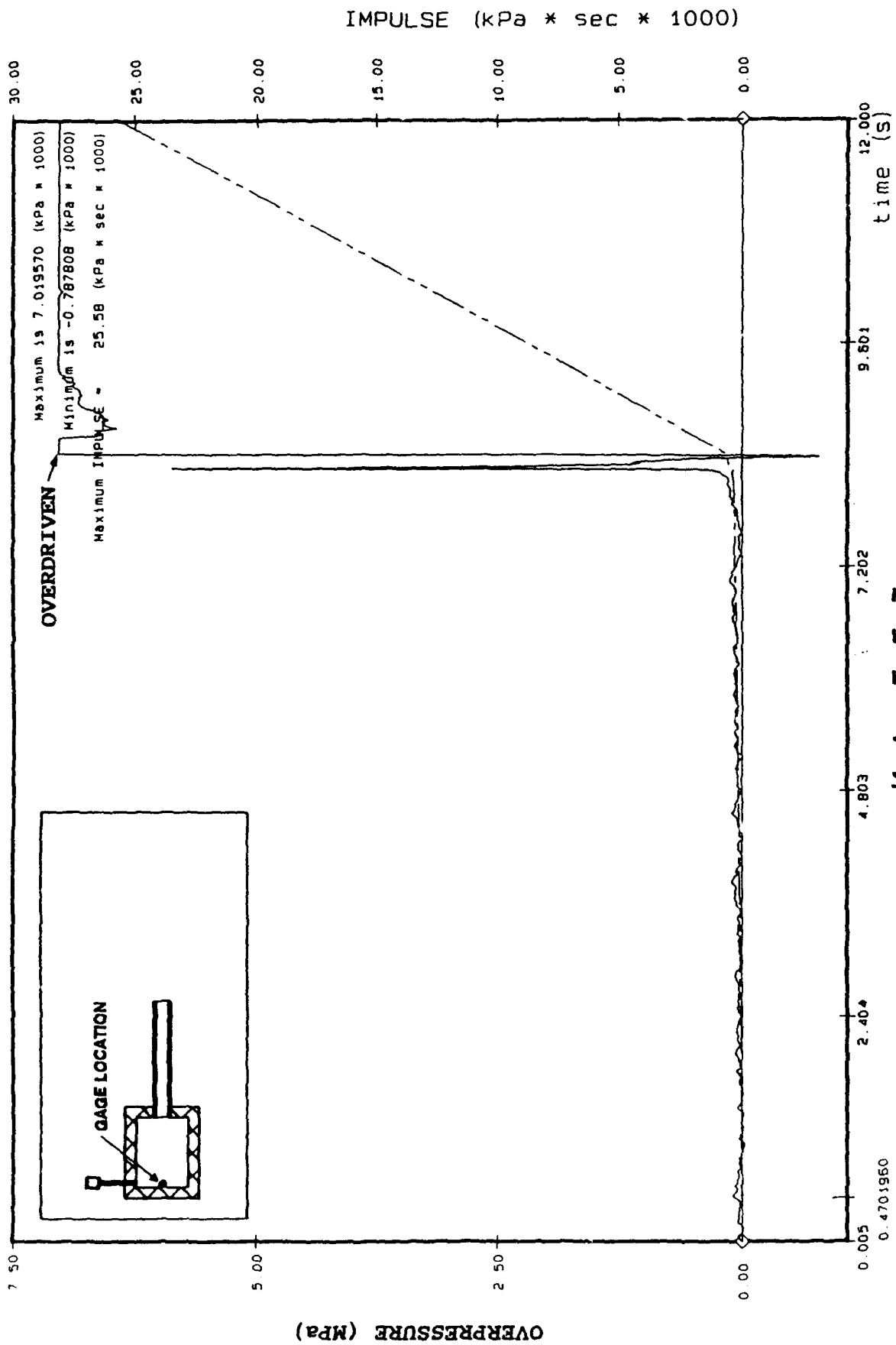
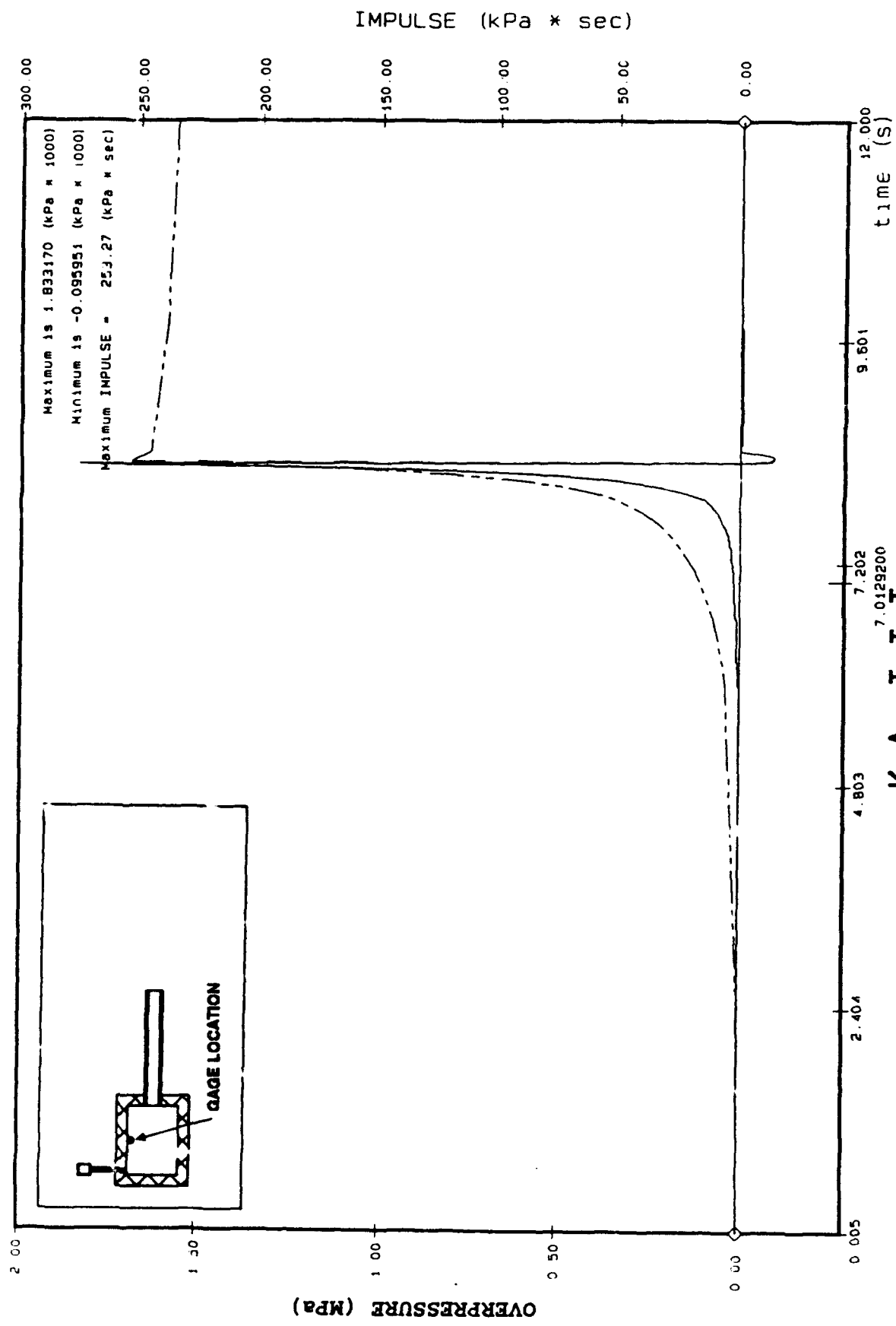


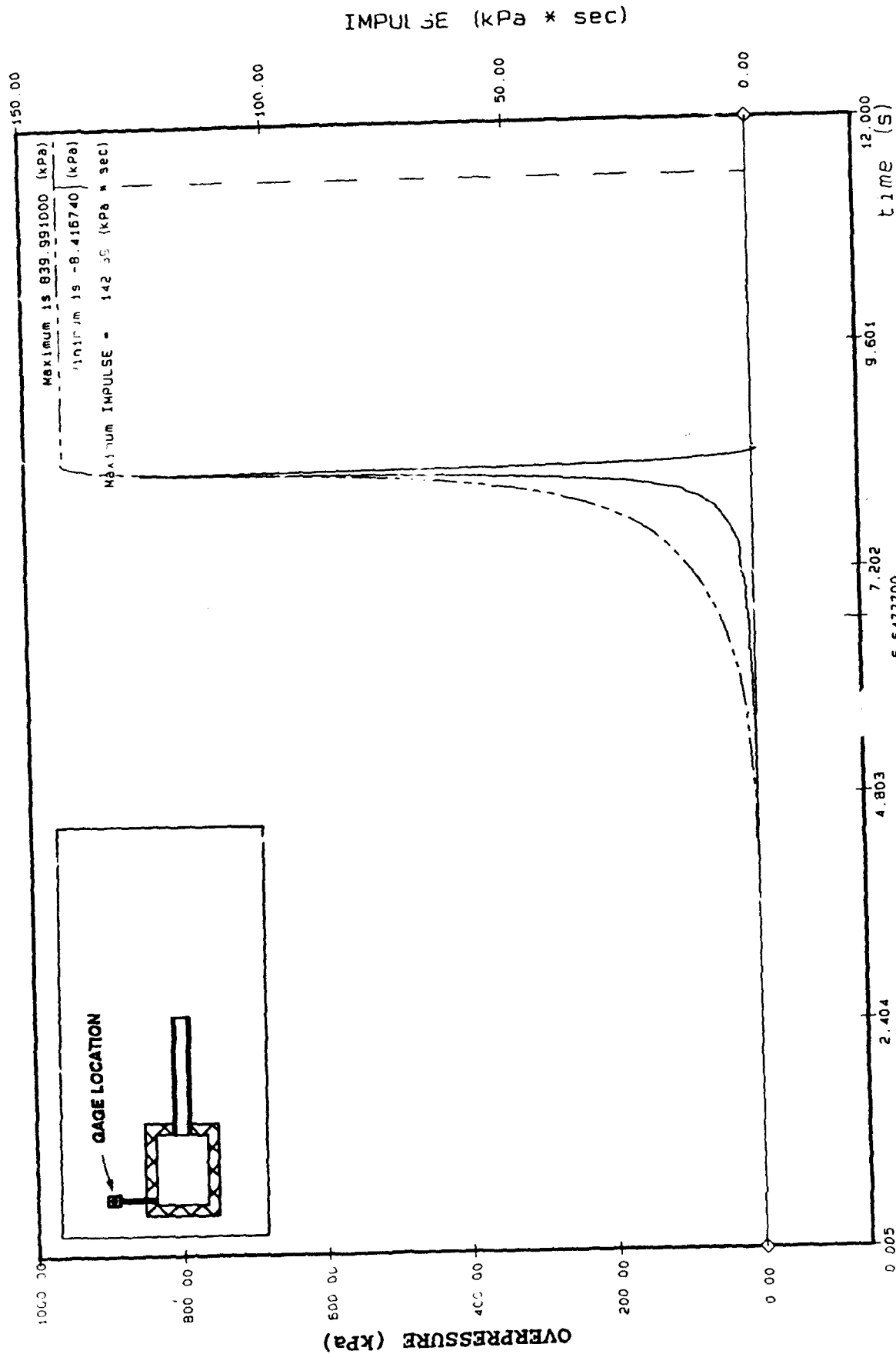
Figure: A4-10



Air Blast Internal Event C4
Pressure Gauge # ABI183T

Figure: A4-11

Filter @ 28.00 Hz



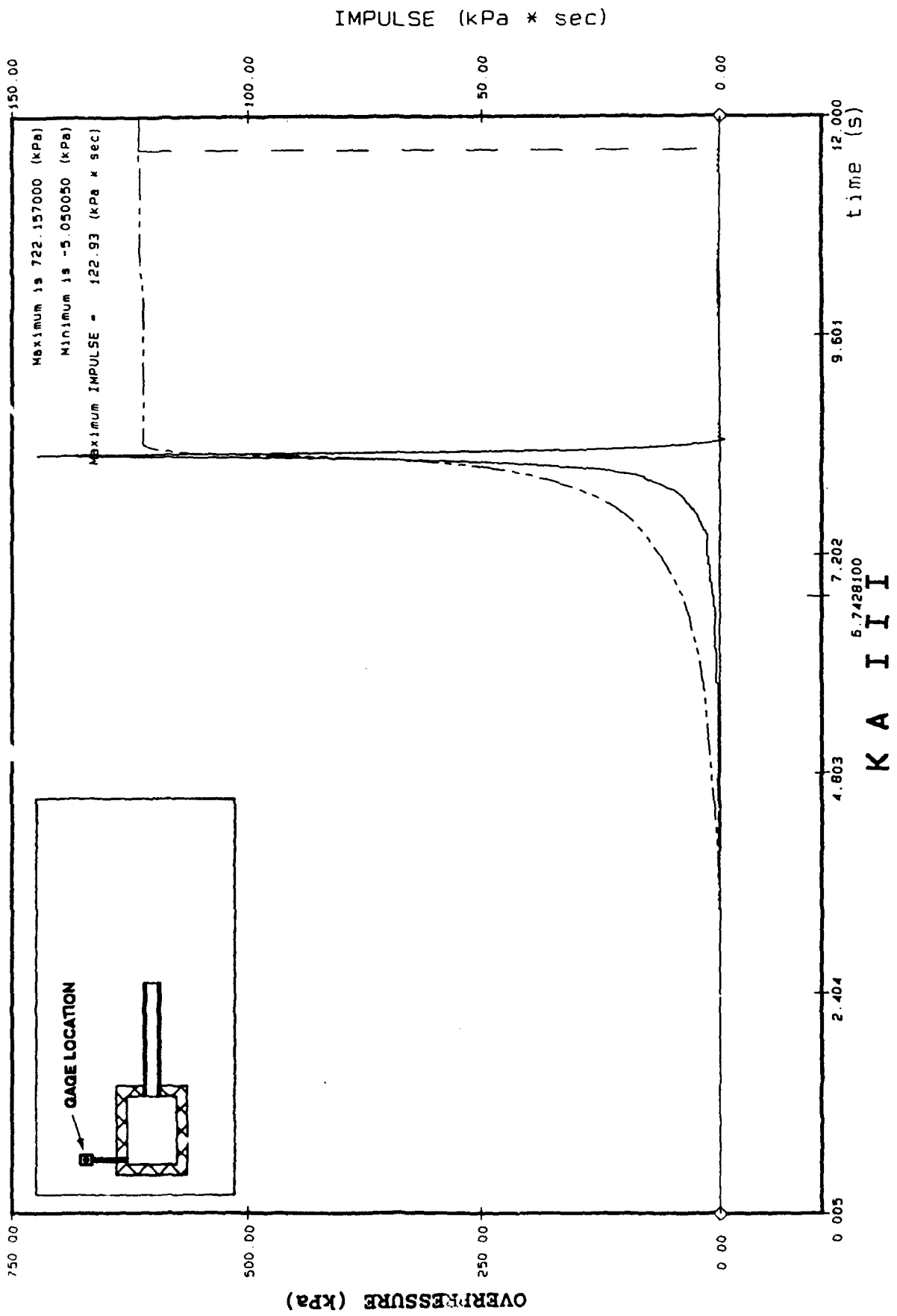
K A I I I

Air Blast Internal Event C4

Pressure Gauge # ABI185

Filter # 28.00 Hz

Figure: A4-12

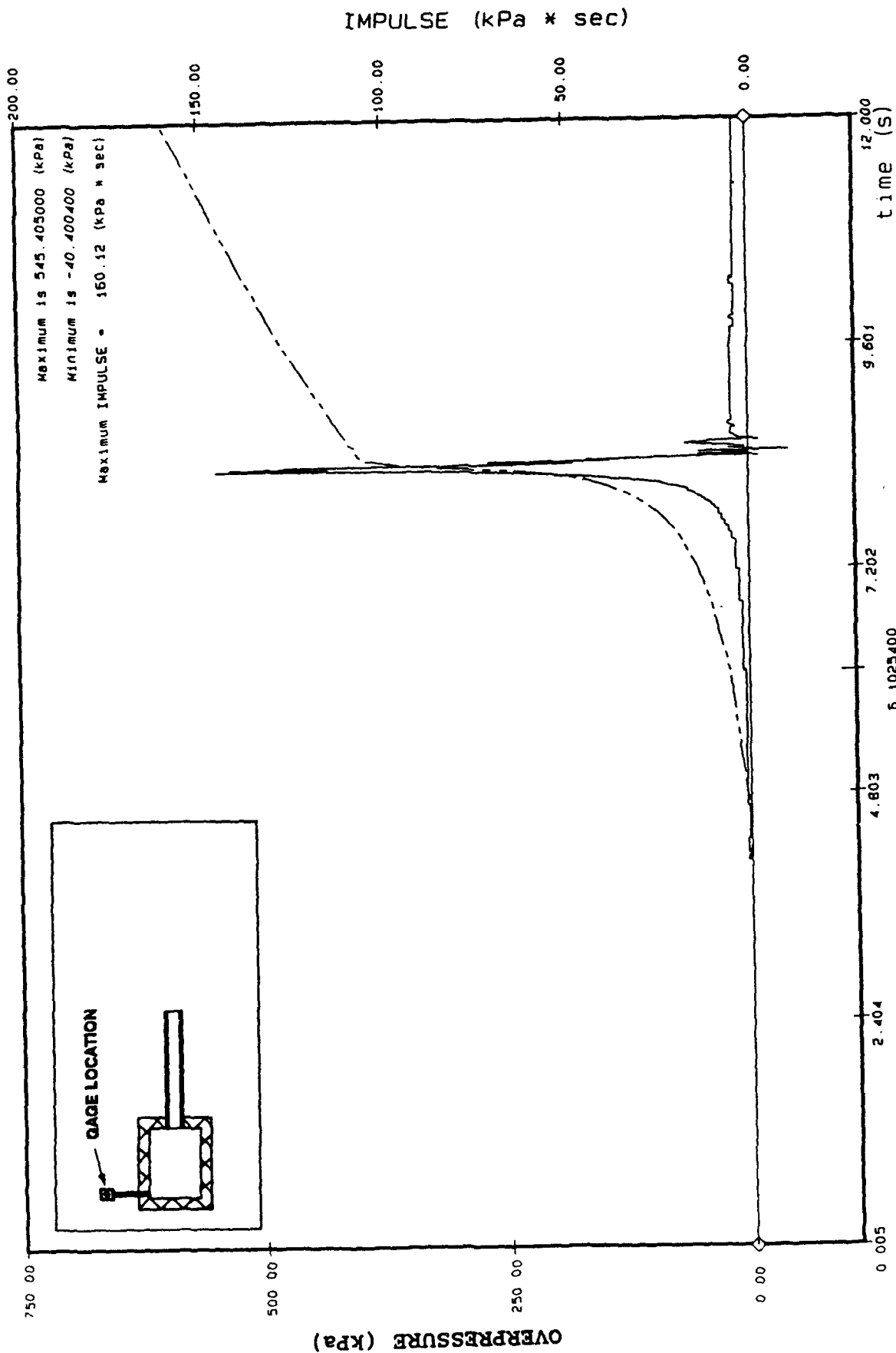


Air Blast Internal Event C4

Pressure Gauge # ABI186

Filter 0 28 00 Hz

Figure: A4-13



K A I I I

Air Blast Internal Event C4

Pressure Gauge # ABI187

Filter # 28.00 Hz

Figure: A4-14

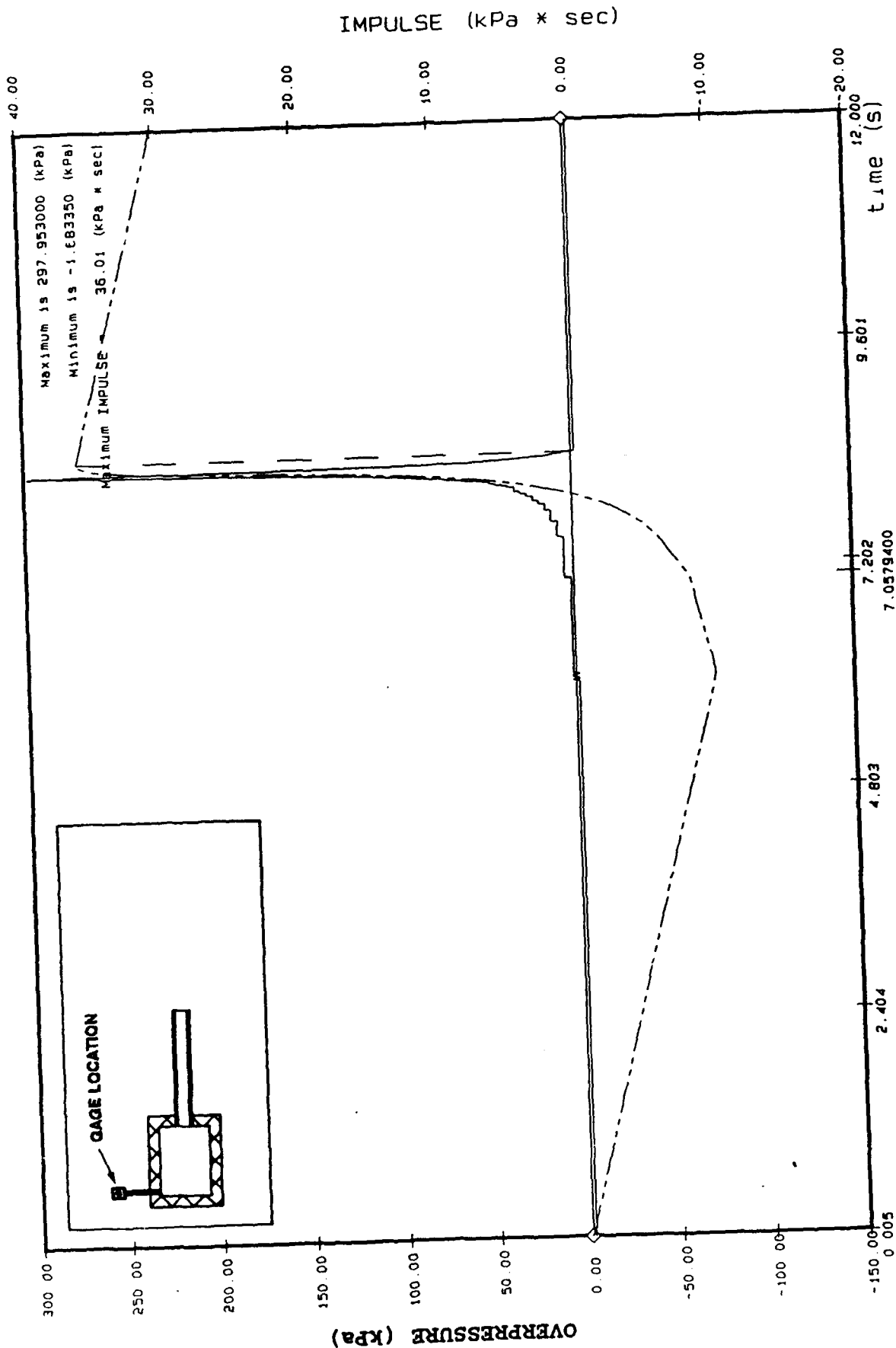
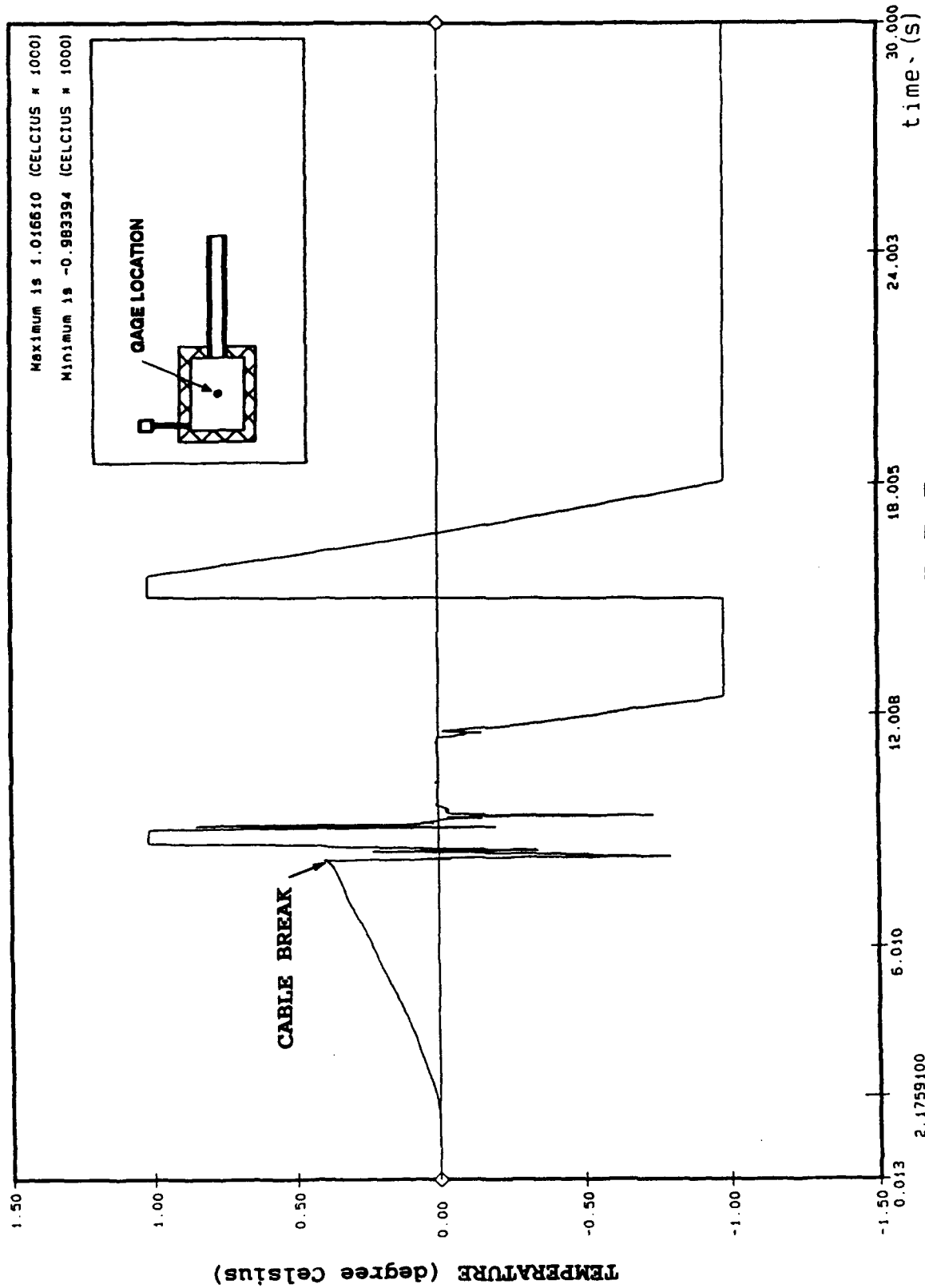


Figure: A4-15



K A I I I

Temperature Experiment C 4

Thermocouple Gauge # THC190

Filter # 11.20 hz

Figure: A4-16

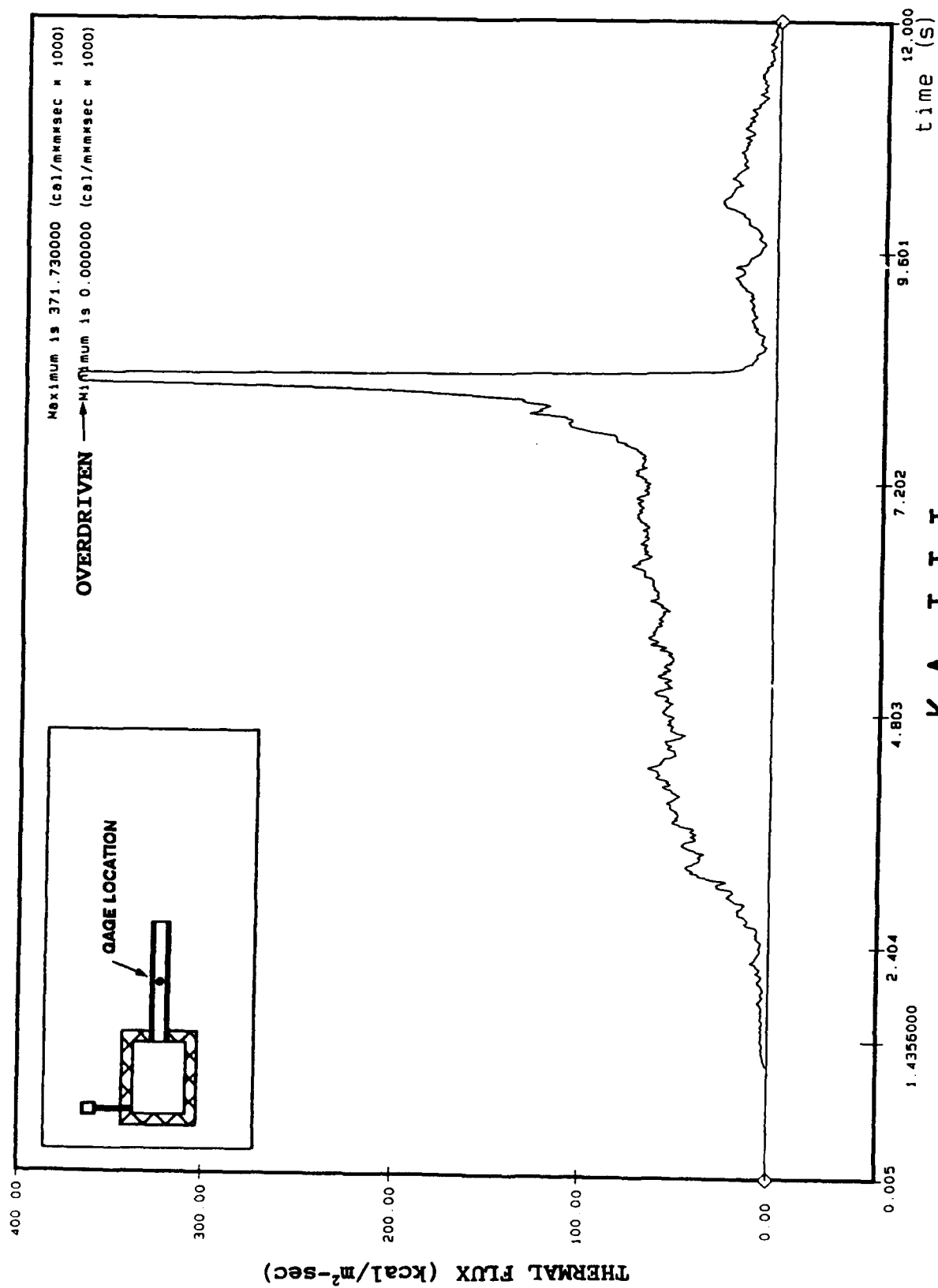
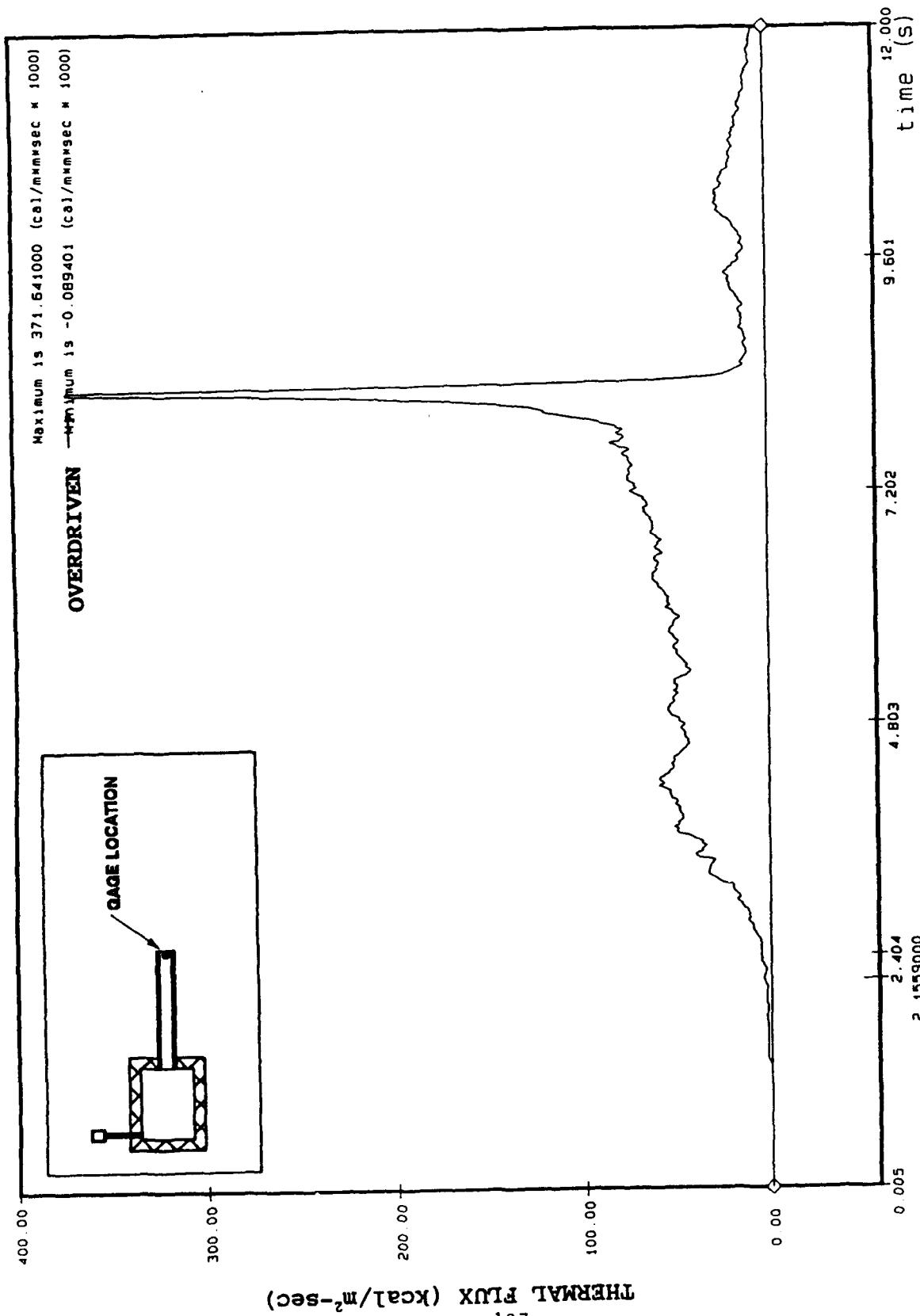


Figure: A4-17



K A I I I
Thermal Flux Event C4
Thermal Flux Gauge # TF192
Filter @ 28.00 Hz

Figure: A4-18